Kinetic and Catalytic Studies of Polyethylene Terephthalate Synthesis

Vorgelegt von

Fatemeh Ahmadnian

Von der Fakultät II - Mathematik und Naturwissenschaften
Der Technischen Universität Berlin
zur Erlangung des akademischen Grades

Doktor der Ingenieurwissenschaften

- Dr. Ing. -

vorgelegte Dissertation

Promotionsausschuss:

Vorsitzende:	Prof. Dr. rer. nat. R. von Klitzing
Berichter:	Prof. Dr. rer. nat. K-H. Reichert
	Prof. Dr. rer. nat. R. Schomäcker
	Prof. Dr. Ing. M. Bartke

Tag der wissenschaftlichen Aussprache: 23.07.08

Berlin, 2008

D 83

'Imagination is more important than knowledge. Knowledge is limited. Imagination encircles the world.'

Albert Einstein

Acknowledgment

I would like to express my deep and sincere gratitude to my supervisor, Professor Karl-Heinz Reichert. His wide knowledge and his logical way of thinking have been of great value for me. His understanding, encouraging and personal guidance have provided a good basis for the present thesis. I am deeply grateful to his detailed and constructive comments and his important support throughout this work.

I wish to express my warm and sincere thanks to Professor Reinhard Schomäcker for his scientific and administrative guidance during my thesis. I greatly appreciate having the chance to teach and supervise lab courses.

My sincere thanks go to the examination committee, Professor Michael Bartke and Professor Regine von Klitzing.

I owe my most sincere gratitude to Dr. Gunter Feix, Dr. Reiner Hagen and Dr. Christofer Hess, for scientific discussions and analytical measurements.

I wish to thank Dr. Geiseler for all his organizatorial helps and supports. He was always ready to help and found always solution for any problem that we faced.

I wish to extend my warmest thanks to all those who have helped me with my work at Technical University Berlin. I would like to thank Astrid for Infrared measurements and also her friendship and support during difficult moments especially for assisting in the organization of scientific symposium on February 2008. Special thanks go to Annette and Annie for all their assistance during my work and teaching duties, to Mrs Wenzel and Mrs Löhr for their sympathetic helps in secretarial works.

I warmly thank all members of research groups of Prof. Schomäcker and Prof. Strasser for warm working atmosphere and funny times in any celebration.

My special appreciation goes to my colleagues, Mohamed, Fernanda and Luis for their scientific assistance in my work and also their friendships and concerns. I am thankful for all beautiful moments that we had together and that nice environment in the group. I would like to thank my former colleagues Marian and Ali.

I wish to thank my friends, Farnoosh, Sara, Pantea, Raha, Zoya, Sohrab, Samira, Arsalan, Juchan, Meena, Rosy and Debby, for good times we spent together in these two years.

I would like deeply to gratitude Milan and Ana Bosnjak for their kindness and support in my residence in Germany. They let me own happy family also in Germany.

I am deeply indebted to my family especially to my parents for their love, continuous support, inspiration and dedication from the first day of my birth. Without them I could not reach to this point now. They share in my entire successes. My special gratitude goes to my lovely sister, my brothers, Mehdi, Nazanin and Safoura for their support and encouragement.

My last but not least gratitude goes to Marijo, for his love, patience, support, concern and dedication during the long process toward this goal. I can not thank him enough.

Thank you all.

Berlin 2008

Abstract of Dissertation

Polyethylene terephthalate synthesis by polycondensation of bis (hydroxyethylene) terephthalate and its low molecular weight oligomers catalyzed by different titanium (IV) based catalysts was investigated. An industrial catalyst, antimony triacetate, was used as a reference catalyst. Polycondensation was carried out in a stirred tank reactor made of aluminium in the temperature range of 250°C to 280°C under 1 mbar vacuum. The products were characterized with respect to conversion of reaction, molecular weight and concentration of side products. For further investigation, differential scanning calorimetry and thermogravimetric analysis techniques were used in nonisothermal mode under nitrogen purging. Differential scanning calorimetry is an appropriate technique for catalyst fast screening of polycondensation reaction. However, some critical points like catalytic activity of sample holder and mass transfer of by-products should be carefully optimized.

Seven different commercially available titanium (IV) compounds were applied which can be mainly classified as chelated and non-chelated titanium derivatives. It was found that non-chelated titanium catalysts were highly active in the synthesis of polyethylene terephthalate nevertheless accelerates the formation of undesired side products. Chelated titanium catalysts showed less activity and more selectivity in the polycondesation reaction. It was also found that the original used titanium compounds were precursors. The catalysts active sites is formed in the beginning of reaction. The exact structure of active species is not known. Probably, the active species is formed by exchange reaction between hydroxyl end groups of monomer and ligands of titanium.

The kinetics of polycondensation reaction catalyzed by titanium tetrabutoxide in melt phase, obeys a second order rate law with respect to the concentration of functional end groups. The overall activation energy of polycodenation reaction is 63 kJ mol^{-1} and that is about 28% less than of antimony triacetate catalyzed polycondensation reaction. A mathematical model was developed to describe kinetic of polycondensation reaction, progress of molecular weight and concentration of side products. The model employed different chemical reactions like reversible polycondensation, degradation reaction and also physical processes like mass transport of ethylene glycol and water. The experimental data were fitted very well by model with respect to conversion, molecular weight and concentration of side products by using of software package PREDICI®. Modeling of molecular weight distribution required modification of the reaction scheme to consider formation of short and long chains of polymers. Good fitting was achieved at lower reaction temperature.

Zusammenfassung der Dissertationsschrift

In dieser Arbeit wurde die durch verschiedene Titan(IV)verbindungen katalysierte Polykondensation von Bis-hydroxyethylenterephtalat und deren niedermolekularen Oligomeren zu Polyethylenterephtalat untersucht. Der industriell verwendete Katalysator Antimontriazetat wurde als Referenzkatalysator verwendet. Untersucht wurde die Polykondensation in einem Rührkesselreaktor aus Aluminium in einem Temperaturbereich von 250 bis 280 °C unter Vakuum von etwa 1 mbar. Während der Reaktion wurden Proben entnommen und der Umsatz, die Molmasse der Polymere und die Konzentration der Nebenprodukte untersucht. Ferner wurde die Polykondensation von Bis-hydroxyethylenterephtalat auch in einem Differentialkalorimeter sowie einer Thermowage bei Atmosphärendruck unter Stickstoff und nicht–isothermen Bedingungen durchgeführt und analysiert. Besonders geeignet für das schnelle Testen von verschiedenen Katalysatoren ist die Methode der Differentialkalorimetrie. Allerdings müssen für zuverlässige Ergebnisse besondere Voraussetzungen hierbei berücksichtigt werden. Dies betrifft insbesondere die Beachtung von Stofftransportprozessen sowie mögliche katalytische Einflüsse des Materials des Probenbehälters.

Als Katalysator für die Synthese von Polyethylenterephtalat wurden sieben verschiedene kommerziell erhältliche Titan(IV)verbindungen verwendet. Hierbei handelt es sich um chelatisierte und nicht-chelatisierte Titankomplexe. Es wurde festgestellt, dass alle nicht–chelatisierten Titankomplexe hoch aktive Katalysatoren für die Polyethylenterephtalatsynthese sind, jedoch katalysieren sie gleichzeitig die Bildung störender Nebenprodukte. Chelatisierte Titanverbindungen hingegen sind katalytisch weniger aktiv und weisen aber eine hohe Selektivität auf. Es wurde festgestellt, dass die untersuchten Titanverbindungen sehr wahrscheinlich nur Vorstufen von katalytisch aktiven Zentren sind, die sich zu Beginn der Reaktion bilden. Die genaue Struktur der aktiven Spezies ist nicht bekannt. Wahrscheinlich werden die aktiven Zentren durch Austauschreaktion zwischen Hydroxylgruppen von Monomeren und den Liganden der Titanverbindungen gebildet.

Die Kinetik der mit Titantetrabutoxid katalysierten Polykondensation von Bis-hydroxyethylenterephthalat in der Schmelze kann durch eine Reaktion zweiter Ordnung bezüglich der Konzentration der funktionellen Gruppen beschrieben werden. Die Bruttoaktivierungsenergie der Polykondensation liegt bei etwa 63 kJ mol^{-1} und ist damit um etwa 28 % niedriger als die der Antimontriazetat katalysierten Polykondensation. Für die mathematische Beschreibung der Kinetik der Polykondensation, der Molmasse der gebildeten Polymeren, sowie der Konzentration der wichtigsten Nebenprodukte wurde ein

Reaktionsmodell entwickelt und durch Parameteranpassung getestet. Das Modell beinhaltet verschiedene chemische Teilschritte wie Polykondensation, Austauschreaktionen, Zersetzungsreaktionen, sowie Stofftransportprozesse von Ethylenglykol und Wasser. Mit Hilfe des Rechenprogramms PREDICI® konnten die experimentellen Ergebnisse sehr gut beschrieben werden. In Bezug auf die Simulation der Molmassenverteilung der Polymeren müssen jedoch Erweiterungen des Reaktionsschemas vorgenommen werden.

Contents

Chapter 1: Introduction to Condensate Polymers

1.1 General Introduction

The class of macromolecular products defined as condensate polymers includes most of synthetic materials manufactured world-wide and used as high-strength and/or high toughness plastics and fibers as well as almost all the hard resins covering very wide range of applications. The definition of such a family of polymer is intended to the condensation methods of polymerization by which they are usually synthesis. This synthetic method from stand point of the polymer chain growth mechanism follows step growth polymerization which proceeds via step-by-step succession of elementary reactions between reactive sites. Each independent step causes the disappearance of two coreacting centres and creates a new linking unit between a pair of molecules. In order to obtain long polymer chain, the reactants must be at least bifunctional, monofunctional reactants act as stopper.

Polyesters (PEs), polyamides (PAs) and polycarbonates (PCs) are commercially important condensate polymers as commodity and engineering polymers with a wide variety of usage which are playing very important role in daily life.

1.2 Polyesters

1.2.1 Historical and economical aspects.

The first studies on synthesis of polyesters go back to the last century [1-3]. It was only in the late 1920s that Carothers undertook an extensive study of this subject but the product could not find great commercial interest [4]. But it was only 15 years after, when Whinfield prepared polyethylene terephthalate (PET) and became widely used [5]. Nowadays, PET is the third largest produced commodity polymer after polyolefins (Figure 1.2.1) [6].

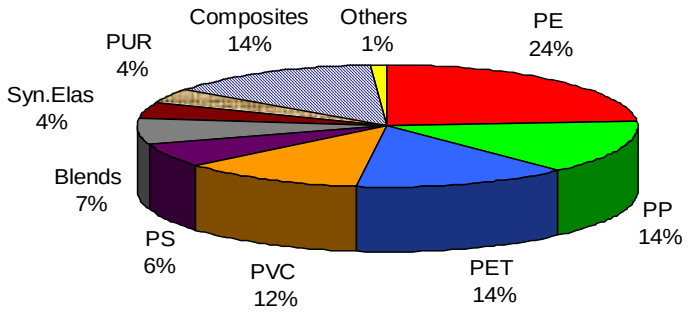

Figure 1.2.1 Diagram of polymer production in 2006 (in weight percentage).

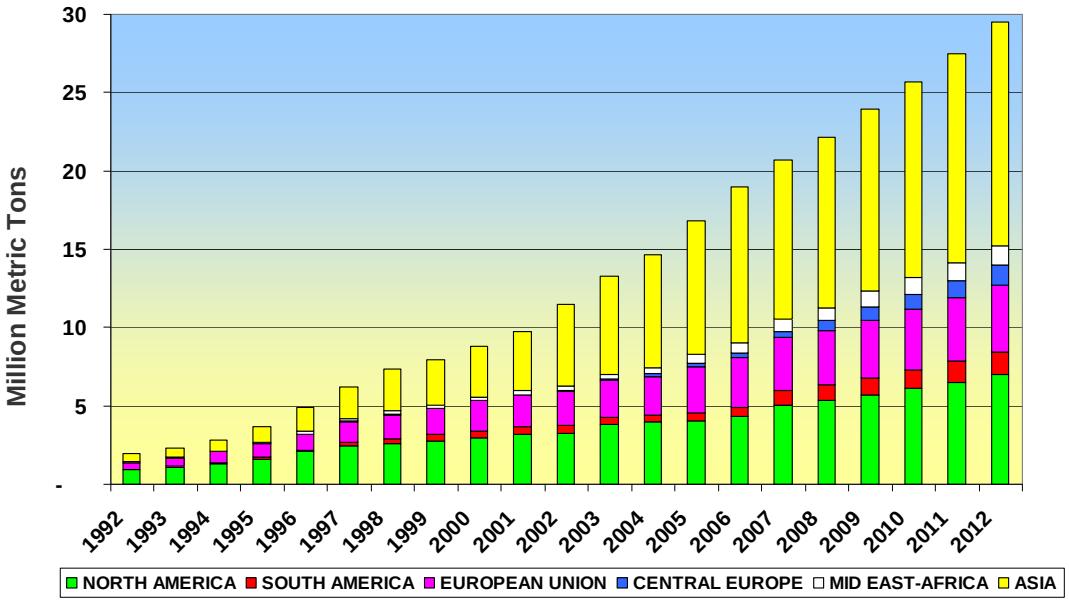

Figure 1.2.2 Regional PET production capacity [6].

Figure 1.2.2 shows the regional PET production capacity in all over the world from 1992 to predicted time of 2012. The total global production of PET in 2007 was about 20 million metric ton. In general, about 63% of PET is used as fibers in staple, filament and woven forms, while the remaining 37% is used as a packaging resin for bottles, containers, sheet and film. Figure 1.2.3, represents consumption pattern of PET in packaging application [6].

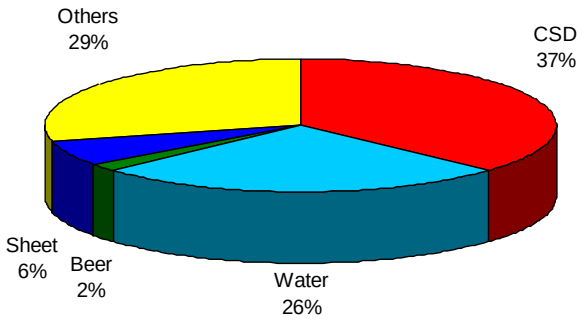

Figure 1.2.3 Consumption pattern of PET in packaging application (wt %) in 2006.

1.2.2 Synthetic methods of polyethylene terephthalate

PET is a polymer formed mainly by polycondensation of purified terephthalic acid (PTA) and ethylene glycol (EG). The synthesis of PET requires two reaction steps. The first step is esterification of PTA with EG, forming a so-called pre-polymer which contains the

monomer bis (hydroxyethylene) terephthalate (BHET) and short-chain oligomers. The esterification by-product, water, is removed via a distillation column system. The second reaction step is polycondensation, in which a transesterification reaction takes place in the melt phase. The by-product, EG, is removed from the melt by using high vacuum [7]. The formation of pre-polymer can also be achieved by transesterification of dimethyl terephthalate (DMT) with EG, releasing the by-product methanol. High purity DMT is easily obtained by distillation and in the early years of PET production, all processes were based on this feedstock. During the late 1960s, highly purified terephthalic acid was produced for the first time on an industrial scale by re-crystallization. Since then, more and more processes have shifted to PTA as feedstock and today more than 70% of global PET production is based on PTA [8].

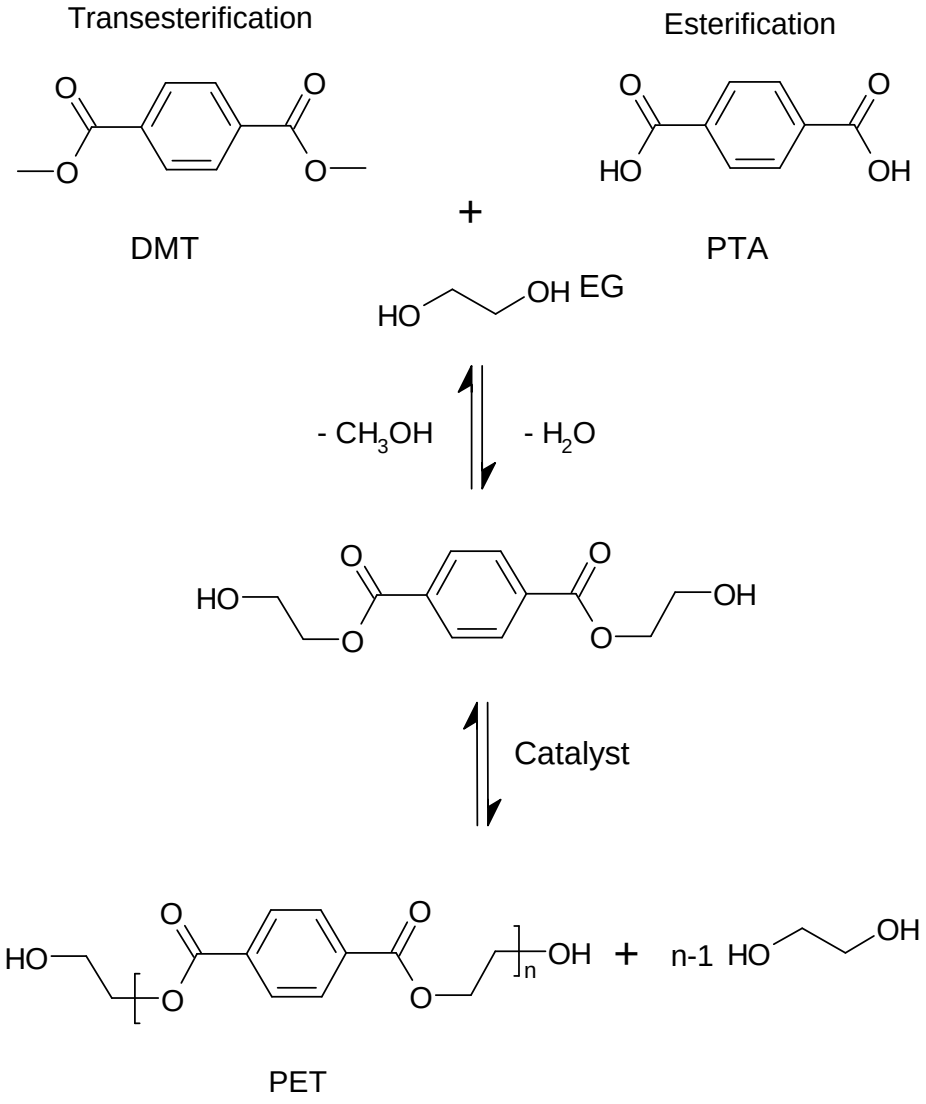

Scheme1.2.1 Reaction scheme of PET production.

Because of the high number of molecules with different chain lengths and compositions present in the polymer, reactions are commonly described as reactions between functional groups. Equal reactivity is assumed for functional groups with the same chemical vicinity, meaning that their reactivity is independent of the chain length of the parent molecules. This concept was initially introduced by Flory [9, 10] and applies without any serious errors if the functional groups are separated by more than three atoms in the chain. If the functional groups in the monomer are separated by only one or two atoms, the reactivity of the monomer and dimer may differ greatly.

PET synthesis is complicated by presence of different side reactions beside the main polycondensation reaction which could be summarized as follows:

1. Thermal degradation of polymer chain and acetaldehyde formation

Thermal degradation of PET is a major problem at temperature above its melting point (260°C) and inevitably occurs in polymer melts during synthesis and processing. The primary degradation reactions have higher activation energies than the polycondensation reactions, and thus become more and more important with increasing reaction temperature. Major consequences for the PET quality are an intrinsic viscosity (IV) drop, formation of carboxyl end groups and acetaldehyde (AA), and yellowing of the polymer. Carboxyl end groups reduce the hydrolytic and thermal stability, and in standard PET grades their concentration should not exceed 25 mmol kg^{-1}. AA migrates into the contents of food packaging, so causing flavour problems of the products. For bottle-grade PET, often an AA content below 1 ppm is specified [8]. The thermal degradation of PET is influenced by metal catalysts. Zimmermann and co-workers [11, 12] have investigated the influence of various metal catalysts on thermal degradation and suggested the following reaction scheme for the catalyzed reaction.

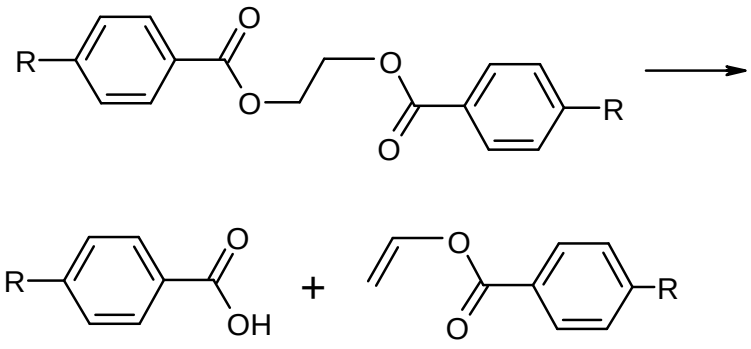

Scheme 1.2.2 Thermal degradation of PET chain.

The most active catalysts were Zn, Co, Cd and Ni.

The polymer chain with vinyl end group is a source of AA formation. It can react with hydroxyl end group and form a new polymer chain and AA as by-product (Scheme 1.2.3).

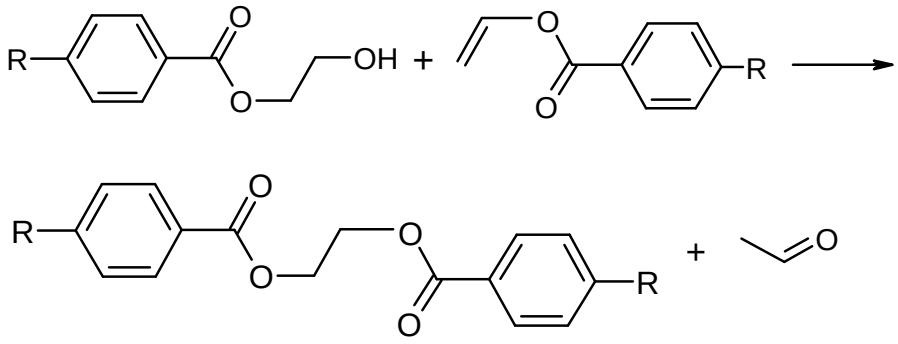

Scheme 1.2.3 Reaction of vinyl end group with hydroxyl end group.

Another source of AA formation is thermal degradation of hydroxyl end group of polymer chain which leads to formation of AA and carboxyl end group (scheme1.2.4).

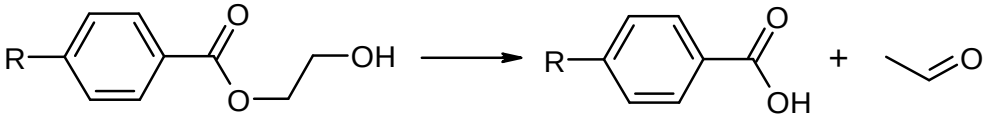

Scheme 1.2.4 Thermal degradation of polymer chain end and formation of acetaldehyde

2- Formation of diethylene glycol

Etherification of EG to form DEG is an important side reaction in PET synthesis. Most of the DEG is generated during the initial stages of polycondensation in the preheating stage and in the low-vacuum stage. Chen and Chen [13] found that most of the DEG is already formed during the esterification stage. DEG is less volatile and, as a diol, it can be incorporated into the PET chain as co-monomer. In some fibre grades, a DEG content of up to 1.5–2.5% is specified to improve the dyeability [8]. Nevertheless, DEG contents should be as low as possible in other PET grades, because DEG decreases the melting point and the thermal stability of the polymer.

Etherification reactions are known to be acid catalyzed. Hornof et al. [14] investigated the influence of metal catalysts (acetates of zinc, Pb and Mn) on the formation of ether bonds. He found that all metals catalyzed etherification, with the strong Lewis acid, Zn, having the highest activity.

3- Yellowing

The polymer colour is regarded as a quality parameter, and low-quality PET grades show yellow colouring. Yellowing of the polymer can be caused by thermal as well as by oxidative degradation and is a severe problem in PET synthesis, especially in the production of bottle grades. The formation mechanisms and the nature of chromophores in PET are still a matter of discussion. Postulated chromophores are polyenaldehydes from the aldol condensation of acetaldehyde [15] and polyenes from polyvinyl esters, as well as quinones [16]. Goodings [15] has proposed aldol condensation as forming polyconjugated species by subsequent reactions of acetaldehyde molecules.

1.2.3 Catalysis

The metal catalysts based on antimony and germanium dominate the industrial production process of PET. Meanwhile a large number of metals and non-metals show a significant catalytic effect but the replacement of antimony and germanium as polycondensation catalysts in an industrial scale has not succeeded until now.

Today, three different antimony compounds are used as polycondensation catalysts; antimony triacetate, antimony trioxide and antimony glycolate. The majority of the polyester is catalysed by antimony trioxide originating from a wide variety of sources. The main drawback of antimony compounds is having negative environmental impact as heavy metal although there is no scientific evidence regarding any negative health impact of antimony used as polycondensation catalyst, but there are variable limitation of antimony content of final product specially in food packaging application which have limitation in the range of 5-20 ppb with respect to the consumer countries (maximum 5 ppb in bottle application for drinking water based on TVO Germany) [17].

Germanium catalyzed polyester were mainly used during the early years in film applications because of its high clarity. Today the main portion of germanium catalyst is still consumed by Japanese polyester producers who like the high brilliancy of the polymer for bottle applications. Assuming an average germanium metal content of 80 ppm, this presents a polyester production of about 0.72 % of the world production. The price of about 500 US$ per kg pure germanium dioxide is the main driving force to gradually replace this catalyst [17].

Titanium based catalysts are very active in the PET synthesis but the main draw back of this catalysts is their poor selectivity causing an increase in concentration of side products and dropping the quality of polymer. The optimal design of titanium compound for

catalysis of PET synthesis is a big challenge in related industries. More information will be presented in chapter 2. Summary of all published data indicate that antimony – free PET based on germanium covers 350000 t/y and antimony – free PET based on titanium, aluminium, magnesium covers about the same amount. This confirmed the former statement: PET based on antimony-free catalysts is still a niche product [18].

1.2.4 Industrial processes of polyethylene terephthalate synthesis in melt phase

The first polyester fiber production was started in 1955 at ICI (GB) with a capacity of 10000 t/y batch wise. Currently, batch plants are mainly used for specialities and niche products. Batch plant capacities span the range from 20 to 60 t/d. The increasing demand for PET gave rise to the development of continuously operated large-scale plants. The capacity of continuous PET plants has grown since the late 1960s from 20 t/d to presently 600 t/d in a single line, with the tendency to still higher capacities. Figure 1.2.4, shows the four specific units that a continuous polycondensation plant is consisted including: Slurry preparation unit, reaction unit, vacuum unit and distillation unit. Reaction unit which is the heart of the production plant consist of one to three esterification reactors two to five pre-polycondensation reactors and one finisher [19].

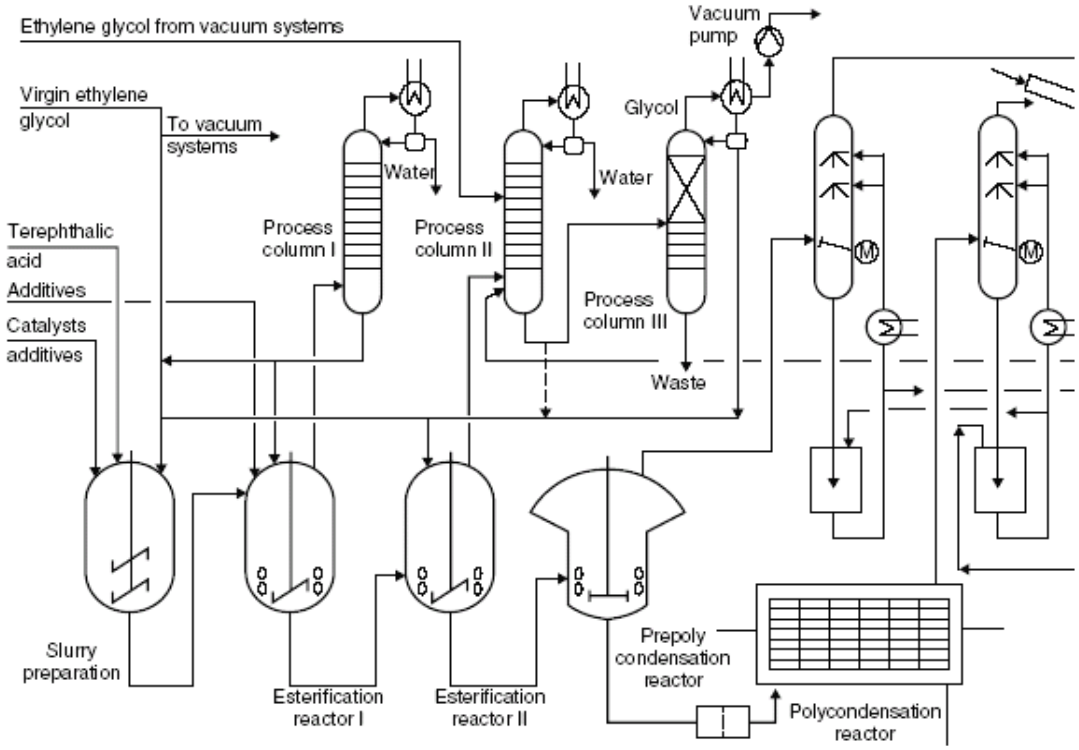

Figure1.2.4 Continuous PET production plant based on Zimmer technology [19].

The monomers PTA and EG are mixed upstream to the esterification reactor in a jacketed slurry preparation unit equipped with a stirrer for highly viscous fluids (e.g. 'Intermig'). The typical molar ratio of EG to PTA lies between 1.1 and 1.3. The esterification temperature and the molar ratio of monomers are the main controlling factors for the average degree of polycondensation of the esterification product (pre-polymer), as well as for its content of carboxyl end groups and DEG. The esterification by-product, water, is removed via a process column in a continuous steady-state mode of operation. The bottom product of the column, being mainly EG, flows back into the esterification reactor. The esterification of PTA is catalyzed by protons and in standard industrial operations neither an additional esterification catalyst nor a polycondensation catalyst is added to the esterification reactor. Some new 'antimony-free' polycondensation catalysts [20] also affect the speed of esterification significantly and it could be advantageous to add them directly into the slurry preparation vessel. The esterification temperature ranges between 235 and 265°C, while the absolute pressure is controlled between ambient pressure and a slight overpressure (0.1–0.4 MPa). At the end of the esterification, the temperature is raised to values between 260 and 285°C and the pressure is often reduced to a moderate vacuum, thus increasing the evaporation of excess EG.

The product of the esterification reactor is fed by gravity into the pre-polycondensation reactor. In the polycondensation reactor, the pre-polymer reacts, forming longer polymer chains and EG is liberated. To shift the chemical equilibrium to the product side, the by-product EG is removed via vacuum (ca. 1 mbar (100 Pa)). EG vapour jet pumps or mechanical rotary piston pumps are used for vacuum generation. In the first quarter of the polycondensation process, the reaction temperature is increased to values between 270 and 295°C and the pressure is slowly reduced with time to avoid high carry over of pre-polymer into the vacuum system. Blade or anchor stirrers are commonly used to renew the surface of the melt and to provide heat which is transferred into the melt by dissipation of the stirrer energy. The stirrer speed is reduced gradually to avoid overheating and reduce power consumption. From the pre-polycondensation stage, the product is pumped by gear pumps through a filter into the finisher. Finisher provides a high specific surface area and short diffusion lengths, thus maintaining high polycondensation rates at reduced temperatures. For a high performance at this step, disc- or cage-type reactors are common. The optimum stirrer design provides a plug flow characteristic with little back mixing. In this case, the residence time distribution is narrow and the average rate of

polycondensation is high. The desired degree of polycondensation, and respectively the final melt viscosity, is set by adjusting the vacuum, the reaction temperature and the average residence time by level control. Figure 1.2.5 shows a view of inside of cage reactor. Figure 1.2.6 represents formation of thin layer of PET which accelerates mass transport phenomena.

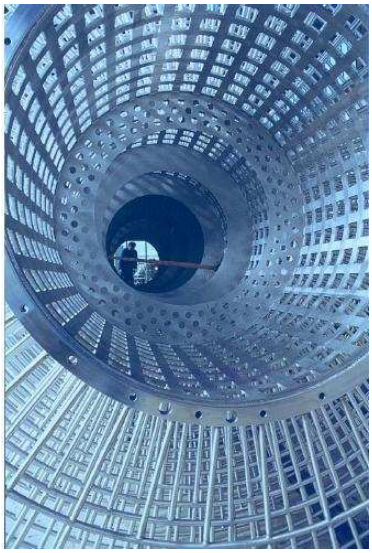

Figure 1.2.5 DISCAGE® reactor [21].

Figure1.2.6 Thin film formation in DISCAGE® reactor [21].

Since 1990, as the production was growing fast and market demand was increasing large and larger plant should be built which was not economically profitable. Furthermore, the price of raw material was increasing to 85% of production costs, therefore the engineering companies start to design and build up new plants in order to minimize production cost by reduction in equipment and installation, building and construction, personal, energy consumption and maintenance costs. In 1996, Uhde Inventa-Fischer introduced the first 4-Reactor single-stream PET technology to the market (Figure 1.2.7) [21].

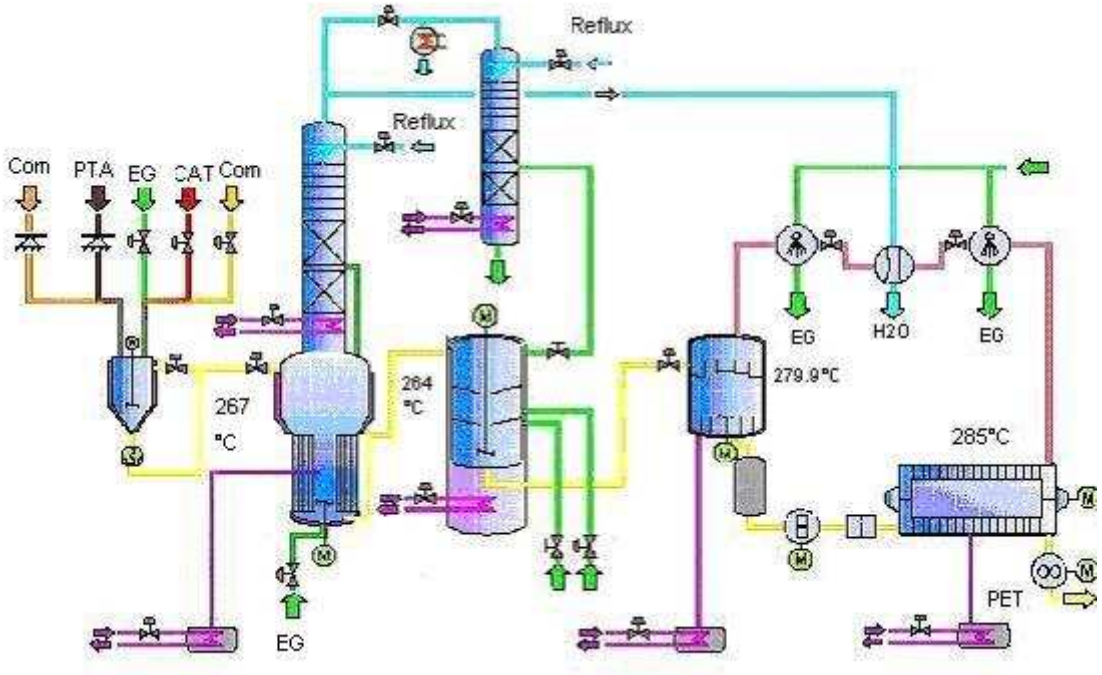

Figure 1.2.7 Flow diagram of 4R-Technology of Uhde Inventa-Fisher [21].

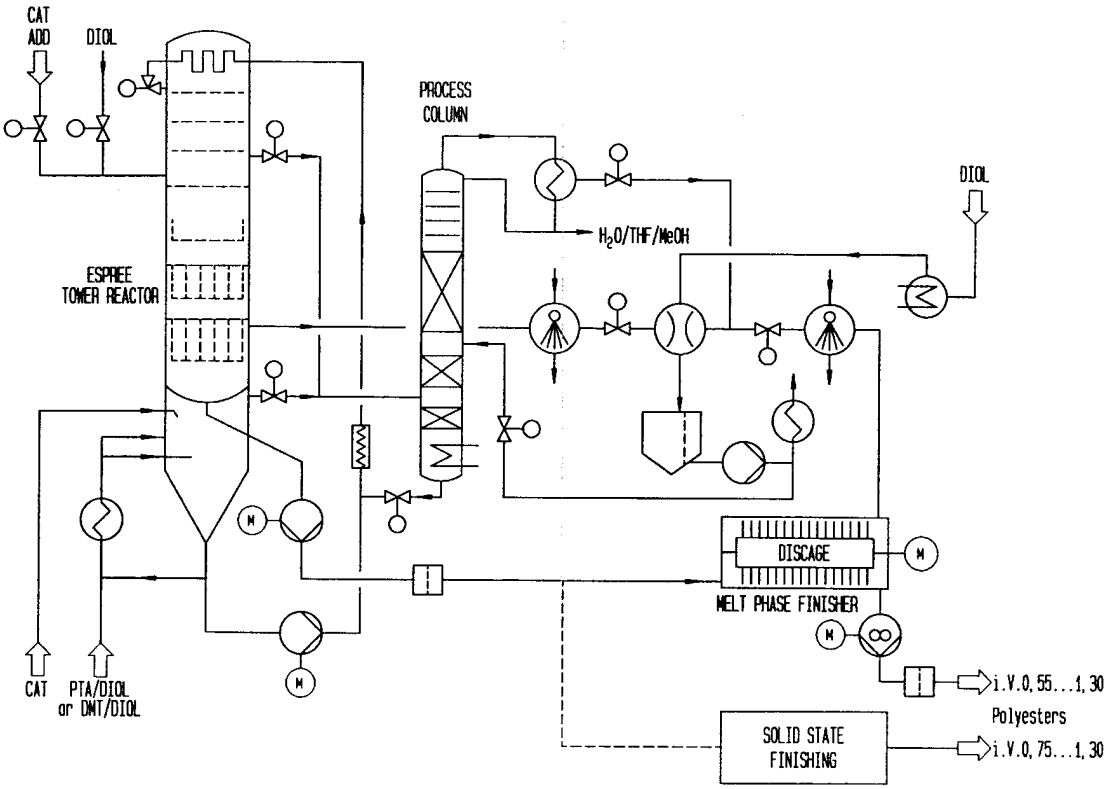

Figure 1.2.8 Flow diagram of 2R-technology of PET production [21].

This company [21] could improve the plant design by introducing 2-reactor single stream PET technology ESPREE ® in 2002 which could reduced the production costs up to 20% (Figure 1.2.8). The reduction of number of reactors was also target by other PET plant designer. Zimmer AG [19] and Aquafil [22] have claimed PET production plant with 3 and 1 reactor respectively.

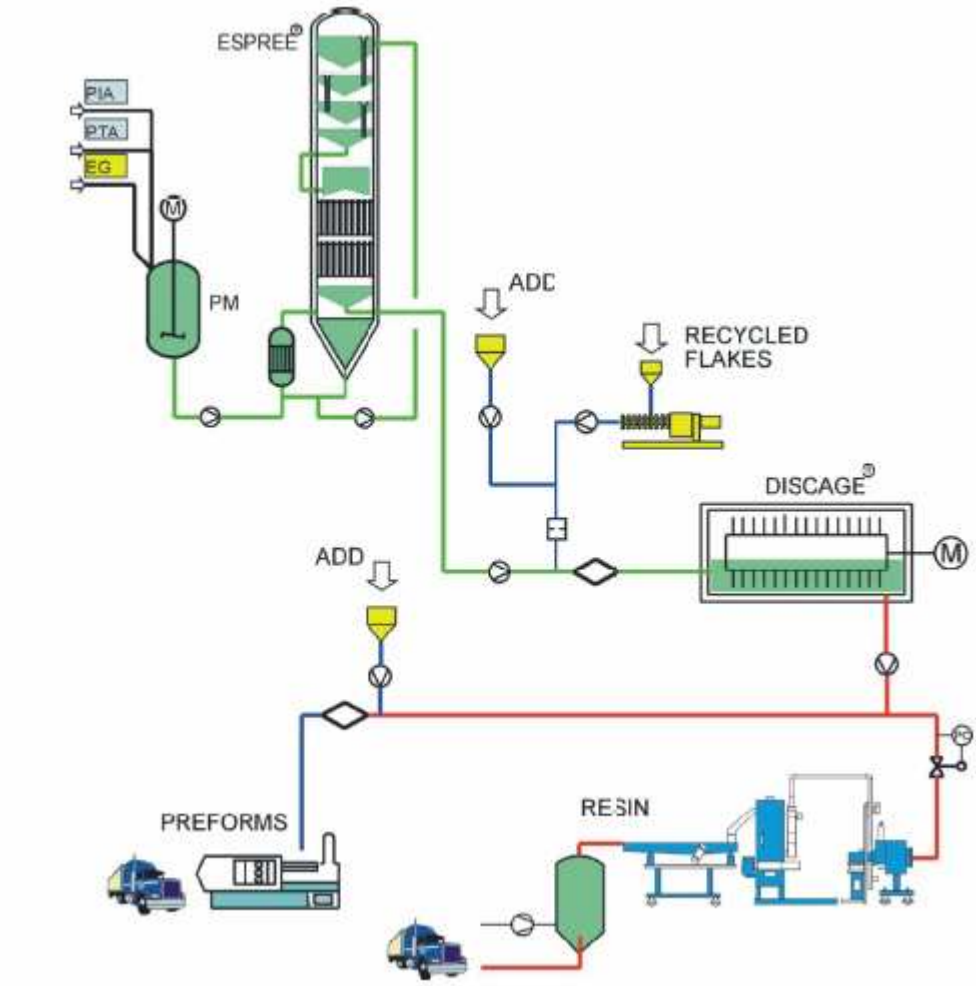

Figure 1.2.9 Scheme of Melt-To-Resin ® Technology of Uhde Inventa-Fisher [21].

The production of bottle-grads resins requires high molecular weight PET which is achieved by polycondensation in solid state under inter atmosphere or vacuum to reach IV of 0.85 dl g^{-1}. This is a long-term energy and investment-intense operation that also impairs quality. In 2004, Uhde Inventa-Fisher[21] announced their new Melt-to-Resin (MTR)® technology which was based on their 2R-process consisting of the brand new ESPREE® tower reactor and the DISCAGE® MV (for medium viscosity) finisher reactor. The technology besides other advantages such as improved product quality and less

maintenance cost, also can increase the profit by 30 to 40 EUR/ton PET on conversion costs compared to the old technology (Figure 1.2.8).

1.2.5 Polyethylene terephthalate synthesis in solid state

Polycondensation of highly viscous PET in the melt phase is limited. The removal of the volatile by-products becomes more difficult due to diffusion inhibited by increasing viscosity of polymer. In addition, undesirable side reactions due to thermal degradation impede the growth of the molecular chains. As a consequence, the reaction rate decreases and decomposition reactions dominate, thus resulting in a decrease in the melt viscosity. As it is able to address these limitations, solid state polycondensation (SSP) has become the method of choice and is therefore so popular. This is the kind of process that can be defined as the polycondensation of semi-crystalline, low molecular weight polymers to high molecular weight polymers occurring below the melting temperature of polymer, but well above the glass transition temperature.

In order to interpret reaction progress in SSP, several key assumptions should be considered; the reactive end groups and the catalyst are located in the amorphous regions, no reaction occurs in crystalline region, polycondensation reaction is reversible reaction but is complicated by the two-phase character of the semi-crystalline polymer [8]. The PET synthesis in SSP is diffusion controlled; therefore it is needed to provide enough interfacial area to allow the efficient removal of by-products from solid phase, by reduce the particle size of polymer. A practically difficulty in this case is the possible tendency of particles to stick which make the process unfeasible. It can be overcome by starting with polymer with sufficiently high crystallinity [26].

SSP can be carried out batch wise or continuously, either under vacuum or an inert gas flow. The continuous process is appropriate for the large-scale production of polyesters used in bottle manufacture. Currently, reactors with capacities of more than 600 t/d have been employed [8].

1.3 Polyamides

1.3.1 Historical and economical aspects

Polyamides or nylons were first synthesized by Gabriel and Maas in 1889 [23]. Carothers continued their work and prepared a large number of nylons in the late 1920’s.

Independent of his efforts, successful attempts to make nylons from ε-caprolactam were undertaken in Germany, and the first commercially produced nylon monofilaments appeared on the German market in 1939. In the U.S. nylon stockings were successfully introduced to the public in May 1940. Britain and Italy followed during World War II, and since the beginning of the 1950's, the production of polyamide fibers has greatly expanded throughout the world, as many new producers entered the field, and the original manufacturers expanded their capacities[24]. The annual demands of PAs increase drastically in application of fiber and automotive. The total PAs consumption in 2006 was about 7.1 million tons in which polyamide 6 (PA 6) has the highest consumption [25] (Figure 1.3.1).

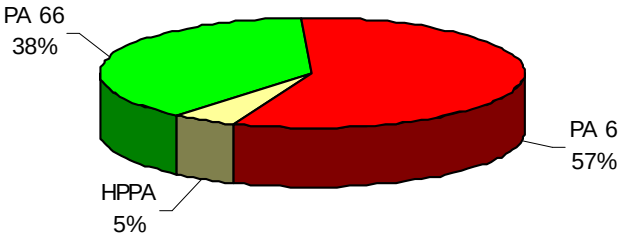

Figure 1.3.1 Global consumption of different polyamides(wt %).

1.3.2 Synthetic methods of polyamides

1.3.2.1. Polycondensation

Amination is occurring by direct reaction of an amine with a carboxyl acid accompanied by elimination of water. The reactive groups may be on a single molecule like an amino acid (AB type) or they can be different molecule, i.e., diamins and dicarboxylic acids. The reaction schemes can be described as follows.

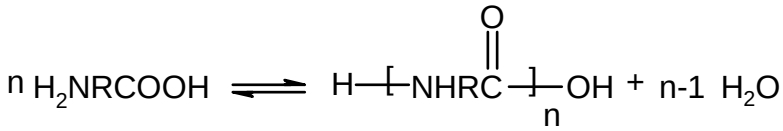

Scheme 1.3.1 AB type of polycondensation reaction in polyamide synthesis.

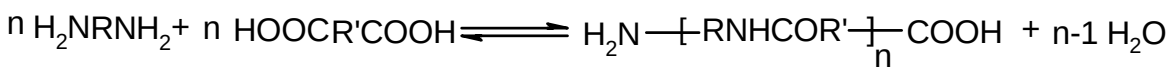

Scheme 1.3.2 AA and BB type of polycondensation reaction in polyamide synthesis.

Polyamide 66

Polyamide 66 (PA 66) is made by condensation of adipic acid with hexamethylene diamine (Scheme 1.3.3). AH salt is formed as an intermediate and subsequent polymerization involving the elimination of water leads to the polymer.

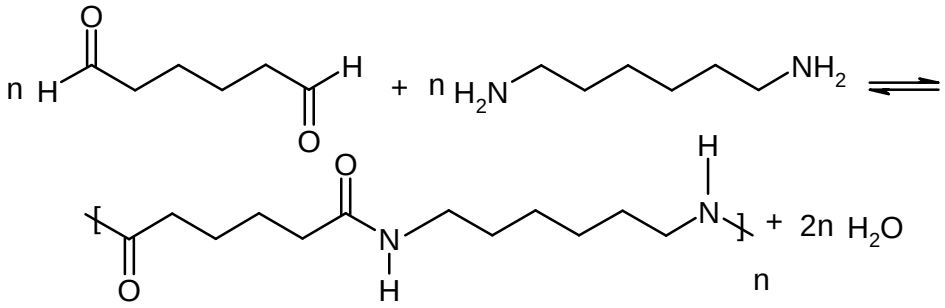

Scheme 1.3.3 Reaction of PA 66 synthesis.

1.3.2.2 Ring-opening polymerization

Ring-opening polymerization is an effective and important method for preparing high molecular weight polymers from cyclic lactate such as ε-caprolactam. Ring-opening Polymerization catalyzed by alkali metals follows a chain growth polymerization mechanism without elimination of a by-product molecule. The reaction shows an induction period which depends on temperature. It is followed by an extremely rapid reaction which is completed in a few minutes. Although salts of phosphorous acid and other phosphorous can catalyzed the polymerization, they are not commonly added to commercial polymerizations. However, ring-opening by hydrolysis follows a step growth mechanism with 3 steps of reactions as hydrolysis reaction, addition reaction and condensation reaction.

Polyamide 6

Polyamide 6 (PA 6) is predominately made by a hydrolytic polymerization mechanism (Scheme1.3.4). The reaction is initiated by hydrolysis of ε-caprolactam with water, and aminocaprolactam is formed in catalytic quantities. ε-caprolactam successfully adds to this chain until a molecular weight of 8000-14000 g mol^{-1} is reached. Subsequently, a condensation polymerization occurs, and the initially formed short chains are linked together to chains of molecular weights between 18000 and 33000 g mol^{-1}. In the final equilibrium step, a molecular weight of 20000- 36000 g mol^{-1} is achieved. Chain stopping elements, either acids or amines, are used to achieve the desired molecular weight.

1. Hydrolysis of ε–caprolactam to aminocaprolactam

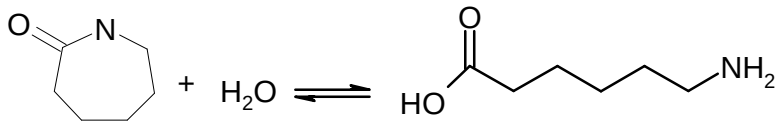

2. Addition of caprolactam to polymaide molecule

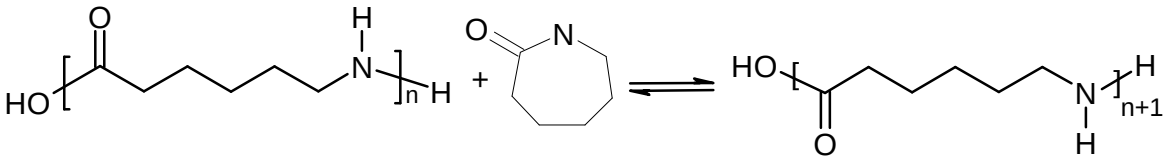

3. Condensation of diffenent polyamide chains

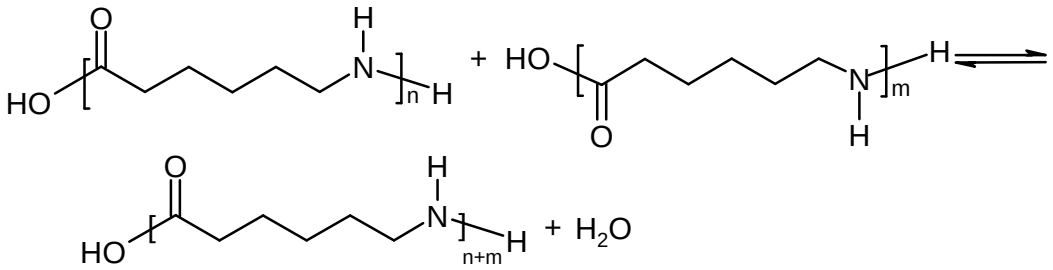

Scheme 1.3.4 Reaction steps of PA 6 synthesis by hydrolytic polymerization

1.3.3 Kinetics

Published results on kinetics of amidation appear to be contradictory [26]. Some researchers contend that the reaction obeys second-order kinetics (first order in both amine and acid end groups) and is not accelerated by catalysts. Several studies of polyamidation, under conditions where the end-group concentrations are relatively low (i.e., conversions above 90%), indicate that a carboxyl catalyzed third-order reaction assumes increasing importance and becomes predominant. So, other researchers have suggested that there is a shift from second- to third-order kinetics, involving catalysis by the carboxyl acid end group, at low water contents and high conversions. In addition, a study of the hydrolysis of amides at 220°C in near-neutral buffered solutions has shown that this reaction is carboxyl-catalyzed. Therefore, some researchers have assumed third-order kinetics (first order in amine ends and second order in carboxyl ends) over the entire water concentration range [26].

For third-order, carboxyl-catalyzed reaction in an anhydrous melt (no reverse reaction), the rate equation is:

$$\frac{-d[COOH]}{dt} = k[COOH]^2[NH_2] \quad (1.3.1)$$

If [COOH]=[NH_2], the integrated rate equation is given by:

$$[COOH]^{-2} - [COOH]_0^{-2} = 2kt \quad (1.3.2)$$

For [COOH] - [NH_2]=D, the integrated rate equation becomes

$$D^{-1}\ln\left(\frac{[COOH]}{[NH_2]}\right) - [COOH]^{-1} = kDt + C \quad (1.3.3)$$

where C is a constant of integration determined by initial conditions.

In the presence of water a carboxyl-catalyzed hydrolysis reaction must be introduced. The rate equation is then given by

$$\frac{-d[COOH]}{dt} = k[COOH]^2 - k_h[COOH][H_2O][CONH] \quad (1.3.4)$$

For kinetic studies at high conversions, where [CONH], concentration of polymer, is essentially constant, and at fixed water vapour pressure and concentration of water in the melt:

$$k_h[H_2O][CONH] = k[COOH]_{eq}[NH_2]_{eq} = kP_{eq} \quad (1.3.5)$$

where the symbol P stands for end product and the rate equation becomes

$$\frac{-d[COOH]}{dt} = k[COOH][P - P_{eq}] \quad (1.3.6)$$

which can be written as following integrated form

$$\ln\left(\frac{[COOH]^2}{[COOH]^2 - [COOH]_{eq}^2}\right) = k[COOH]_{eq}^2 t + C \quad (1.3.7)$$

The catalysts applied for the polyamides synthesis are bromic acid, hypophosphorus acids and hypophosphite salts and phosphonic acids and according to the type of catalyst used, a psudo-second-order kinetic contribution were reported [26].

Various values have been reported for activation energy of polyamidation in the range of 47-100 kJ mol^{-1}. The activation energy of chain end diffusion of polyamide is less than other type of polycondensation reaction. Therefore, the reaction rate is not affected by viscosity of medium, except that water removal may become more limiting in nonagitated high viscose melt. Another well-established principle is that similar to polyester, reactivity of a functional end group is not affected by the length of parent molecule.

During formation of PA 66, equilibrium constant is not constant as in other cases. Here the thermodynamic of liquid phase plays very important role. The equilibrium constant is not a function of concentration but a function of activity [27]. Therefore, the equilibrium constant can be defined as:

$$K = \frac{k}{k'} = \frac{a_L a_w}{a_A a_c} = \frac{\gamma_L x_L \gamma_w x_w}{\gamma_A x_A \gamma_c x_c} = K_\gamma \frac{x_L x_w}{x_A x_c} = K_\gamma K_{app} \quad (1.3.8)$$

where k, k' are rate constant of forward and backward reactions respectively. a_i, γi, x_i are activity, activity coefficient and molar fraction of each species. The activity coefficient of water can be determined by the following equation:

$$\gamma_w = \exp(6.390 - \frac{2258}{T}) \quad (1.3.9)$$

The apparent equilibrium constant is written as:

$$K_{app} = K_0 \exp(-\frac{\Delta H}{R}(\frac{1}{T} - \frac{1}{T_0})) \quad (1.3.10)$$

It was found [27] that the frequency factor of the Arrhenius expression has the following dependency to molar fraction of volatile water:

$$K_0 = \exp((1 - 0.47\exp(-\frac{\sqrt{x_w}}{0.2}))(8.45 - 4.2x_w) \quad (1.3.11)$$

Therefore, the rate of reversible polycondensation reaction to form PA 66 is expressed:

$$R = k[COOH]([NH_2][COOH] - \frac{[H_2O][CONH]}{K_{app}}) \quad (1.3.12)$$

A value of 95 kJ mol^{-1} for activation energy was reported in literature [28].

1.3.4 Industrial processes of polyamide production

1.3.4.1 Polyamide 6

PA 6 can be produced in batch and continuous operation. The batch operation is nowadays applied for very small production. Continuous processes are used by the major manufacturers of PA 6. Continuous production could be done in a single stage or two stage processes. The so-called VK-tube (Vereinfacht Kontinuierlich = simplified continuous) was developed in Germany. It is a vertical tube operated at atmospheric pressure wherein heating and pre-polymerization take place in the upper part and polymer is formed in the lower section [29]. The middle and the lower part of the VK-tube are built as a tubular reactor. Very even cooling is realized from the middle to the lower part of the

VK-tube to achieve a high degree of conversion which ensures that the density of the melt increases constantly downwards to the outlet. Thus back-mixing is prevented and plug flow is guaranteed. The polymer melt, which is kept very close to the chemical equilibrium, is discharged continuously by a gear pump and sent to the pelletizer. A scheme of the BASF process [30] shows a VK tube feeding a pelletizer followed by a water extraction unit (Figure 1.3.2).

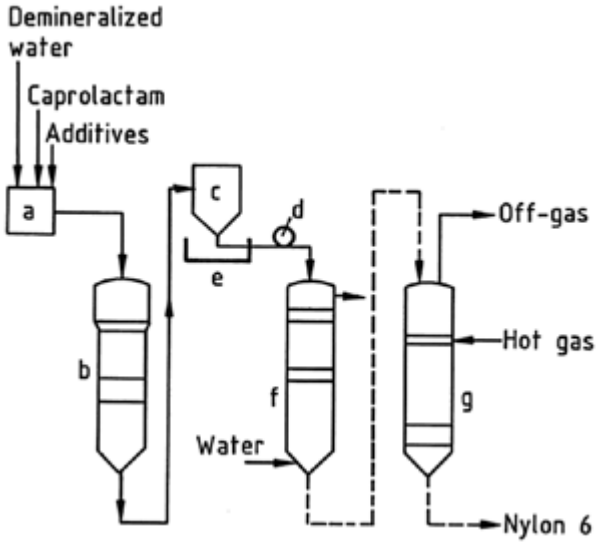

Figure 1.3.2 Flow diagram of PA 6 process of BASF [30].
a) Feed tank; b) VK tube; c) Pourer; d) Pelletizer; e) Water bath; f) Extractor; g)Dryer

A process [31] involving vacuum extraction is shown in Figure 1.3.3. Claim is made that controlling initial conversion to 45% yields a product with less than 2% of cyclic oligomers with vacuum that does not require prolonged heating at less than 665 Pa [32].

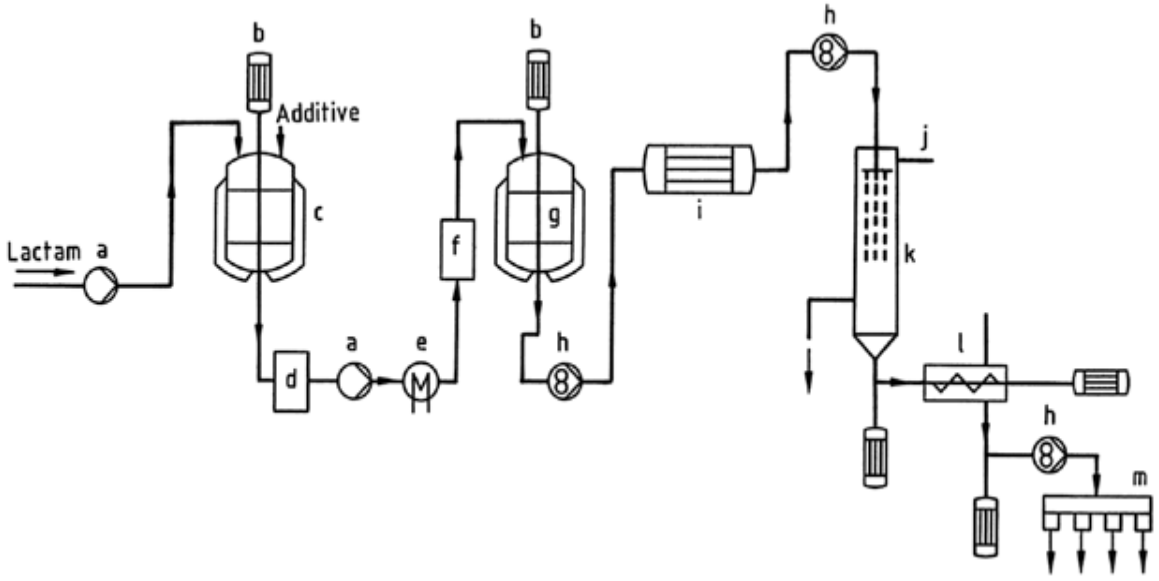

Figure 1.3.3 Flow diagram of PA 6 process of Allied Chemical [31].
a) Pump; b) Stirrer; c) Holding tank; d) Filter; e) Flow meter; f) Pre-heater; g) Hydrolyzer; h) Metering pump; i) Polyaddition reactor; j) Vent; k) Vacuum flasher; l) Finisher; m) Spinning heads.

In technology supplied by Uhde Inventa-Fischer [21], the VK-tube is developed as a continuously stirred tank reactor with a built-in evaporator. This is the zone where the reaction is initialized and the water content, which is important for the achievement of a certain degree of polymerization, is adjusted (Figure 1.3.4).

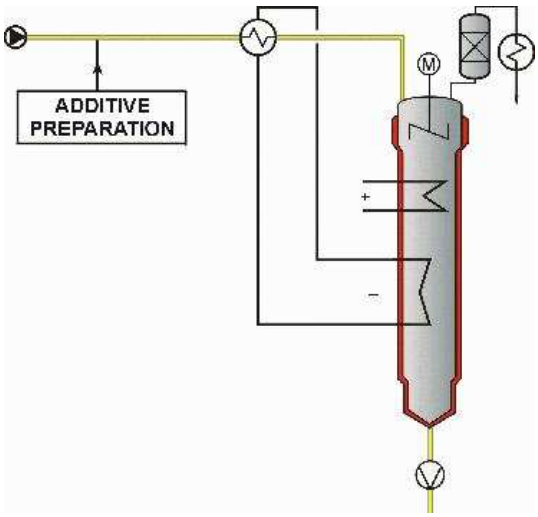

Figure 1.3.4 Simplified flow diagram of one-step PA 6 process of Uhde Inventa-Fisher [21].

Two-stage polymerization consists of a pre-polymerizer along with a VK-tube has been proven, in a wide range of applications, to be reliable, very flexible, and economical as well. The pre-polymerizer, as well as the VK-tube, are equipped in the top section with

tie-heat exchangers providing a large heat transfer area. Prior to the pre-polymerizer, the inlet product is pre-heated in a vessel and excess water is evaporated using the reaction enthalpy which is given off in the VK-tube. The pre-polymerizer is operated under controlled pressure which leads to a high conversion of the caprolactam and to a low residence time in the polymerization process ahead. In order to produce a polymer with a high viscosity, the pressure in the VK-tube can be reduced from atmospheric pressure down to a precisely controlled vacuum. The water content in the polymer is adjusted by the formation of a thin polymer film at the top of the VK-tube. The lower part of the VK-tube is provided with a melt cooling system to achieve a high degree of polymerization. The polymer melt is discharged at a constant rate by an adjustable gear pump. The special design of the pre-polymerizer and the VK-polymerizer internals ensure a high homogeneity of the product. Figure 1.3.5, represents a simple flow diagram of the two stage technology provided by Uhde Inventa-Fisher [21].

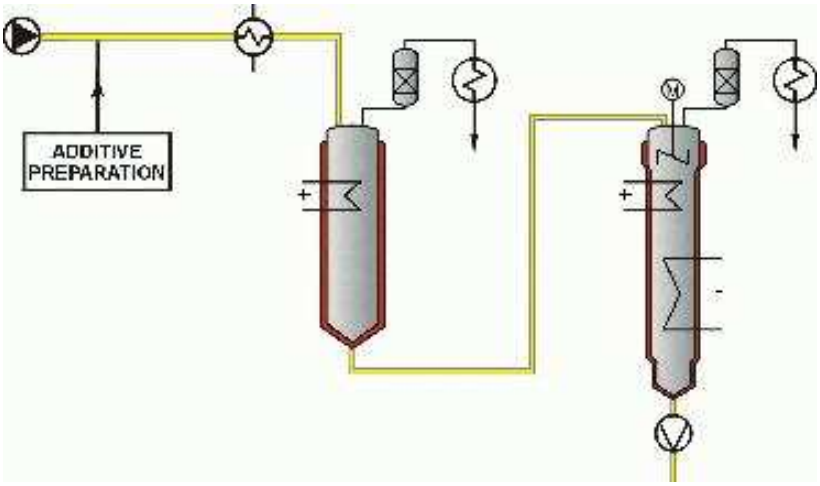

Figure 1.3.5 Simplified flow diagram of two-step PA 6 process of Uhde Inventa Fisher [21].

1.3.4.2 Polyamide 66

Polycondensation of PA 66 and its processing in the molten stage is far more sensitive than in the case of PA 6. This also applies to its raw materials basis. Only a few companies worldwide avail themselves of the PA 66 process or know about the plant technology. PA 66 is either made from AH salt or its two components: adipic acid (ADA) and hexamethylene diamine (HMD).

Preparation of AH salt solution

Mixing of the two components ADA and HMD requires exact dosing, temperature and process control. Even during storage, liquid HMD must be kept within a low temperature range. HMD is a vivid reagent, which is especially sensitive to O_2 and CO_2. The process for preparing an AH salt solution from ADA and HMD is continuous. After mixing the two components together with water, the pH-value is precisely corrected, in order to achieve the end-group equivalence necessary for PA 66 polycondensation. The final concentration of the AH salt solution is about 50% by weight. If the starting material is solid AH salt, it is first dissolved in water and afterwards concentrated continuously by evaporation of a part of the water. From this point, the process is the same as using liquid salt solutions from the beginning, comprising the two components ADA and HMD [21].

Batch polycondensation

The stored salt solution is concentrated under pressure to 65 – 80 % before charging to an autoclave. The essential features are heating to 210°C under autogeneous pressure to reach a pressure of 1.75 MPa, gradually increasing the temperature to about 275°C while releasing steam at a rate which maintains the pressure, reducing the pressure at a rate that avoids cooling and finally holding the batch at atmospheric or reduced pressure to obtain the target molecular mass before extruding the polymer under inert gas pressure. This procedure is designed to assure that there is enough water present to avoid freezing of the batch before the melting point has been reached. Water also minimizes excessive loss of diamine. Stirred autoclaves are used but are normally unnecessary. The extrudate is in a wide ribbon that is quenched with water which is subsequently removed by jet blowers. The ribbon is cut into chips which are blended and packaged [33, 34]. The polycondensation autoclaves ensure a gentle polycondensation due to the size and favourable arrangement of the internal heat exchange surfaces. The capacity of batch polycondensation plants is up to 25 t/d in one line [21].

Continuous polycondensation

The same concerns for control of the rate of removal of water and loss of diamine exist as in batch polymerization, but the situation is complicated by the needs of a continuous

process. Typically, a first stage involves evaporation/reaction with controlled loss of water to form a pre-polymer and minimize loss of diamine (Figure 1.3.6).

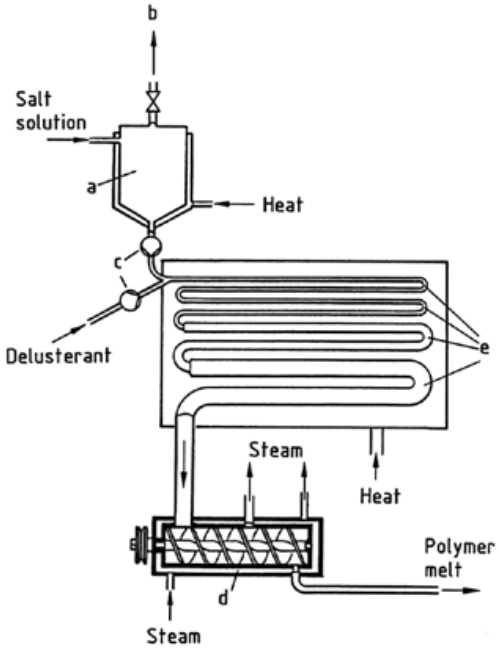

Figure 1.3.6 Continuous polymerizer for PA 66 [7].
a) Evaporator/reactor; b) Vent; c) Pump; d) Finisher; e) Flash tubes

Further reaction occurs in subsequent stages with controlled evaporation in devices known as “separators” and “flashers”. The desired molecular weight and water content are obtained in a “finisher”. However large patent literature exist that claims improvement in each of these devices or combinations thereof for process simplification [7].

1.4 Polycarbonates

1.4.1 Historical aspects

The existence of polycarbonate (PC) resins has been known for nearly a century. However the real beginnings of commercial polycarbonate resin technology occurred on 1950s when two major international chemicals companies, General Electric and Bayer announced their inventions almost simultaneously which based on the reaction of phosgene and salt of bisphenol A (BPA) to produce the bisphenol A polycarbonate [35, 36]. Many alternative formulations were published and patented but none of them could take the place of original PBA.

1.4.2 Polycarbonate synthesis and processes

The chemistry employed to make polycarbonate resins depending on process applied include interfacial, trasesterification and solution-based methods. The methods differ in reaction medium, reaction condition, catalysts and monomeric raw material, but they have one raw material common to all methods: phosgene which provides the source of carbonate carbonyl moiety at some stage of monomer or polymer synthesis. The commercially most important monomer is BPA however many other type of bisphenol have been converted to polycarbonate but very few of them have been used in industry for PC production. Examples include 1,1-bis(4-hydroxyphenyl)cyclohexane (bisphenol C, BPC), 2,2-bis(3,5-dibromo-4-hydroxyphenyl)propane, (tetrabromobisphenol A, TBBPA), and 2,2-bis(3,5-dimethyl-4-hydroxyphenyl)propane, (tetramethylbisphenol A, TMBPA)[7].

1.4.2.1 Melt transesterification

1.4.2.1.1 Synthesis and catalysis

Transesterification is carried out in melt phase. The carbonyl is provided by carbonyl ester. The other monomers are aromatic diols which have the thermal stability at melt condition to survive the polymerization reaction. The transesterifcation leads to the exchange of hydroxylic reagents with diol releasing the monohydroxylic agent from the reactant as a reaction by-product (Scheme1.4.1).

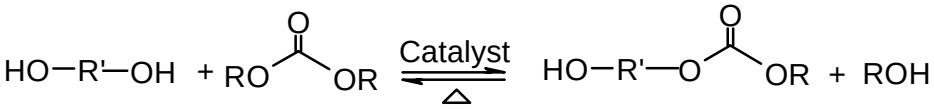

Scheme 1.4.1 Transesterification reaction.

Typical catalysts for melt transesterification are basic catalysts like lithium, sodium or potassium hydroxide. The reaction is also catalyzed by titanium teterabutoxide much like polyesterification reaction [37]. The catalysts can adjust the reaction rate. They react with aromatic diols to form diolates prior to reaction with the carbonate ester.

The resin molecular weight is controlled by manipulating the residence time of the reactant system at high temperature and high vacuum in the melt phase. The chain prolongation can be continued and polymer remains as living polymer but it can be controlled by adding high boiling reactive monofunctional phenols chain as terminator in the initial formulation.

The following reaction is the polycondensation of diphenyl carbonate (DPC) and BPA:

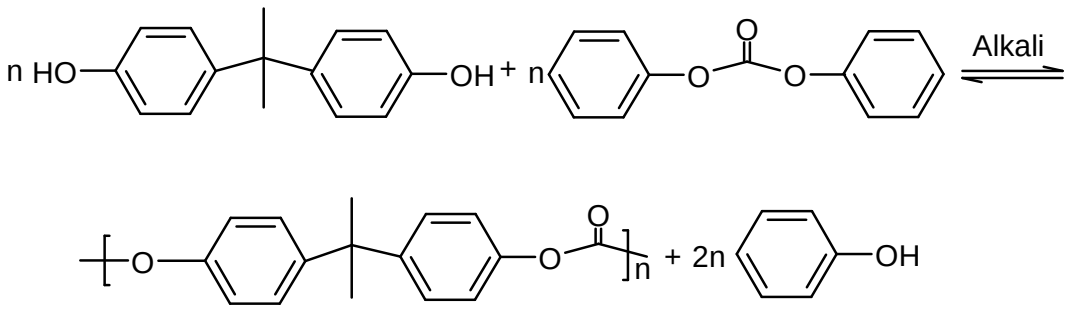

Scheme 1.4.2 Polycondensation of diphenyl carbonate and BPA.

Phosgene provides reaction with a phenolate salt to produce the condensate salt. In spite of intensive research to find alternative routes to diaryl carbonate, this rout still is commercially used.

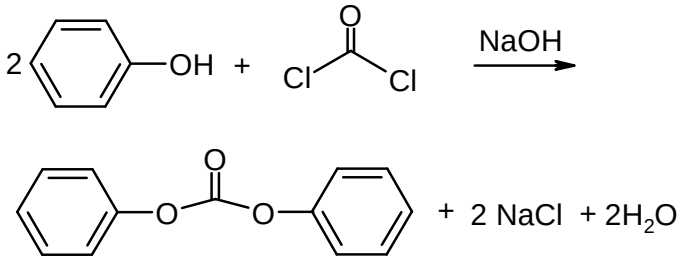

Scheme 1.4.3 Formation of diphenyl carbonate by phosgenation of phenol.

1.4.2.1.2 Kinetic and mass transfer phenomena

The transesterification is a reversible reaction and the reaction by-product (phenol) must be distilled off continuously to facilitate the forward reaction. Phenol is removed from the melt phase by applying a high vacuum. As the polymer molecular weight raises, the melt viscosity increases rapidly and hence, the polymerization becomes mass transfer controlled.

The liquid-vapour equilibrium has to be taken into account at least for two components: phenol and DPC. As phenol is removed from the melt polycondensation reactor, some DPC is also removed from the reactor because DPC exhibits moderate vapour pressure at the reaction temperature. Any loss of DPC during reaction will cause significant variations in the concentration of reactive end groups (phenyl carbonate and hydroxyl group) that, in turn, will make high molecular weight polymers difficult to obtain. Therefore it is important to keep the stoichiometric ratio of the two functional end groups during the course of polycondensation. To do so, an appropriate initial DPC/BPA molar ratio needs

to be employed to compensate for the loss of DPC in a reflux column. The concentrations of phenol and DPC in both the vapour phase and the liquid phase need to be calculated. The following vapour pressure equations are reported in literature [38] for phenol and DPC:

$$\ln P_p^0 = 7.13 - \frac{1.52\times10^3}{T - 98.58} \tag{1.4.1}$$

$$\ln P_{DPC}^0 = (-\frac{1.48\times10^4}{1.987})\frac{1}{T} + 19.55 \tag{1.4.2}$$

Since the transesterifcation reaction occurs to some extent even without any catalyst, the rate constant of polycondensation could be express in the following form:

$$k = k_u + k_c[Cat] \tag{1.4.3}$$

where [Cat] is the catalyst concentration k_u represents the rate constant for uncatalyzed transesterification and k_c represents the rate constant for the catalyzed transesterification. The forward and reverse reaction rates for the uncatalyzed transesterification are reported [38] to be:

$$k_u = (3.108\times10^7)\exp(-\frac{105712}{RT}) \quad [\text{l mol}^{-1}\ \text{min}^{-1}] \tag{1.4.4}$$

$$k_u^{'} = (2.028\times10^7)\exp(-\frac{188225}{RT}) \quad [\text{l mol}^{-1}\ \text{min}^{-1}] \tag{1.4.5}$$

and for the catalyzed reactions:

$$k_c = (9.62\times10^8)\exp(-\frac{58102}{RT}) \quad [\text{l}^2\ \text{mol}^{-2}\ \text{min}^{-1}] \tag{1.4.6}$$

$$k_c^{'} = (8.04\times10^7)\exp(-\frac{50536}{RT}) \quad [\text{l}^2\ \text{mol}^{-2}\ \text{min}^{-1}] \tag{1.4.7}$$

1.4.2.1.3 Transesterification process

Transesterifiction process usually involves preliminary melting of precursor diaryl carbonates and BPA. The molten reagent, along with carefully metered catalysts and chain terminators, are fed to a mixer under reduced pressure. The reaction is usually catalyzed with very small amounts of alkali at 190 – 320°C and reduced pressure (down to ca. 0.1 kPa). The temperature is initially low and the pressure is slightly reduced (e.g., 200°C at 20 kPa). During the course of reaction the temperature is raised and the pressure reduced. Mass transfer and hence the speed with which phenol can be removed are reduced with increasing viscosity. Reactors are needed that provide a high rate of surface renewal.

These may be wiped-film evaporators, single or twins extruders, reactor of rotating disk type [39, 40].

1.4.2.2 Polycarbonate synthesis in solution

Solution PC synthesis was the first process pursued commercially. In this synthetic method, all the reactants are soluble in the reaction matrix. The differences with transesterification is application of organic solvents like methylene chloride and organic base such as pyridine which is sufficiently basic to succeed in dissolving the aromatic diol to produce reactive pyridinium salts as reaction by-product [41, 42].

1.4.2.2.1 Solution polycondensation process

Commercial solution processes in PC production are batch processes [41, 42]. The reactants are placed in a stirred tank reactor. Typically, methylene chloride, pyridine, BPA and chain terminator are added to the reaction vessel. Phosgen is bubbled into the stirred mixture. At the conclusion of the reaction, the pyridinium hydrochloride must be removed from the reaction solution prior to polymer isolation. The removal of the pyridinium hydrochloride is usually accomplished by multiple aqueous acid and water washes. The major disadvantages of the solution process are in the difficulty in removing all traces of pyridine and pyridinium hydrochloride from the polymer solution and in the cost of recovery/purification of the pyridine.

1.4.2.3 Interfacial polycondensation

1.4.2.3.1 Synthetic aspects

The interfacial synthesis involves reaction at the boundary between two immiscible solvents which are protic and aprotic respectively. Some reactant dissolved in the aprotic organic solvent layer and some in protic aqueous layer. During the reaction, the monomers react in the interface with the polymerizing resin growing into and remaining dissolved in aprotic phase. The typical solvents used in industry are methylene chloride and aqueous caustic. The caustic dissolves aromatic diol and the phenolic chain terminators. The methylene chloride layer dissolves the carbonate source which invariably is phosgene [43, 44]. The overall reaction scheme is shown in scheme 1.4.4.

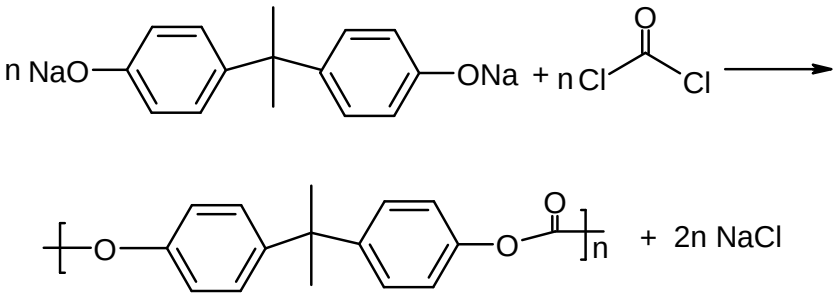

Scheme 1.4.4 Synthesis of PC via interfacial rout of reaction

The synthesis proceeds in three steps: Phosgenation of BPA, formation of oligomeric carbonates with phenolic and chloroformate end groups; which will follow by polycondensation of oligomers. The phosgenation is started by dispersion of two phases. In phosgenation step, the concentration of BPA is very important. Since at high concentration a fourth solid phase might be present.

In all interfacial procedures vigorous agitation is necessary to promote practical reaction rate. The reaction is exothermic and provisions must be made to control reflux of the volatile methylene chloride. The concentration above 26 % of resins in methylene chloride can results in metastable solutions whose coagulation or high viscosities can cause problems in production facilities.

In polycondensation step, a monofunctional phenol is added as chain terminator to control the molecular weight of the final polycarbonate. At this step reaction rate decreases. The final polycondensation stages are catalyzed by tertiary amines.

1.4.2.3.2 Kinetic and mass transfer phenomena

Phosgenation is generally mass transfer limited and its rate depends on mixing as well as on pH and the volume ratio of the organic and aqueous phases. Although the polycondensation reaction of end groups is slower, both rates still show the same dependencies due to the interfacial nature of the reaction. The reaction rate could be influenced by following phenomena:

- Dispersion of two phases. Rates always depend on mixing. Effective kinetic rate constant can be formulated as a function of energy dissipation or interfacial area.
- Type of emulsion (oil in water (o/w) as well as water in oil (w/o)).
- The partition of phenols between the phases and its pH dependence. Kosky et al. [45] studied the reaction hydrolysis taking into account the different phases and the

partitioning of BPA between them. Monofunctional phenols with better solubility in the organic phase show a better efficiency as chain terminators.

- Mass transfer to and across the boundaries.

1.4.2.3.3 Interfacial polycondensation processes

Interfacial polymerization developed first at Farbenfabriken Bayer AG [46], is employed by most polycarbonate manufactures by three techniques: batch, semi batch and continuous process.

Batch interfacial process

The reactants and reaction media are charged into a single vessel where the polymerization takes place. Phosgene is bubbled into rapidly stirred vessel at a rate which is tailored to the parameters of the system insuring maximum phosgene uptake. pH value decreases during reaction therefore additional caustic is added as reaction progress. At the end of reaction the aqueous solution is separated from PC/methylene chloride solution. The polymer solution is purified and isolated.

The batch process has some drawbacks. Since chain terminators are added in the initial charge diaryl carbonates, low molecular weight oligomers are produced which leads to broadening of molecular weight distribution. Furthermore, the batch processes are also plagued with the problems of batch to batch variability which requires very excellent process controls.

Semi batch interfacial process

Semi batch operations use a sequence of stirred tank reactors to promote the polycarbonate synthesis. Commercial systems can include two to four reactors[47, 48]. Three series reactors are common process configuration. These three reactors configurations allow sequential programming of pH, addition of chain terminators and phase transfer agents. The first reactor is charged similarly to the single batch interfacial reactor. Methylene chloride, caustic and BPA chloroformates are added and subsequently treated by phosgene gas. In general the whole reaction mixture is transferred to second reactor when pH of around 10 is reached. There, a phase transfer agent, ($[R_4N^+]Cl^-$) is added and polymer molecular weight increases.

The polydispersity index of semi batch process is similar to that for batch process. If chain terminating agent is added in the second reactor after production of BPA oligomers, the level of low molecular weight oligomers are reduced relative to batch process. However, control system must be precise in order to avoid product variability.

Continuous interfacial synthesis

Continuous polycarbonate processes are only variants of the semi batch process [49]. Here the functions of the first reactor are preformed by continuous mixer where phosgenation takes place. The reactants are fed into the system with all reactants concentrations carefully set and rate of addition in precisely maintained. The mixture is sent to another stirred tank reactor in which the oligomerization takes place. The produced heat is removed by cooling jacket. After reaching a certain degree of polymerization, the product which is mixed with fresh phenol is conveyed to the tubular reactors where the main polycondensation will occur. Figure 1.4.1 shows a simplified flow diagram of this process. The polydispersity index is in the same range as in batch process. The products have consistent properties.

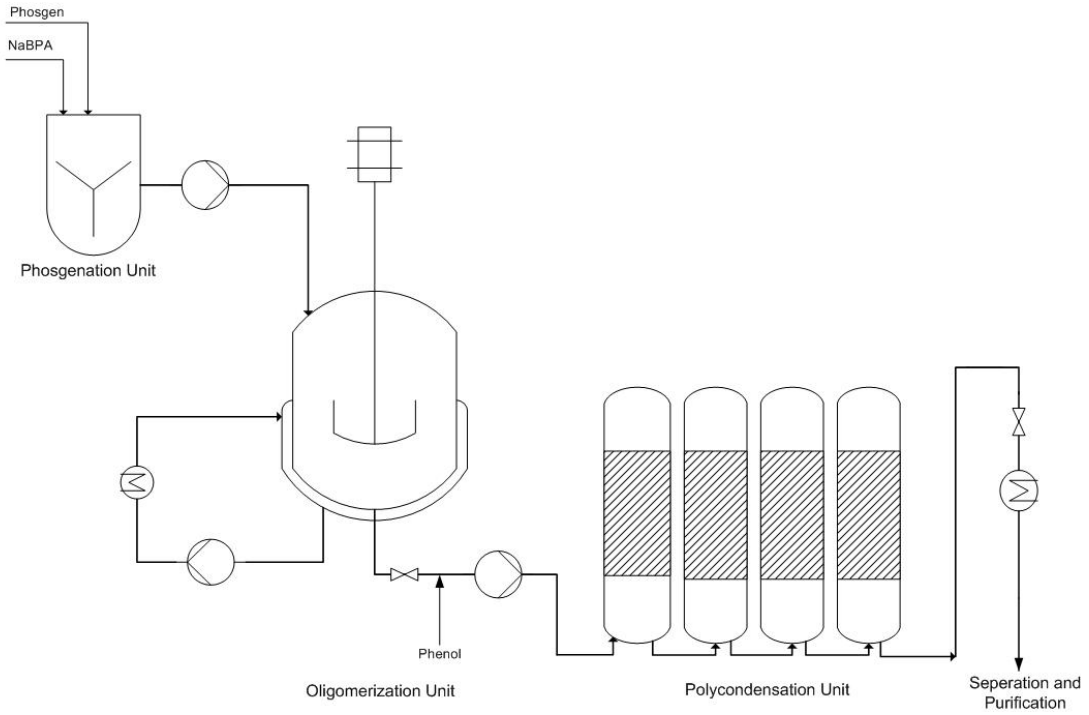

Figure 1.4.1 Simplified flow diagram of continuously operated PC synthesis.

1.5 Objectives of project

Antimony compounds are still the main catalyst of choice in PET synthesis in production plants. This is due to the high selectivity of this compound in the course of polycondensation reaction. However, because of the main disadvantage of this catalyst as a heavy metal, intensive attempts have been invested to replace it by a more environmentally friendly catalyst.

Despite of releasing huge number of patents claiming titanium compounds being the best choice of replacement of antimony, but the fundamental aspects and mechanism of catalysis in PET synthesis is poorly understood. The reason lies in the nature of reaction (reversible and parallel side reactions) and in the reaction condition (high temperature causing side reaction, variation of pressure from 3 bar to 0.1 mbar, high viscosity).

The aim of this project was to understand fundamental aspect of titanium-based catalyst PET synthesis by screening of different commercially available titanium-based compounds. Furthermore, optimization of differential scanning calorimetry and thermogravimetric analysis as fast screening technique was in major interest. Another objective was developing a comprehensive mathematical model to be able to simulate kinetic, molecular weight, concentration of side products and molecular weight distribution. A set of reliable experimental data should be achieved by developing a lab scale stirred tank reactor equipped with a very precise online data acquisition.

1.6 References

[1] J. Berzelius, *Ann.*, **26**, (1847)

[2] A. V. Laurenco, *Ann. Chem. Phys*., **67**, 293 (1863)

[3] K. Kraut, Justus Liebigs *Ann. Chem*., **150**, 1(1869)

[4] W.H. Carothers, *J. Am. Chem. Soc*., **51**, 2548 (1929)

[5] J. R. Whinfield, J. T. Dickson, Br. Pat. **578 079** (1941)

[6] U. K. Thiele, *POLYESTER BOTTLE RESINS, Production, Processing, Properties and Recycling*, Heidelberg Business Media GmbH, 2007, ISBN 978-3-9807497-4-9

[7] Ullmann Encyclopedia of Industrial Chemistry, 4th Edition, John Wiley & Sons (2000)

[8] J. Scheirs, T. E. Long, *Modern Polyesters: Chemistry and Technology of Polyesters and Copolyesters*, John Wiley & Sons (2003)

[9] P. J. Flory, *J. Am. Chem. Soc.*, **58**, 1877 (1936)

[10] P. J. Flory, *Principles of Polymer Chemistry*, Cornell University Press, Ithaca, New York (1953)

[11] H. Zimmermann, D. D. Chu, *Faserforschung Textiltechnik*, **24**, 445 (1973)

[12] H. Zimmermann, *Faserforschung Textiltechnik*, **13**, 481 (1962)

[13] J.-W. Chen, L.-W. Chen, *J. Polym. Sci., Polym.Chem. Ed.*, **36**, 3073 (1998)

[14] V. Hornof, *J. Macromol. Sci. Chem.*, **A15**, 503 (1981)

[15] E. P. Goodings, *Soc. Chem. Ind. (London)*, Monograph No. **13**, 211 (1961)

[16] M. Edge, R. Wiles, N. S. Allen, W. A. McDonald, S. V. Mortlock, *Polymer*., **36**, 227 (1995)

[17] U. K. Thiele, *Inter. J. Polym. Mat.*, **50**, 387 (2001)

[18] U. K. Thiele, *The European PET Conference***,** Barcelona, October 2006

[19] WWW.Zimmer-AG.de

[20] K. C. Cannon, S.R. Seshadri, R. R. Dirks, EP Pat. **0 970 983 A2** (2000)

[21] www.Uhde-Inventa-fischer.com

[22] www.Aquafileng.com

[23] S. Gabriel, T. Maass. R., **32**, 1266 (1889)

[24] H. E. Stepniczka, *Ind. Eng. Chem. Prod. Res. Develop*., **12**, 1 (1973)

[25] F. Charaf**,** *Polyamide 2007 World Congress*, Zurich, June 2007

[26] H. F. Mark, N. M. Bikales, C. G. Overberger, G. Menges, *Encyclopaedia of Polymer Science and Engineering*, 2nd Edition, volume 11, John Wiley & Sons (1988)

[27] M. Steppan, *J. Appl. Polym. Sci*., **33**, 2333 (1987)

[28] M. A. Schaffer, K. B. Mcauley, M. F Cunningham, E. K. Marchildon, *Ind. Eng. Chem. Res*., **42**, 2948 (2003)

[29] H. Jacobs, C. Schweigman, *Fifth European/Second International Symposium on Chemical Reaction Engineering*, Amsterdam, 1972

[30] G. S. Kirshenbaum, *High Performance Polymers: Their Origin and Development*, Elsevier (1986)

[31] I. C. Twilley, G. J. Coll, Jr., D. W. H. Roth, (Allied Chemical), US Pat. **3 578 640** (1968)

[32] I. C. Twilley, D. W. H. Roth, R. A. Lofquis, (Allied Chemical), CA Pat. **823 290** (1967)

[33] G. De, W. Graves, (Du Pont), US Pat. **2 289 774** (1939)

[34] W. G. Johnson, (Du Pont), US Pat. **3 491 177**, (1967)

[35] H. Schnell, L. Bottenbruch, H. Krimm, (Bayer AG), Belg. Pat. **532 543** (1954)

[36] D.W. Fox, (General Electric Company), Australian Pat. **221 192** (1955)

[37] G. W. Parshall, S. D. Ittel, *Homogeneous Catalysis*, 2nd Edition, John Wiley & Sons, (1992)

[38] B. G. Woo, K. Y. Choi, W. H. Song, S. H. Lee, *J. Appl. Polym. Sci.,* **80**, 1253 (2001)

[39] U. Curtius, L. Bottenbruch, H. Schnell, (Bayer AG), US Pat. **3442 854** (1969)

[40] H. Yamana, T. Kuni, H. Nakai, (Mitsubbishi Gas Chemical Co.), US Pat. **3 888 826** (1975)

[41] K. Dik, G. Ham, J. Gross, (Dow Chemical Co.), US Pat. **4378 454** (1983)

[42] J. H. Vestergaard, (General Electric Co.), US Pat. **3 989 672** (1976)

[43] M. Rabinovitz, Y. Cohen, M. Halpern, *Angew. Chem. Int. Ed. Engl*., **25**, 690 (1986)

[44] D. Landini, A. Maia, A. Rampoldi, *J. Org. Chem*., **51**, 5474 (1986)

[45] P. K. Kosky, J. M. Silva, *Ind. Eng. Chem. Res*., **30**, 468 (1991)

[46] W. Alewelt, G. Jacobs, D. Margotte, E. Lax (Bayer AG), US Pat. **4 127 561** (1978)

[47] T. Megumi, S. Kondo, (Mitsubishi Gas Chemical Co.), US Pat. **4 097 457** (1978)

[48] H. Koda, T. Megumi, H. Yoshizahi, (Mitsubishi Gas Chemical Co.), US Pat. **4 413 103** (1983)

[49] H. Vernaleken, O. Court, K. Weirauch, (Bayer AG), US Pat. **3 674740** (1972)

[50] P. Horn, H. Kuerten, (BASF SE), US Pat. **3 945969** (1978)

Chapter 2: Screening of Different Titanium (IV) Catalysts in Polyethylene Terephthalate Synthesis

Abstract

Polycondensation of bis (hydroxyethylene) terephthalate and its oligomers to polyethylene terephthalate catalyzed by different chelated and non-chelated titanium (IV) catalysts in lab scale stirred tank reactor and micro scale crucible of differential scanning calorimetry was investigated. Different titanium compounds showed different activity and selectivity in polyethylene terephthalate synthesis. The nature of ligand of catalyst has a significant effect on catalyst activity and selectivity. In general, non-chelated organic titanium (IV) derivatives were more active and less selective than corresponding chelated compounds. In chelated titanium compounds, the activity was affected by nature of multidentate and monodentate ligands simultaneously. In solid state polycondensation reaction, the same results were achieved with respect to effect of catalyst type on catalytic activity. Polycondensation progress is characterized by an initial induction period which depends on the type of catalyst. The original used titanium compounds seem to be catalyst precursors and are probably activated by ligand exchange reaction.

2.1 Introduction

In production of polyethylene terephthalate (PET), the presence of catalyst is essential. Although large number of papers and reviews published on kinetic and catalytic aspects of PET formation, the mechanism of catalysis is not fully understood [1]. Thus, testing of a new catalyst is by far empirical by trial and error process. Despite of the high efficiency of antimony catalysts, drawbacks to the use of these compounds are the formation of side-products (such as acetaldehyde) and catalyst decomposition depositing elemental antimony, which imparts an undesirable gray color to the polymer. Intensive efforts have been invested in industries in the search of other stable efficient and more environmentally friendly antimony-free catalysts, such as those based on titanium [2, 3]. A huge numbers of patents had been appeared but few companies are producing PET based on antimony-free catalysts. Table 2.1 names the companies which produce PET with titanium catalysts. However, these PET products are mostly used in fiber application.

Table 2.1 Companies producing PET based on titanium catalysts [3]

Company	Catalyst name	Catalyst type
Mitsui	MP Catalysts	Ti/Mg
Mitsubishi Chemicals	NC2 Catalysts	Ti/Mg
Teijin	Purity ®	Ti-based
Acordis	C94	Ti/Si
Lorgi-Zimmer	Ecocat B & C ®	Ti/P
Invista	Special Products	Ti-based
UIF	NN	Ti-based
Sachtleben Chemie	Hombifast	Alkali-titanate

All published mechanism for metal catalyzed PET synthesis can be categorized in two classes. In first category, a nucleophilic attack of hydroxyl end group to the carbon of carbonyl group is assumed to be activated by formation of metal alkoxide following with formation of 7 or 5 member ring chelating complex [4-6] (scheme 2.1).

In second category, the activation is supposed to occur by complexation of metal catalyst with carbonyl or ester oxygen [7-12] (scheme 2.2).

Furthermore, the reported results show contradiction in the catalytic behavior of titanium-based catalysts. Weingart et al.[5] reported that the activity of titanium is independent of its ligand nature. However, Laricheva et al.[13] found some differences in activity with respect

to the nature of attached ligands. Otton et al. [14, 15] showed that the activity of titanium catalysts is affected by the type of reaction medium and the kinetic of catalyzed reaction depends on the reaction medium. Furthermore, possible deactivation of titanium catalyst during polycondensation is an open question which is not fully understood, since it was reported that the polymeric form of titanium compounds as product of hydrolysis is still catalytically active [13].

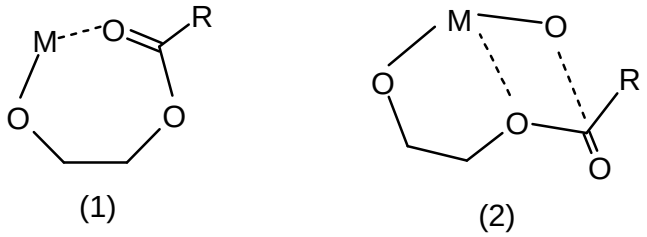

Scheme 2.1 Formation of 7 member ring (1) and 5 member ring (2) in activation step of metal catalyzed polycondensation.

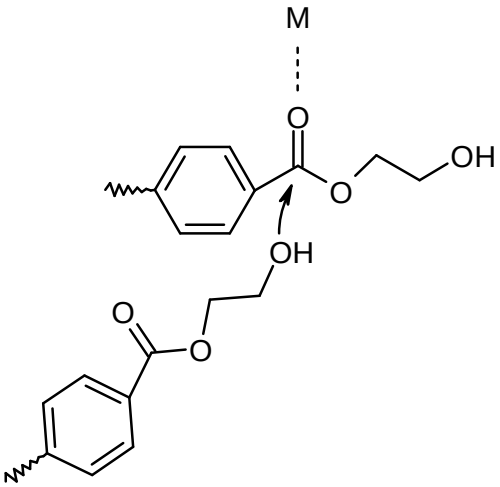

Scheme 2.2 Complexation of metal to the carbonyl oxygen to activate nucleophilic attack for chain prolongation.

The aim of this chapter is to study catalysis aspects of different titanium-based catalyzed polycondensation reaction and express a reaction progress rout that can explain best the experimental results by screening of different patented catalysts.

2.2 Experimental part

2.2.1 Chemicals

Bis (hydroxyethylene) terephthalate (BHET) (> 99%) was from Aldrich, ethylene glycol (EG) (>99%) was from Merck, titanium (IV) tetrabutoxid (Cat 1) (>98%) and chlorotriisopropoxy titanium (IV) (Cat 3) (> 98%) were from Fulka, tetrakis

(diethylamido) titanium (IV) (Cat 2) (>99.999%), titanium (IV) tert-butoxide (Cat 4) (purum), titanium (IV) bis (ammonium lactate) dihydroxide (Cat 5) (50 wt% in water), diisopropoxytitanium bis (acetylacetonate) (Cat 6) (75 wt% in isopropanol) and titanium (IV) (triethanolaminato) isopropoxide (Cat 7) (80 wt% in isopropanol) were from Aldrich. PET oligomer with chain length of 4-5 units was from Equipolymers GmbH. Antimony triacetate (> 98%) was from Uhde Inventa-Fischer and was mixed with EG. Model molecule ethylene glycol monobenzoat (EGMB) was synthesised by method of Santacesaria et al. [4]. All the applied chemicals were used without further purification.

2.2.2 Preparation of sample for catalyst screening

The preliminary studies of different sample preparation methods showed that the most reliable and reproducible method of sample preparation is the following: 1 µl of Cat 1 was added to the appropriate amount of molten BHET (5-25 g) at 110°C and stirred at this temperature for 15 min. The product was cooled down and ground to fine powder and used for catalysts screening. The expressed catalysts concentration in mol ppm is based on mol of titanium atom to mol of BHET.

2.2.3 Catalyst fast screening

Differential scanning calorimetry instrument, DSC 6, from Perkin Elmer was used as catalysts fast screening method. Aluminium crucible was filled with about 10 mg of sample and inserted in the DSC oven. Nitrogen gas (50 ml min^{-1}) was purging over the sample to carry away the by-product as it formed.

2.2.4 Reuse of catalyst after pre-polycondensation

The desired amount of catalyst was added to molten BHET in a glass vessel and mixed for 10 min before starting reaction by applying vacuum at 260°C. The pre-polycondensation was running for 1 and 4 h and was stopped by breaking vacuum with nitrogen flow. The polymeric product was depolymerised by cooking in EG under reflux. After complete depolymerization, the product was cooled down to room temperature and EG was removed by vacuum at 50°C. Then fresh BHET was added to the obtained powder to adjust catalyst concentration, mixed and introduced to DSC crucible for screening.

2.2.5 Polycondensation in lab scale stirred tank reactor

200 g of PET oligomer was filled into a 200 ml aluminium reactor equipped by a helical stirrer. The oligomers were molten by heating the reactor under nitrogen flow. Catalyst was added to the molten oligomers at 260°C then vacuum was applied which reached to the value of 1 mbar after 20 min. Stirring rate was 200 rpm. After 4 h of reaction time, polycondensation was stopped by purging with nitrogen. PET melt was removed from reactor and cooled down to ambient temperature under nitrogen flow.

2.2.6 Solid state polycondensation

The reaction apparatus for solid state polycondensation involved a series of 3 reaction tubes, which were connected to a vacuum line to reach a vacuum of 1 mbar and immersed in a salt bath having constant temperature with a precision of ±2 °C. The SSP process of PET included three stages, i.e., drying, polycondensation, and cooling. The drying process was carried out at 120°C for 24 h under nitrogen flow, the polycondensation process was performed at 230°C for different times (1, 2, 4 and 6 h) and finally cooling to ambient temperature was done under nitrogen flow.

The drying process reduced the concentration of water in PET resin since presence of water in PET particles usually leads to a decrease in molecular weight because of hydrolysis of polymer. Careful removal of water in pre-polymer particles is very important. The pre-polymer particles were classified into three different fractions with average particle sizes of 700, 400 and 200 µm by grinding and sieving of PET product from melt phase polycondensation.

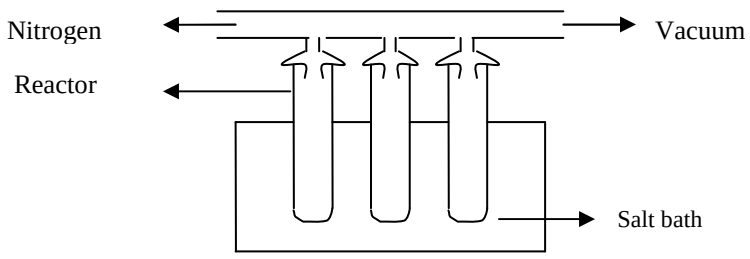

Figure 2.1 Scheme of solid state apparatus.

2.2.7 Thermogravimetric analysis

Thermogravimetric analysis setup, TGA-209 F3 Tarsus, from Netzsch was applied for studying thermal decomposition of polymer and catalysts. 10 mg of sample was filled into the aluminium crucible with 80 µl volume and located on the sample holder of TGA and heated up till desired temperature. Nitrogen was used as purging gas with purging rate of 20 ml min^{-1}. The oven of the TGA was first evacuated and then refilled with nitrogen before each run.

2.2.8 Infrared spectroscopy

Infrared spectroscopic (IR) investigations were done on an attenuated total reflection Fourier transform (ATR/FTIR) spectrometer of the type Spectrum One from Mettler Toledo. Mixtures of catalysts and monomer (1 to 2 molar ratio) were prepared by heating the mixtures in DSC crucible for a certain time under nitrogen flow. The product was then cooled down to ambient temperature under nitrogen, taken from crucible and mounted on sample holder of IR spectrometer.

2.3 Differential scanning calorimetry

2.3.1 Principle of data acquisition

DSC belongs to the family of thermal analysis methods. Thermodynamic data (heat capacity, phase transition, enthalpy) and kinetic data can be determined by methods of thermal analysis. The advantage of thermal analysis is the easy handling and the output of valuable information of small samples. DSC is a technique for measuring the energy necessary to establish a nearly zero temperature difference between a substance and an inert reference material, as the two specimens are subjected to identical temperature regimes in an environment heated or cooled at a controlled rate. There are two types of DSC systems in common use.

1- Heat flux DSC

In heat flux DSC, the sample and reference are connected by a low resistance heat flow path (a metal disc) symmetrically. The assembly is enclosed in a single furnace. Enthalpy or heat capacity changes in the sample cause a difference in its temperature relative to the reference; the resulting heat flow is small compared with that in differential thermal analysis because the sample and reference are in good thermal contact.

2- Power compensation DSC

In this system the temperatures of the sample and reference are controlled independently using separate, identical furnaces. The temperatures of the sample and reference are made identical by varying the power input to the two furnaces; the energy required to do this is a measure of the enthalpy or heat capacity change in the sample relative to the reference.

In DSC, when a change of heat capacity, phase transition or reaction occurs, the equilibrium between sample and reference is disturbed. The sample temperature is higher (exothermic event) or lower (endothermic event) than the reference. This temperature difference is detected and heat flow is calculated.

$$\Delta \dot{Q} = -K\ \Delta T \tag{2.1}$$

$\Delta \dot{Q}$ is the heat flow and the constant K has to be determined by calibration. The difference of heat flowing to the sample and reference is given by

$$\Delta \dot{Q} = (\dot{Q}_S - \dot{Q}_R) + (C_{p,MS} - C_{p,MR})\,\beta \tag{2.2}$$

$\dot{Q}_S$ is the heat flow to the sample, $\dot{Q}_R$ is the heat flow to the reference, $C_{p,MS}$ is heat capacity of the sample measuring system, $C_{p,MR}$ is heat capacity of the reference measuring system and $\beta = dT_s/dt$ is heating rate. The heat flow in the sample with a chemical reaction is given by,

$$\dot{Q}_S = C_{p,s}\frac{dT_s}{dt} + \dot{Q}_{chem} \tag{2.3}$$

where $C_{p,s}$ is heat capacity of the sample and $\dot{Q}_{chem}$ is heat flow by chemical reaction which is given by following equation,

$$\dot{Q}_{chem} = R\ V\ (-\Delta H_R) \tag{2.4}$$

R is reaction rate; V is reaction volume and ΔH_R is molar reaction enthalpy. For the inert reference,

$$\dot{Q}_R = C_{p,R}\frac{dT_R}{dt} = C_{p,R}\,\beta \tag{2.5}$$

where $C_{p,R}$ is heat capacity of the reference.

Since the measuring systems of sample and reference were made of same material with the same heat capacity, therefore the second part of equation (2.2) is negligible.

$$\Delta \dot{Q} = (\dot{Q}_S - \dot{Q}_R) = C_{p,s} \frac{dT_s}{dt} + \dot{Q}_{chem} - C_{p,R}\, \beta \tag{2.6}$$

During reaction dT_s/dt is not identical with β. This unknown parameter must be eliminated. It is considered that there is a heat flow resistance R_{MS} between the sample measuring system at temperature T_{MS} and the sample at temperature T_S,

$$\Delta \dot{Q} = \frac{T_{MS} - T_S}{R_{MS}} \tag{2.7}$$

The term dT_s/dt can be eliminated by differentiation the previous equation with time. With approximation of $dT_{MS}/dt = \beta$,

$$\Delta \dot{Q} = \dot{Q}_{chem} + (C_{p,s} - C_{p,R})\, \beta - C_{p,s}\, R_{MS} \frac{d\Delta \dot{Q}}{dt} \tag{2.8}$$

$$\Delta \dot{Q} = \dot{Q}_{chem} + \Delta C_p\, \beta - \tau \frac{d\Delta \dot{Q}}{dt} \tag{2.9}$$

The detected signal contains three contributions. First, there is the heat flow from reaction $\dot{Q}_{chem}$. Second, there is a term which is dependent on the difference of the heat capacities of the sample and the reference. The third contribution is influenced by the so called time constant $\tau = C_{p,s}\, R_{MS}$ of the measuring system and the slope of the measured signal. The third term reflects the time lag between the chemical heat flow and the reaction of the compensation heater.

2.3.2 Principle of catalysts screening

The DSC thermogram of polycondensation reaction is shown in figure 2.2. The first endothermic peak is due to the melting of monomer, the second peak represents evaporation of by-product EG. Since evaporation of EG is assumed to be fast compare to polycondensation, this peak represents polycondensation reaction of BHET. The absence of mass transfer limitation at present condition was drawn by running polycondensation reactions at different gas purging rate and different amounts of reaction mass. The bell shape of the reaction peak is due to the fact that rate of polycondensation is a function of temperature and concentration of functional end groups and it increases with increasing temperature and decreases with decreasing of concentration of functional groups. At lower temperatures the effect of temperature is dominant while at higher temperatures the effect

of concentration of functional end groups is dominant. At a certain temperature these two effects compensate each other and reaction has maximum rate. According to Wolf et al.[16] and Reichert et al. [17] the temperature at which maximum reaction rate occurs, was taken to define an activity index. The activity index (AI) is defined as $1/T_{max}$ with an error of 0.5%. The faster the reaction, the larger the value of AI, the more active is the catalyst.

In DSC thermogram of PET synthesis catalyzed by titanium compounds, an endothermic peak at about 300°C can be observed at catalyst concentration of 150 mol ppm. The onset temperature of this peak depends on the type and concentration of titanium catalyst. Furthermore the color of the polymeric product at endset temperature of this peak is much darker than that of the product at onset temperature. Probably, this peak represents a thermal degradation of polymer formed. The onset temperature (T_{deg}) of degradation peak was used as degradation index.

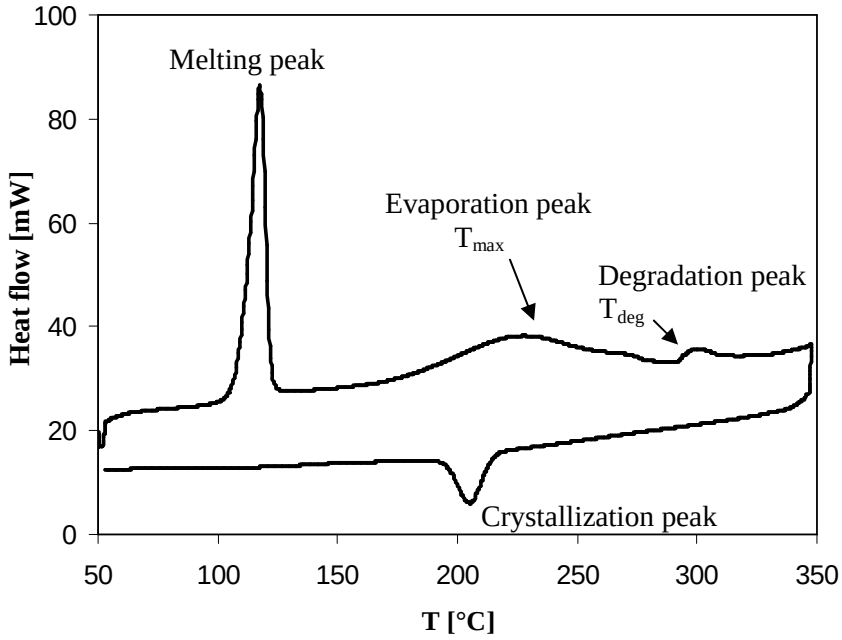

Figure 2.2 DSC thermogram of BHET polycondensation, [Cat 1]: 150 mol ppm, 10 K/min.

(a) (b)

Figure 2.3 The color of polymeric product (a) before and (b) after appearance of degradation peak.

2.4 Results and discussion

Figure 2.4, represents the activity index of Cat 1 and antimony triacetate with respect to the catalysts concentration. It was observed that considerable activity of titanium achieved by only application of 10 mol ppm of catalyst; however the first maximum of reaction peak in case of antimony needs minimum 500 mol ppm of catalyst.

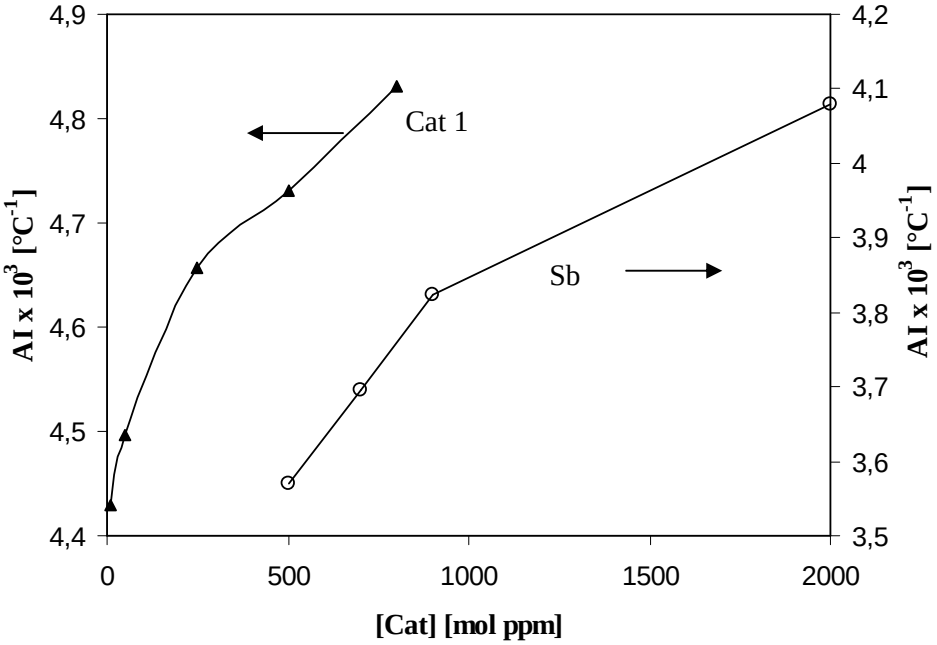

Figure 2.4 Dependency of activity index on concentration of catalysts in polycondensation of BHET.

2.4.1 Effect of sample preparation method on activity of titanium (IV) catalyst

It was found that preparation of reaction mixture in presence of different solvents has an effect on catalytic activity of Cat 1. Mixing of reaction mixture in presence of butanol shows lower activity than in presence of EG, however adding of catalyst to molten BHET in absence of any solvent has highest activity (Table 2.2).

Table 2.2 Effect of sample preparation on activity of catalyst

Sample	AI [°C^{-1}]
Mixed in Bu	4.32±0.5%
Mixed in EG	4.70±0.5%
Mixed in molten BHET	4.72±0.5%

2.4.2 Effect of titanium (IV) ligands on catalytic activity

The influence of ligands attached to titanium on catalytic activity was studied for two categories of the titanium compounds. First category (scheme 2.3) involves non-chelated titanium (IV) derivatives with general name of tetraalkyl titanate, consist of monodentate ligands of alkyl chains with differences in structure of ligand and electronegativity of atoms bonded to titanium.

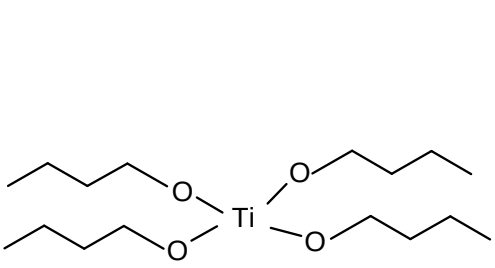

Titanium(IV) tetrabutoxide
(Cat 1)

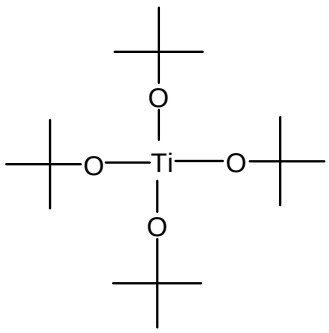

Titanium(IV) tertbutoxide
(Cat 2)

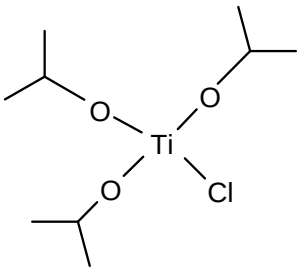

Chloroisopropoxy titanium (IV)
(Cat 3)

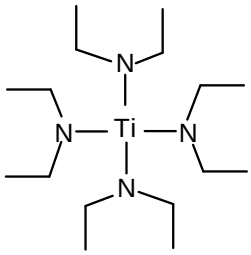

Tetrakis (diethylamido)titanium(IV)
(Cat 4)

Scheme 2.3 Non-chelated titanium (IV) catalysts.

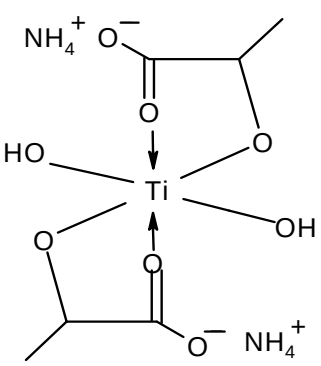

titanium (IV) bis (ammonium lactato)
dihydroxide (Cat 5)

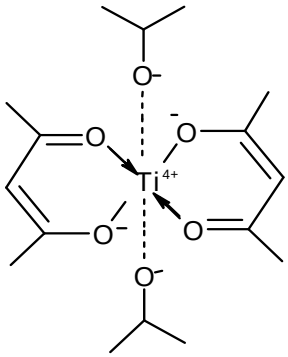

Diisopropoxytitanium bis
(acetylacetonate) (Cat 6)

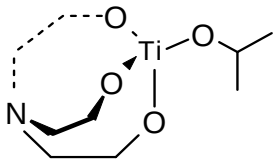

Titanium (IV) (triethanlaminato)
isopropoxide (Cat 7)

Scheme 2.4 Chelated titanium (IV) catalysts.

Second category (scheme 2.4) of titanium catalysts, titanate chelates, consist of chelated titanium (IV) derivatives with differences in nature of multidentate ligands.

Table 2.3, represents the activity of all catalysts studied. Cat 1 and Cat 5 show the highest and the lowest activity index respectively. A slight drop in activity of Cat 1 to Cat 4 was detected. The nature of monodentate ligands tested has no significant effect on catalytic activity in PET synthesis. The external stereo structure of monodentate ligands has no evidence effect on titanium catalytic activity since the activity of Cat 1 and Cat 2 are almost the same. The electronegativity of attached atom to titanium (O, Cl, N) also can not influence the activity of titanium strongly, because the presence of an electronegative atom like chlorine in Cat 3 results in same activity as Cat 1. In general one can say, Irregardless of nature and structure of ligands, the catalytic activity of titanium compounds containing monodentate ligands, tetraalkyl titanates, is very high and similar to each other. Whereas, the activity indices of chelated titanium catalysts depend more strongly on the nature of ligand and larger differences in activity was detected among this type of catalysts.

Table 2.3 Activity index of titanium (IV) catalysts, [Ti]:500 mol ppm

Catalyst	**AI ×10^3** [°C^{-1}]
Cat 1	4.72±0.5%
Cat 2	4.69±0.5%
Cat 3	4.67±0.5%
Cat 4	4.67±0.5%
Cat 6	4.69±0.5%
Cat 7	4.48±0.5%
Cat 5	4.38±0.5%

2.4.3 Effect of titanium (IV) ligand nature on polymer degradation in the course of polycondensation

The nature of ligands are affecting onset temperature of degradation of polymer formed (Table 2.4). Tetraalkyl titanates have lower T_{deg} than the chelated types of titanium derivatives. The most active catalyst of this group in degradation reaction is tetrakis (diethylamido) titanate. Nonetheless, chelated titanium catalysts have similar behaviour and are less active than non-chelated catalysts in polymer degradation. Cat 5 shows least activity in polymer degradation.

Table 2.4 Effect of ligand nature of titanium (IV) on onset temperature of degradation reaction of product formed in DSC, [Ti]:500 mol ppm

Catalyst	T_{deg} [°C]
Cat 4	260
Cat 1	273
Cat 3	275
Cat 2	287
Cat 7	298
Cat 6	303
Cat 5	303

2.4.4 Thermal stability of titanium (IV) compounds with different ligands

Thermograms of different titanium compounds are presented in figure 2.5.

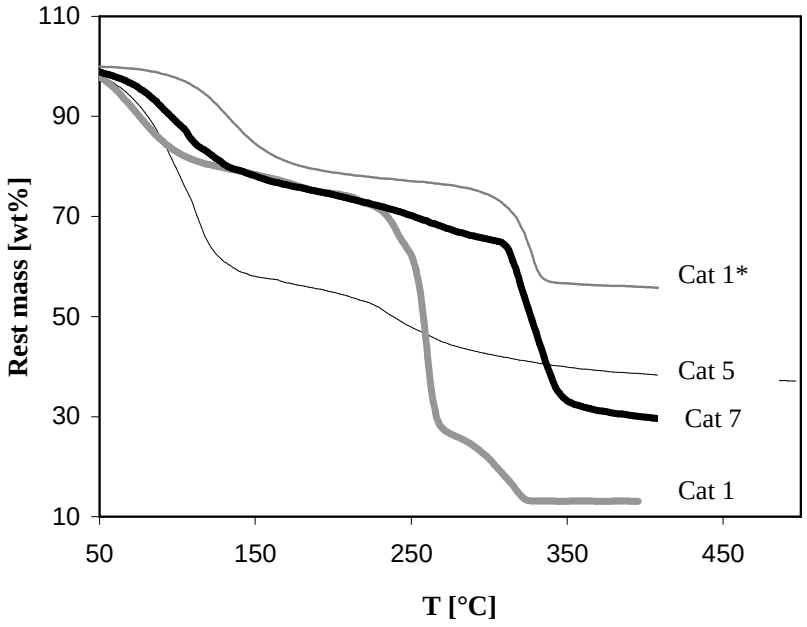

Figure 2.5 TGA thermogram of thermal decomposition of different titanium-based catalysts under nitrogen flow. Cat 1*: Product of mixture of Cat 1 and EG.

The first mass loss seen in all thermograms is due to the removal of residual solvent which is followed by mass loss due to thermal decomposition of catalyst compound. Cat 1 has lowest thermal stability and shows almost complete decomposition. However, by mixing of Cat 1 with EG for 2 h at room temperature and removing the excess of EG (Cat 1^{*}), the residual shows a better stability than original product. Cat 1 is reacting with EG forming a more stable compound. It indicates that at reaction condition which EG is present, Cat 1 is converted to a more stable structure. Cat 5 and Cat 7 have higher thermal stability than Cat

1, but decomposition is also taking place at polycondensation temperature. The catalysts which are more thermally stable were found to be less active in polycondensation reaction.

2.3.5 Catalyst screening in lab scale stirred tank reactor

The activity of catalysts was screened in stirred tank reactor by measuring torque of stirrer online during polycondensation. Since torque of stirrer depends on viscosity of reaction mixture and viscosity is correlated to progress of polycondensation, one can follow conversion of reaction and thereby activity of catalyst. Figure 2.6, presents the change of torque in the course of polycondensation catalyzed by different catalysts. The measurements show an induction time for titanium catalysts. Since different titanium catalysts show different induction periods in PET synthesis, the induction period is not caused by physical effects like sensitivity of torque measuring system. In case of antimony catalyst, it was found that this period is an inhibition period and is relatively long and can be due to an interaction of antimony with hydroxyl end groups of monomer preventing formation of active sites [18]. With consumption of hydroxyl end groups in the course of polycondensation, the catalytic activity of antimony is increasing. The induction period of titanium based catalysts might be of different nature and varies with catalyst type. However, variation of catalyst concentration did not change the duration of induction, it only change slightly the slope of torque measured during induction period and strong change in slope was detected in the polycondensation period.

It is believed that induction period of titanium catalysts is due to formation of active sites which is depending on the nature of ligands of catalyst. That might be reflected in different capability of titanium compounds to form titanium alkoxide by ligand exchange reaction with hydroxyl end groups of monomer and oligomers. The ligand exchange capability of Cat 1 is very high since it is known that butoxide groups attached to titanium can be exchanged easily. However, in Cat 5, the hydroxide groups are rather stable and ligand exchange reactions should happen by breakage of the chelating ring. In this sense the original titanium catalysts are precursors and are activated in the first stage of reaction. This fact can also be observed in preparation of sample for catalyst screening in DSC. Activation of Cat 1 in molten BHET is a time dependent procedure and optimal activity is achieved after 15 min of mixing (Table 2.5). This illustrates that total concentration of active species is formed only after a certain time of mixing.

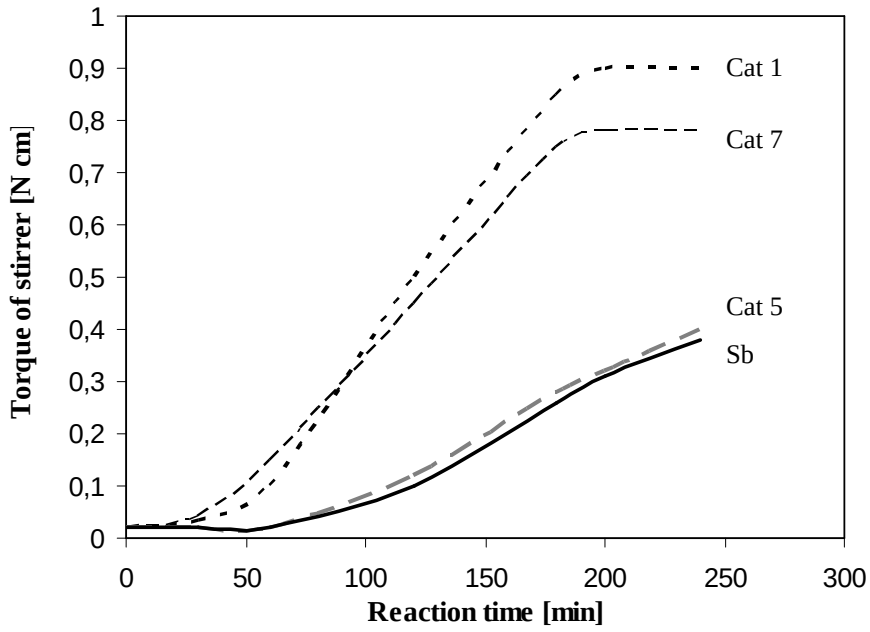

Figure 2.6 Torque of stirrer during polycondensation of BHET and its oligomers in stirred tank reactor at 260°C under vacuum in presence of different catalysts. [Ti]: 20 wt ppm and [Sb]:250 wt ppm.

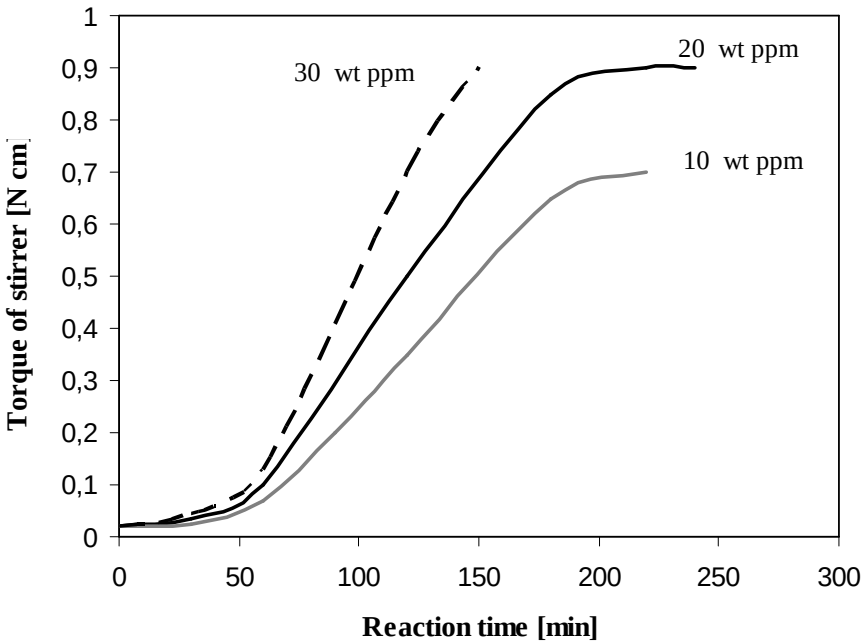

Figure 2.7 Variation of torque of stirrer with change of concentration of Cat 1 at 260°C.

Table 2.5 Effect of mixing time of reaction mixture at 110°C on activity index, [Cat 1]: 500 mol ppm

Mixing time [min]	**AI ×10^3** [°C^{-1}]
5	4.34±0.5%
10	4.55±0.5%
15	4.72±0.5%
30	4.72±0.5%

Table 2.6 Data of PET produced in stirred tank reactor, at 260°C under vacuum (1 mbar) for 3 h, [Ti]: 20 wt ppm, [Sb]: 250 wt ppm

Catalyst	**Intrinsic viscosity** [dl g^{-1}]	**[COOH]** [mmol kg^{-1}]	**[Acetaldehyde]** [µmol kg^{-1}]	**dM$_T$/dt** [mN cm min^{-1}]
Cat 1	0.66	13	9.5	6.1
Cat 7	0.54	7	7.0	4.8
Cat 5	0.43	5	3.4	2.2
Sb	0.42	4	3.3	2.2

The maximum slope of torque-time curve is related to activity of catalyst and used as another kind of activity index. The obtained values (Table 2.6) are in good agreement with the values of activity indices obtained by DSC measurements. The Characterization of polymeric samples of different catalysts is summarized in table 2.6. Cat 5 has moderate activity and better selectivity than other catalysts and shows similar values as antimony with application of only 20 wt ppm compare to 250 wt ppm of antimony.

2.4.6 Thermal stability of polymer

Figure 2.8, represents thermograms of thermal degradation of PET synthesised by different catalysts at 260°C. No significant difference in thermal stability of PET produced at this temperature can be seen. PET produced by antimony is slightly more stable than PET synthesised by titanium catalysts.

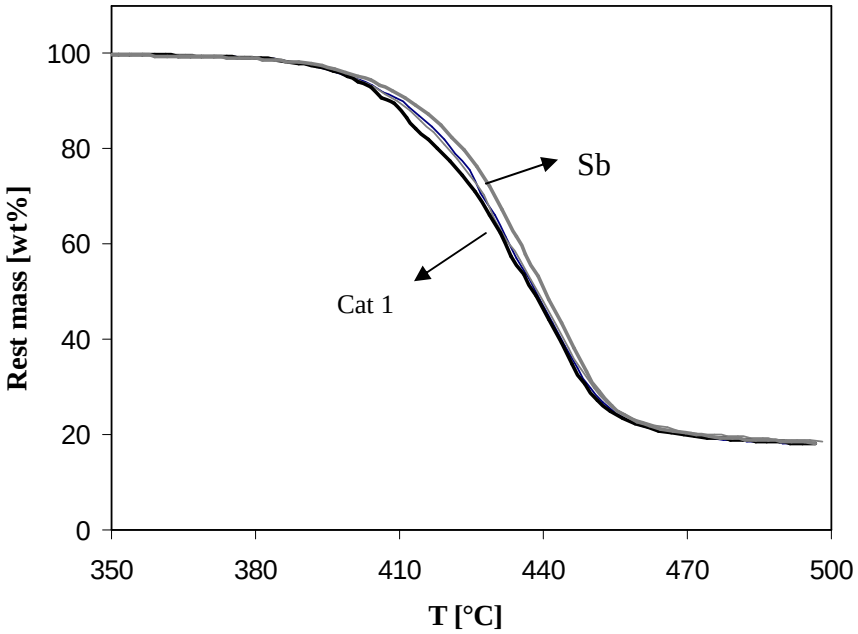

Figure 2.8 TGA thermogram of PET thermal degradation synthesised by different catalysts, under nitrogen flow, [Ti]: 20 wt ppm, [Sb]: 250 wt ppm.

2.4.7 Effect of reuse of catalyst after pre-polycondensation on its catalytic activity

Reuse of Cat 1 after pre-polycondensation at 260°C for different times did not lead to considerable variation on the catalyst activity (Table 2.7). This indicates that catalyst is not severely deactivated and the concentration of active species remained almost constant in the course of polycondensation and is in agreement with the obtained kinetic results which will be reported in the next chapter.

Table 2.7 Effect of pre-polycondensation period on activity index, [Cat 1]:500 mol ppm

Pre-polycondensation period [h]	**AI ×10^3** [°C^{-1}]
0	4.72±0.5%
1	4.58±0.5%
4	4.57±0.5%

2.4.8 Solid state polycondensation

The polymer products of polycondensation in melt with different catalysts (for polymer specification see table 2.6) were used for post polycondensation in solid state.

2.4.8.1 Optimization of reaction operational condition

The reaction condition was optimized with respect to the removal of by-product in such ways; nitrogen purging through a fixed non-stirred bed, nitrogen purging through a stirred bed and vacuum. It was found that working under vacuum is the most effective way to carry away the produced by-product.

Table 2.8 Comparison of efficiency of by-product removal method [Cat 1]: 20 wt ppm

Removal method	**Molecular weight** [g/mol]
Nitrogen- non-stirred bed	63827
Nitrogen- stirred bed	71751
Vacuum	79508

2.4.8.2 Catalyst screening in solid state polycondensation

The increase of number average molecular weight with time is shown in figure 2.8. Taking the initial slope of curves of different catalysts and normalize them with respect to the catalyst concentration, the activity indices shown in table 2.9 are obtained. This shows that titanium catalysts are more active than antimony catalyst. Also, in solid state polycondensation, different types of titanium catalysts have different activity and their activity order is in agreement with activity order in the melt phase polycondensation. The lower activity of titanium catalysts in SSP might be caused by the lower mobility of the chain end to reach catalyst active species with low concentration compare to higher concentration of antimony which is more accessible for chain end.

Table 2.9 Normalized activity index of different catalysts in solid state polycondensation at 230°C

Catalyst	**AI×10^6** [$g^2\ mol^{-2}h^{-1}$]
Cat 1	393
Cat 2	388
Cat 5	384
Sb	47

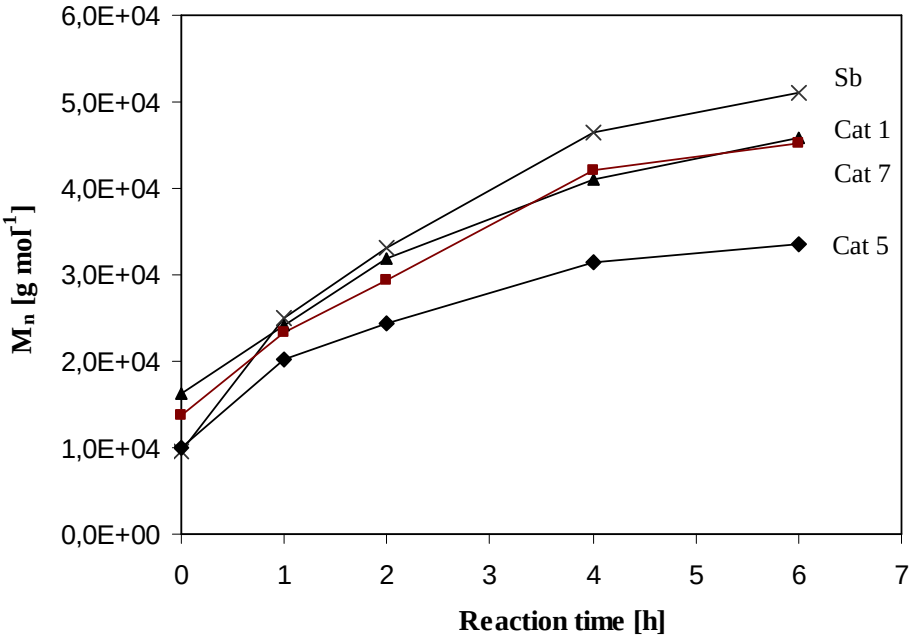

Figure 2.8 Number average molecular weight of PET during solid state polycondensation at 230°C under vacuum, [Ti]: 20 wt ppm, [Sb]: 250 wt ppm.

2.4.8.3 Effect of polymer particle size on polycondensation progress

It is known that at high temperature, solid state polycondensation is mass transfer controlled in case of particles with larger diameter.

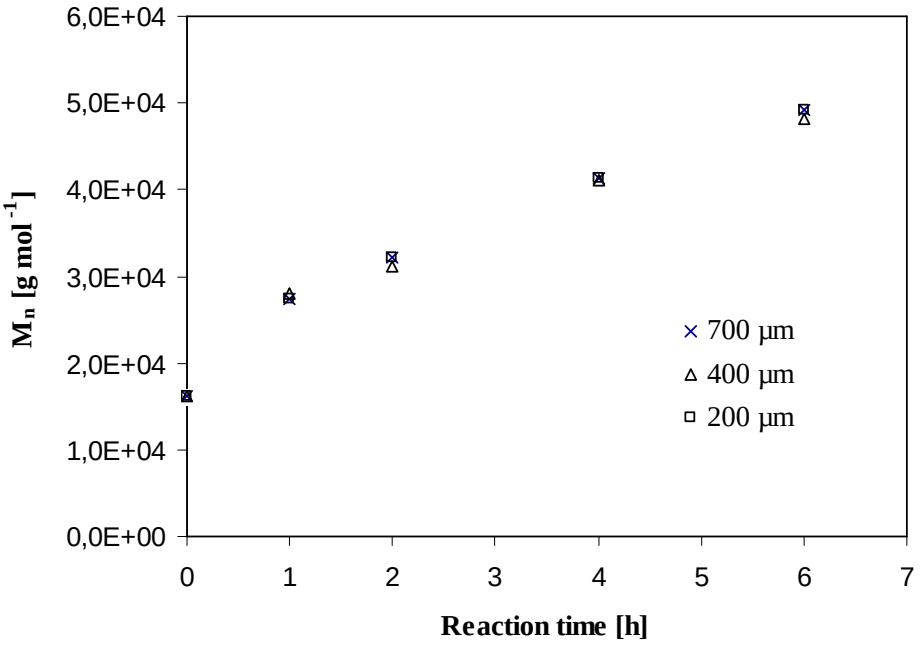

Figure 2.9 Number average molecular weight of PET particle with different sizes during solid state polycondensation at 230°C under vacuum.

The effect of particles size in titanium catalyzed solid state polycondensation was studied (Figure 2.9). It was found that for particles with diameters less than 1 mm, the reaction is completely chemistry controlled and mass transfer limitations are absent.

2.4.9 Infrared spectroscopic studies

Pure EGMB has several absorption bands in the range of 1067-1262 cm^{-1} due to C-O vibration, a doublet at 1710-1717 cm^{-1} due to carbonyl stretching and various bands between 1365-1497 cm^{-1} that corresponds to benzene. Hydroxyl end group vibration appeared by a broad peak at about 3091-3657 cm^{-1}. The change of spectrum of EGMB mixed with Cat 1 with molar ratio of 1 to 1 was investigated (Figure 2.10 and 2.11). The spectrum did not show significant changes at 100°C while increasing temperature to 140°C led to disappearing of the peaks corresponding to hydroxyl end groups. This indicates that ligand exchange reaction was happened between butyl groups of catalyst and hydroxyl end groups of EGMG and titanium alkoxide was formed. Furthermore, a new peak at about 1550 cm^{-1} was appeared, which might be due to complexation to the titanium centre.

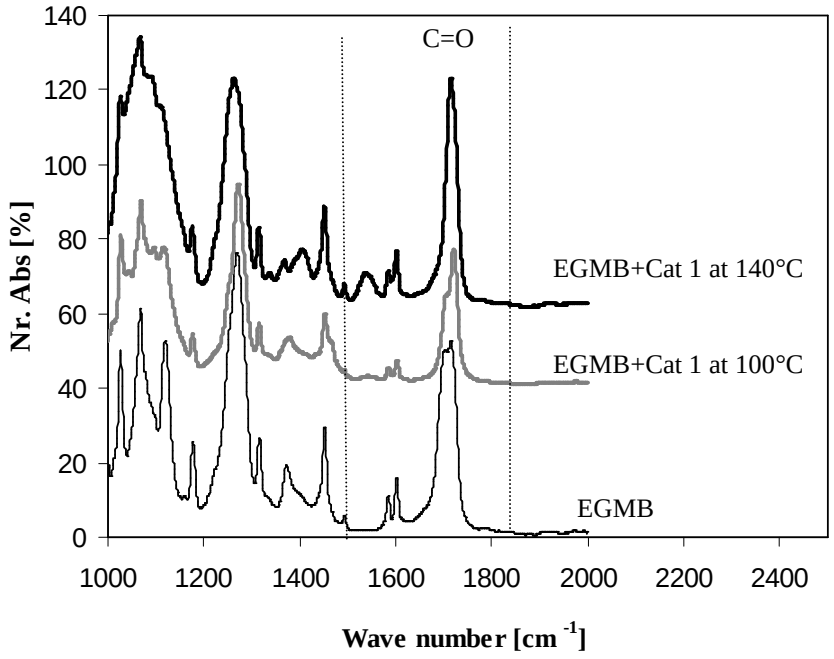

Figure 2.10 IR spectra of EGMB, mixture of EGMB and Cat 1 at 100°C and 140°C in the range of 1000-2000 cm^{-1}.

Figure 2.12 and 2.13 represent the IR spectra of BHET, Cat 1 and Cat 5 and mixture of each catalyst with BHET (molar ratio of 1 to 2) at 120°C and 260°C. In spectra of Cat 1-

BHET mixture heated at 140°C for 15 min, a shift at C=O stretching vibration and appearance of new bands in the range of 1550 cm^{-1} were observed. The shift of C-O vibration of ester oxygen also could be seen in the spectrum. These results might be an indication of restricted carbonyl and ester oxygen vibration which could be due to complex formation at the titanium coordination site. It was the same in case of Cat 7. Therefore, active species formation starts at earlier stage of reaction.

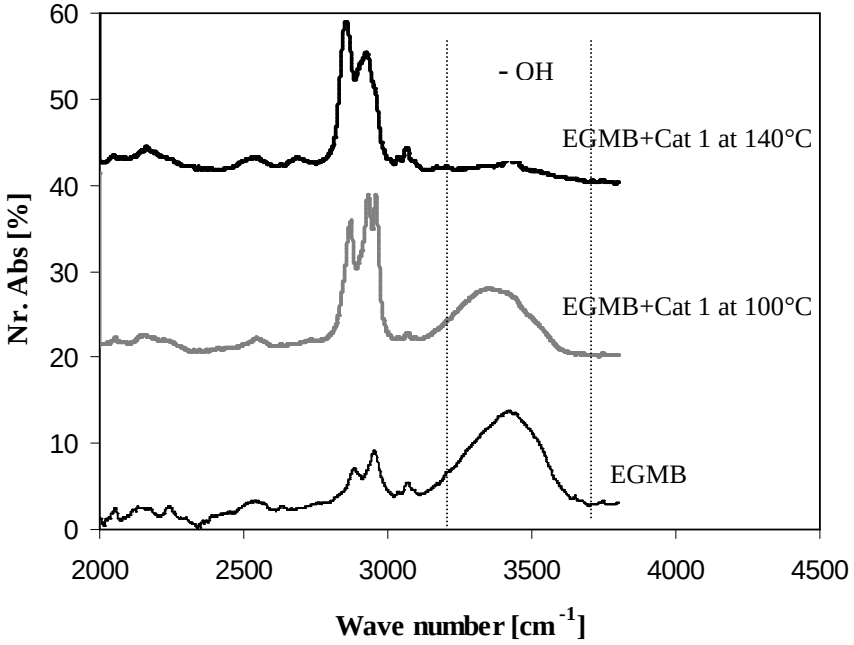

Figure 2.11 IR spectra of EGMB, mixture of EGMB and Cat 1 at 100°C and 140°C in the range of 2000-3600 cm^{-1}.

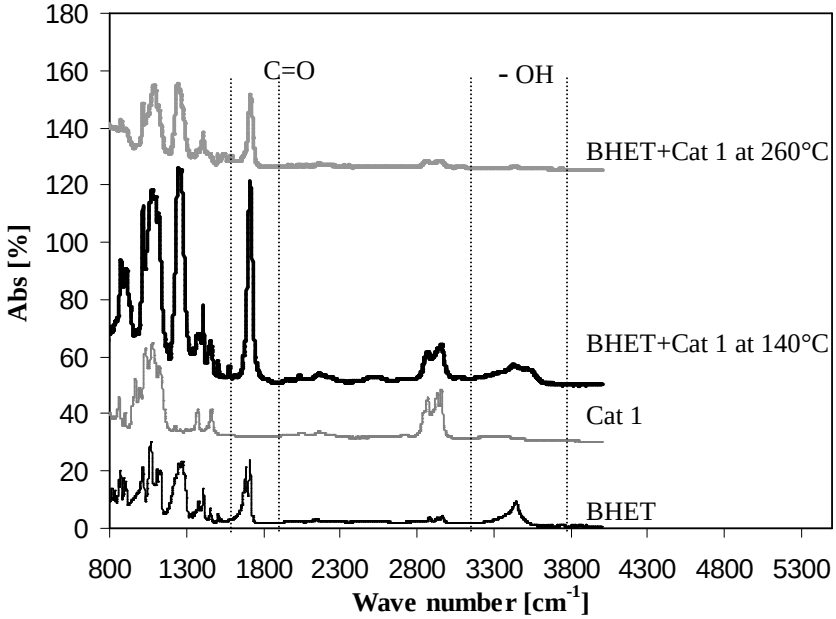

Figure 2.12 IR spectra of BHET, Cat 1, BHET-Cat 1 mixture (2 to 1 molar ratio) at 140 and 260°C.

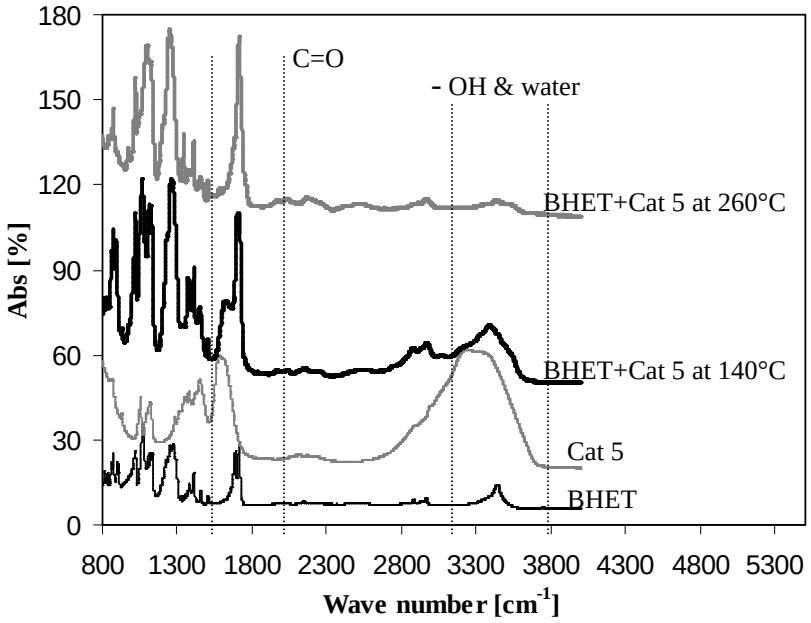

Figure 2.13 IR spectra of BHET, Cat 5, BHET-Cat 5 mixture (2 to 1 molar ratio) at 140 and 260°C.

However spectrum of BHET-Cat 5 at 140°C does not present any significant change in any absorption peaks. This is due to more stability of chelating ligands against ligand exchange reaction. Furthermore, in addition of complexation, one can observe presence of hydroxides groups showing titanium hydroxide is stable and no chain prolongation could happen from these two positions by ligand exchange.

The mechanism of activation step of titanium catalyzed polycondensation is in agreement with the mechanism proposed by Weingart et al.[5], which is assuming, first exchange of initial ligands by hydroxyl end groups of monomer or oligomers. In case of non-chelated titanium derivatives, the exchange reaction of organic monodentate ligands by hydroxyl end group is very fast. Nevertheless, in chelated compounds, in addition of nature of multidentate ligands, nature of monodetate ligands attached to titanium play very important role in formation of active species. Next step is intramolecular complexation of titanium to the ester oxygen of attached chain to form a favourable stable complex of chelating glycolate and rendering carbonyl for nucleophilic attack of terminal oxygen. The other titanium coordination site might be occupied either by initial ligand (like Cat 5) or one of the reaction components which can improve the selectivity or cause side reaction respectively.

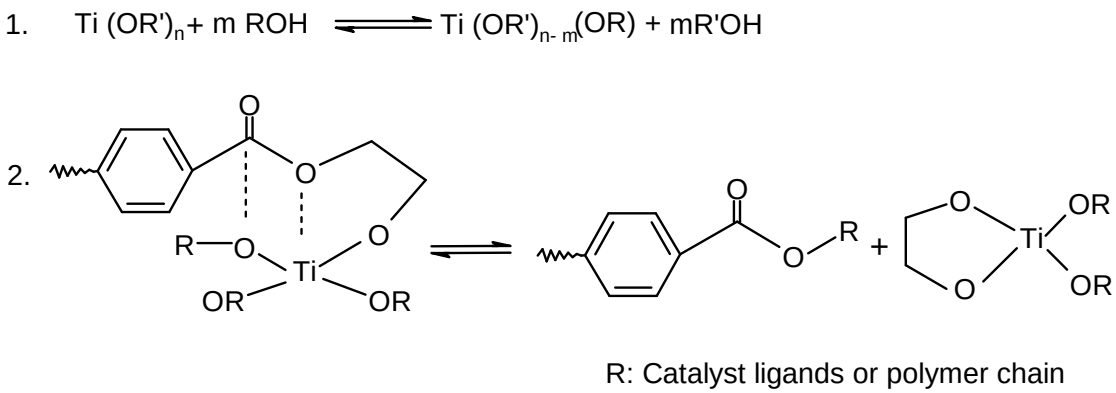

Scheme 2.5 Proposed activation steps in titanium catalyzed PET synthesis.

2.5 Conclusion

The comparative studies show that all titanium compounds used are catalyst precursors and the nature of active form of catalyst is different for different titanium compounds with respect to ligand nature. But formation of a five member ring might be a common characteristic pattern of the active form of all tested catalysts.

Appropriate design of titanium catalysts might be achieved by application of multidentate ligand acting as a cage for metal centre and fixation of titanium on the surface of an appropriate support.

2.6 References

[1] J. Scheirs, T. E. Long, *Modern Polyesters: Chemistry and Technology of Polyesters and Copolyesters*, John Wiley & Sons (2003)

[2] U. K. Thiele, *Inter. J. Polym. Mater.*, **5**, 387 (2001)

[3] U. K. Thiele, *Chem. Fiber. Inter.*, **54**, 162 (2004)

[4] B. Apicella, M. Di Serio, L. Fiocca, R. Po, E. Santacesaria, *J. Appl. Polym. Sci*., **69**, 2423 (1998)

[5] F. Weingart, *PhD Thesis*, University of Stuttgart (1994)

[6] S. B. Maerov, *J. Polym. Chem*., **17**, 4033 (1979**)**

[7] K. Tomita, *Polymer*, **14,** 50 (1973)

[8] K. Tomita, H. Ida, *Polymer*., **16**, 185 (1975)

[9] K. Tomita, *Nippon Kagaku Kaishi*, 514, (1975)

[10] K. H. Wolf, *PhD Thesis*, University of Stuttgart (1976)

[11] K. H. Wolf, H. Herlinger, *Angew. Makromol. Chemie*, **65**, 13, (1977)

[12] J. S. Chung, *J. Macromol. Sci.-Chem*., **27(4),** 479 (1990)

[13] T. N. Laricheva, M. I. Siling, *Russian. Chem. Rev.*, **65 (3)** 279 (1996)

[14] J. Otton, S. Ratton, *J. Polym. Sci.: Part A: Poylm. Chem.*, **26**, 2183 (1988)

[15] J. Otton, S. Ratton, *J. Polym. Sci.: Part A: Poylm. Chem.*, **26**, 2199 (1988)

[16] K. H. Wolf, B. Kuester, H. Herlinger, C. J. Tschang, E. Schollmeyer, *Angew. Makromol. Chem.*, **68**, 23 (1978)

[17] F.-A. El-Toufaili, G. Feix, K.-H. Reichert, *Thermochim. Acta.*, **432**, 101 (2005)

[18] R. W. Stevenson, *J. Polym. Sci., Part A-1*, **7**,395 (1969)

Chapter 3: Kinetic Studies of Polyethylene Terephthalate Synthesis with Titanium Tetrabutoxide and Application of Thermogravimetric Analysis

Abstract

Thermogravimetric analysis was used to study the kinetic of polycondensation of bis (hydroxyethylene) terephthalate catalyzed by titanium tetrabutoxide. Polycondensation reaction can be modelled best with a second order reaction with respect to hydroxyl end groups concentration. Kinetic data depends on the mode of operation in thermogravimetric analysis. In nonisothermal mode, the overall activation energy was determined by model-free method and the frequency factor was found to be affected by catalyst concentration. The kinetic study of isothermal reaction in thermogravimetric analysis is complex due to the fact that isothermal condition are reached only at relative high conversion of reaction and also high activity of the catalyst studied. Kinetic investigation of polyethylene terephthalate degradation indicates high degradation activity of titanium catalysts in comparison to antimony catalysts.

3.1 Introduction

Thermogravimetric analysis (TGA) was used as a technique for catalyst screening for the first time by Bhatty et al. [1], in 1986. They used the onset temperature of thermogram at which initial mass loss occurs as activity index. In 1997, Zimmerer et al. [2] applied TGA to examine the kinetics of polycondensation reaction in order to estimate the mass transfer influence and optimize reaction condition. They considered also monomer evaporation in their mathematical model. Moreover, they studied diffusion of EG within the melt by changing the thickness of the polymer layer. Rieckmann et al. [3] also applied TGA to study the kinetic of PET synthesis and tried to consider mass transfer effects. Reichert et al. [4] studied the kinetics of hydrotalcite catalyzed BHET polycondensation by TGA and applying nonisothermal mode of operation.

The aim of this chapter is to optimize TGA for quantitative study of titanium catalyzed PET synthesis and obtain kinetic data of polycondensation and degradation reaction by application of this method.

3.2 Experimental part

3.2.1 Sample preparation

Sample preparation technique is the same as described method in chapter 2.

3.2.2 Polycondensation in lab scale stirred tank reactor

Polycondensation was also run in a lab scale stirred tank reactor made of glass with a volume of 200 ml equipped with a special helical type of stirrer. Polycondensation was performed with 120 g monomer and 10 wt ppm of Cat 1 at different temperatures 250, 255, 260°C and 0.1 mbar with stirring speed of 200 rpm for different reaction times 2, 3 and 4 h.

3.2.3 Polymer decomposition

The polymer decomposition was studied in TGA as described in chapter 2. The polymer particles used were synthesized in lab scale stirred tank reactor at 280°C for 4 h. Concentration of Cat 1 in PET synthesis was 50 wt ppm. 250 wt ppm of antimony triacetate was used to synthesize PET as reference material.

3.3 Thermogravimetric analysis

3.3.1 Apparatus

Thermogravimetry, TGA-209 F3 Tarsus, from Netzsch company was applied in this investigation. This instrument offers a resolution of 0.1 µg and operates between room temperature and 1000°C with freely selectable heating rates from 0.001 K min^{-1} up to 100 K min^{-1}. The accurate sample temperature is detected by a thermocouple in direct contact with the sample crucible. Through the reliable vertical construction with sample carrier lift, the thermo-balance as a top-loader is easy and safe to use, with no hang-down wires or exposed fragile parts. The inner room of oven can be flashed with purge gas (nitrogen) and it is supported by protective gas to provide an inert atmosphere with in the oven and microbalance chamber. 10 mg of prepared sample was filled into the aluminium crucible with 80 µl volume which was located on the sample holder of TGA. Nitrogen was used as purging gas with purging rate of 20 ml min^{-1}. The vertical construction of sample holder provided efficient purging. The oven of the TGA was first evacuated and then purged with nitrogen before each run. Isothermal polycondensation of BHET was investigated at 220, 230, 240 and 250°C for 40 min reaction time. Nonisothermal runs were performed at heating rates of 1, 5 and 20 K min^{-1} starting at 30°C and ending at 300°C.

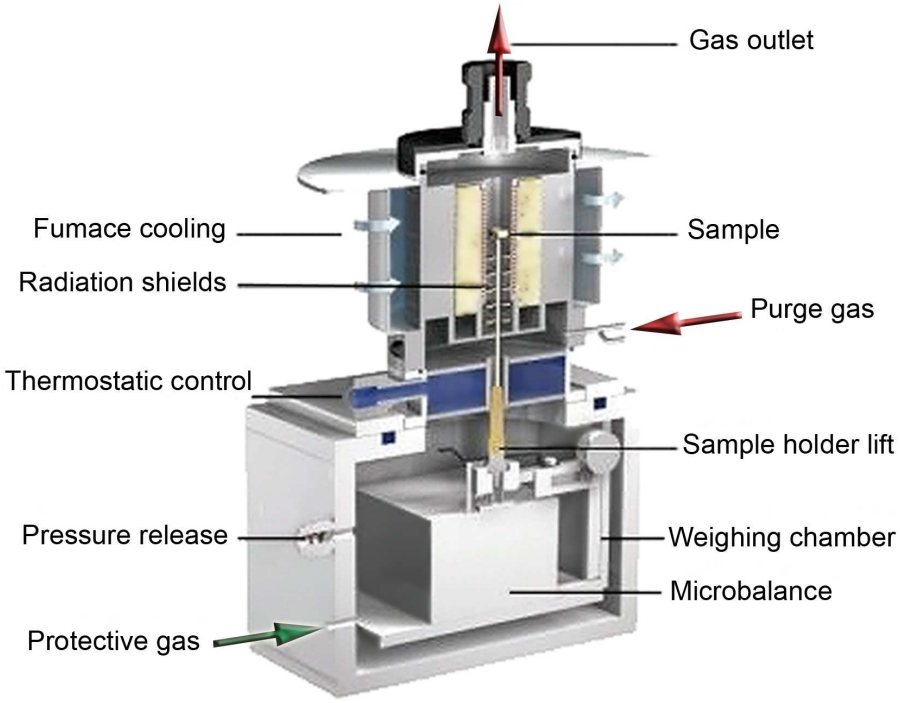

Figure 3.1 Scheme of TGA-209 F3 Tarsus.

3.3.2 Principle of screening

A thermogram obtained from dynamic heating of a BHET-catalyst mixture is shown in figure 3.2. Mass loss starts at a certain temperature indicating onset of polycondensation with onset temperature of T_o. On the other hand, a temperature (T_m) can be obtained at which rate of mass loss has a maximum. In addition, the total mass loss which is due to EG evaporation can be correlated to the total conversion of polycondensation. These parameters can be applied as activity ordering indices in catalyst screening. TGA measurements are reproducible with standard deviation less than 1% for each of these parameters.

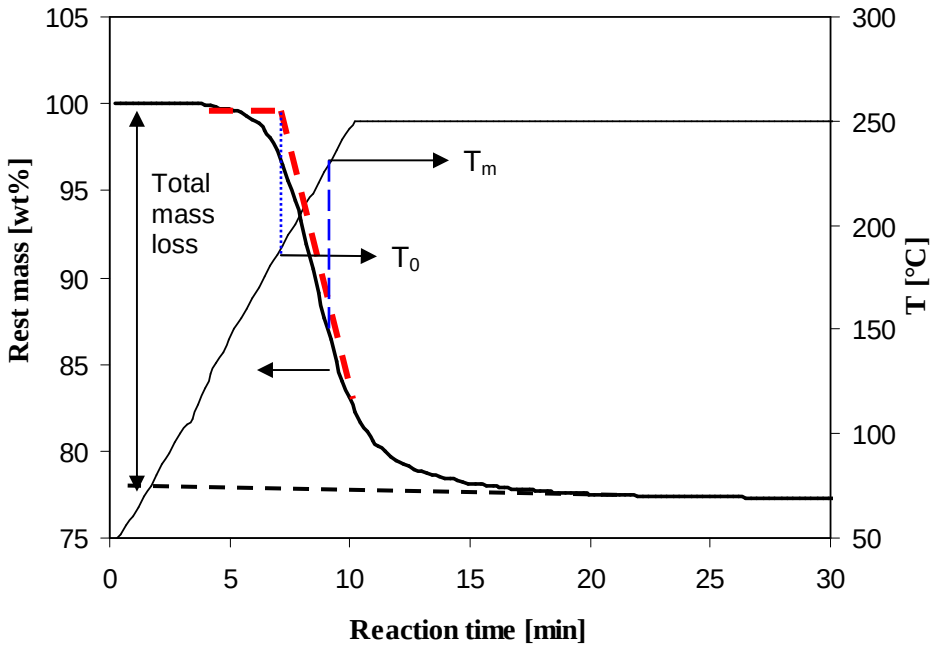

Figure 3.2 TGA thermogram of BHET polycondensation with 10 mol ppm of Cat 1.

3.4 Results and discussion

3.4.1 Optimization of thermogravimetric analysis for quantitative study

The micro-scale of the TGA crucibles provides micro-scale diffusion path length and thereby mass transfer limitations might be avoided. The main draw back of this system is the absence of effective mixing of reaction mass. However it can be seen that reaction mixture within the TGA crucible is moving very strongly and stimulates self-mixing thereby. Another problem can be the catalytic activity of the crucible itself. It was found that aluminium crucibles have least catalytic activity [5]. Moreover, monomer evaporation

is present during polycondensation of BHET [2,4], since polycondensation of BHET in an open crucible has a mass loss much higher than expected for complete conversion equal to 24.4 wt% (Figure 3.3).

$$\frac{Total\ mass\ loss}{Monomer\ mass} = \frac{Molar\ mass\ of\ EG}{Molar\ mass\ of\ BHET} = \frac{62}{254} = 0.244 \qquad (3.1)$$

Increasing mass loss with decreasing monomer amount is due to increase of specific surface exposed to purging gas and increase of mobility of the melt leading to enhancement in evaporation rate. To reduce monomer evaporation, a lid with a hole in the centre covered the aluminium crucible in all polycondensation runs.

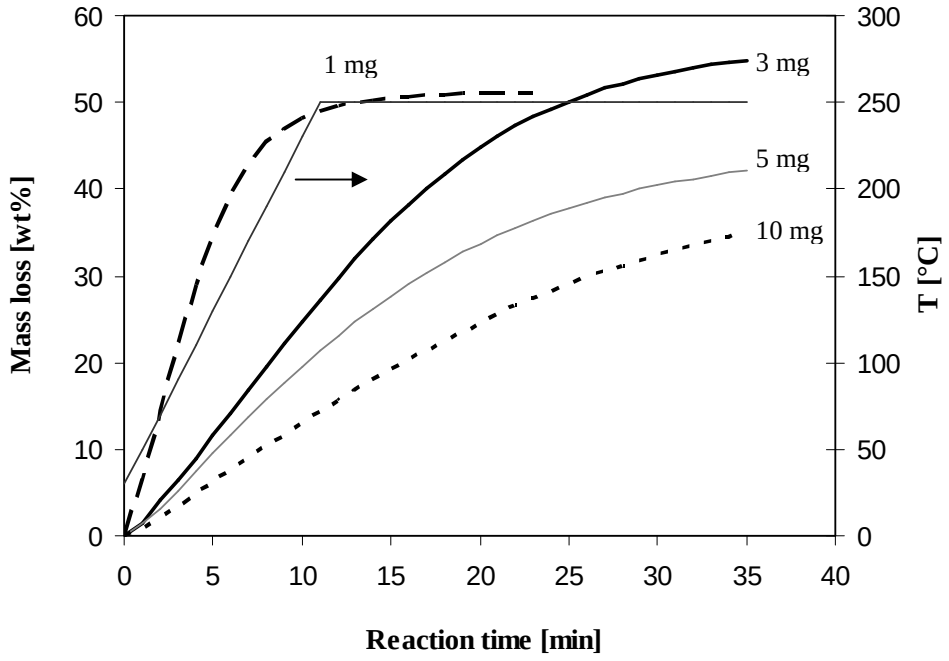

Figure 3.3 Thermograms of polycondensation of BHET with different weight of monomer in an open crucible at 250°C.

Another important point in application of TGA is the mode of operation. Running the reaction merely isothermal was not possible. Since the heating rate and heating time from ambient to reaction temperature have effect on mass loss and consequently concentration of hydroxyl end groups. These effects however were considered in the kinetic studies. Figure 3.4, represents the thermogram of BHET polycondensation in quasi-isothermal mode of operation with different initial heating rates. At high heating rate the thermal lag between sample and oven is highest and at lower heating rate, higher conversion is

achieved before reaching the isothermal regime. Therefore, 20 K min^{-1} was chosen as optimal heating rate for isothermal runs in TGA.

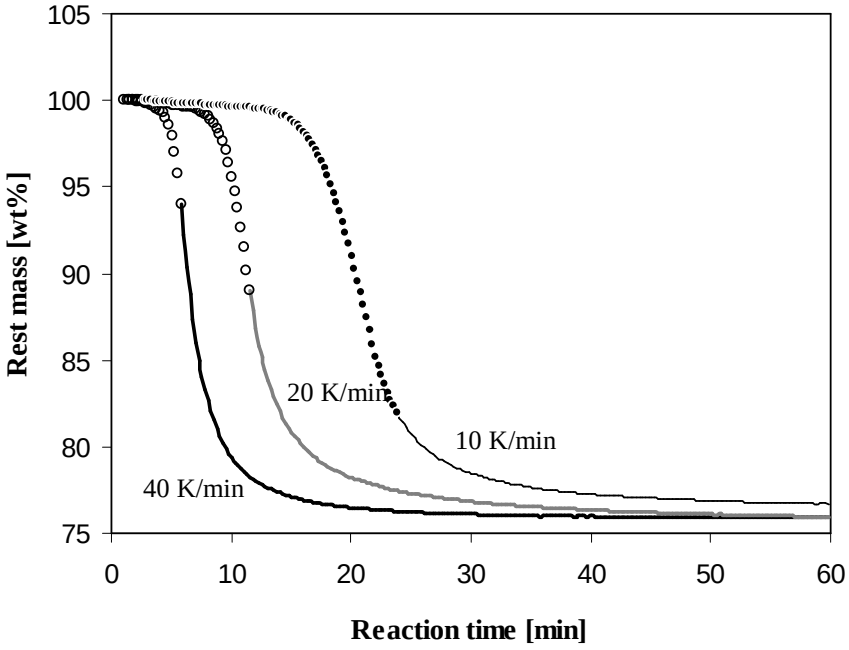

Figure 3.4 Effect of initial heating rate on mass loss of reaction mixture of BHET polycondensation at 250°C, [Cat 1]: 10 mol ppm. Dots indicate nonisothermal and lines isothermal regimes.

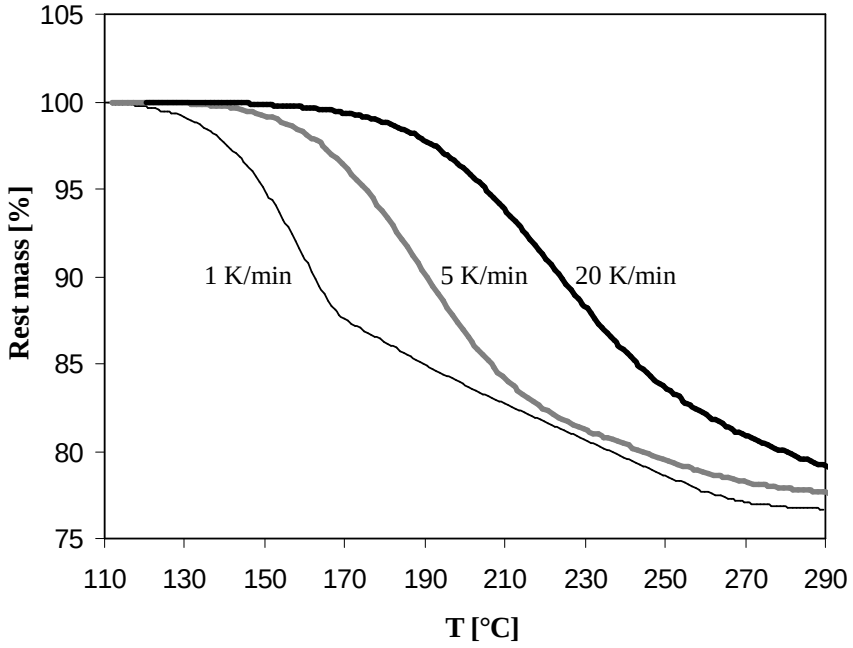

Figure 3.5 Effect of heating rate on mass loss of reaction mixture of BHET polycondensation, [Cat 1]: 10 mol ppm.

Nonisothermal runs were performed by heating up the reaction mixture at 1, 5 and 20 K min^{-1}. Figure 3.5, represents the thermograms of nonisothermal runs. Heating rate has

significant effect on the onset temperature of reaction. The reason is that the true sample temperature lags behind recorded temperature caused by heat transfer effects. Furthermore, time effect should also be considered. A low heating rate has the advantage of overcoming of temperature lag. However, in this case, the melt solidifies partially due to increase in molecular weight of product and kings are formed in the thermogram of polycondensation as can be seen in figure 3.5. Therefore, 5 K min^{-1} was used as optimal heating rate for nonisothermal mode of TGA operation.

3.4.2 Mass transport limitations

The effect of mass transfer limitations with in the melt and melt-gas interface was studied. The absence of mass transfer limitations on gas side of the melt-gas interface was demonstrated with different gas purging rate since the purging rate had no significant effect on total mass loss and the lid used to cover crucible did not affect the EG removal (Table 3.1).

Table 3.1 Effect of purging rate on total mass loss of polycondensation of 50 mol ppm Cat 1-BHET mixture at 5 K min^{-1} in covered crucible

Purging rate [ml min^{-1}]	**Total mass loss** [wt%]
20	22.5±0.5
30	22.6±0.5
40	22.6±0.5

Table 3.2 Effect of sample weight on total mass loss of polycondensation of 50 mol ppm Cat 1-BHET mixture at 5 K min^{-1} in covered crucible

Sample weight [mg]	**Total mass loss** [wt%]
3	23±0.5
7	22.4±0.5
10	22.5±0.5

Mass transfer phenomenon within the melt was studied by changing the amount of sample. In published article [3], this effect was evaluated in TGA crucible with respect to polymer film thickness. However in this investigation no uniform film was observed in the crucible. The polymer formed was located in the form of an O-ring in the periphery of

the crucible. Therefore, it is unreliable to use film thickness as parameter for mass transfer studies. The obtained total mass loss of polycondensation of BHET catalysed by 50 mol ppm Cat 1 in covered crucible was presented in the table 3.2. The results show no influence of amount of reaction mixture on total mass loss. Mass transfer limitations within the melt are negligible.

3.4.3 Kinetic of polycondensation

Quantitative evaluation of thermograms which is corresponding to calculation of hydroxyl end groups concentration with respect to mass loss in TGA was done according to the method of Reichert et al.[9] by considering volume change during reaction.

The number of moles of produced EG as a function of time, $n_{t,EG}$, is calculated by the following equation:

$$n_{t,EG} = \frac{mass\ loss}{M_{EG}} \tag{3.2}$$

where M_{EG} is the molar mass of EG.

The initial number of hydroxyl end groups, $n_{o,OH}$, is given by:

$$n_{o,OH} = 2n_{o,BHET} = \frac{2m_{o,BHET}}{M_{BHET}} \tag{3.3}$$

where $n_{o,BHET}$ is the initial number of moles of BHET, $m_{o,BHET}$ is the initial mass of BHET and M_{BHET} is the molar mass of BHET. In each condensation step two hydroxyl end groups are consumed and one EG is produced. The number of moles of hydroxyl end groups remaining after a reaction time t, $n_{t,OH}$, can be calculated from the amount of produced EG by the following equation:

$$n_{t,OH} = n_{o,OH} - 2n_{t,EG} = \frac{2m_{o,BHET}}{M_{BHET}} - \frac{2mass\ loss}{M_{EG}} \tag{3.4}$$

For kinetic studies it is required to convert the number of moles of hydroxyl end groups into concentration via dividing it by the melt volume:

$$[OH]_t = \frac{n_{t,OH}}{V_t} \tag{3.5}$$

To calculate melt volume, PET is considered as polymer with different segments in table 3.3.

Table 3.3 Different segments of PET and their physical properties

Segment	Symbol	V_m^{298} [l mol^{-1}]	E [l mol^{-1}.K^{-1}]	M [g mol^{-1}]	Density [g ml^{-1}]
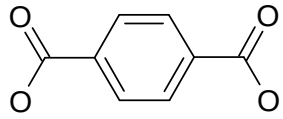	T	0.1115	6.97×10^{-5}	164.11	1.472
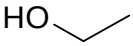	HE	0.0455	2.84×10^{-5}	45.07	0.991
	E	0.0327	2.04×10^{-5}	28.06	0.858

The molar volume of the polymer segments at any temperature T, V_m^T, can be calculated by:

$$V_m^T = V_m^{298} + E(T - 298) \tag{3.6}$$

where, E is molar expansivity. The volume of the melt at any time, V_t, is given by:

$$V_t = n_{t,HE} V_{m,HE} + n_{t,ET} V_{m,ET} + n_{t,TE} V_{m,TE} \tag{3.7}$$

The concentration of hydroxyl end groups in lab scale reactor was calculated by analysis of intrinsic viscosity and carboxyl end groups concentration of polymer product.

[OH] = [E]-[COOH] (3.8)

Kinetic studies are based on following assumption:

1- Polycondensation is considered as a reaction between hydroxyl end groups.

2- All hydroxyl end groups have the same activity irregardless of the chain length of the parent molecules.

3- Polycondensation reaction is considered as irreversible reaction due to fast and efficient removal of EG (Scheme 3.1).

Side reactions are negligible in TGA since the online IR spectra of evolved gas of polycondensation reaction in TGA, represented no IR bands corresponding to side products and was mainly showing bands corresponding to EG bellow 150 mol ppm of Cat 1 concentration while in concentration above 150 mol ppm of Cat 1, peaks corresponding to water and carbon dioxide were detected which show presence of side reactions.

Furthermore, the results were approved by application of DSC and appearance of degradation peaks discussed in chapter 2 (Table 3.4).

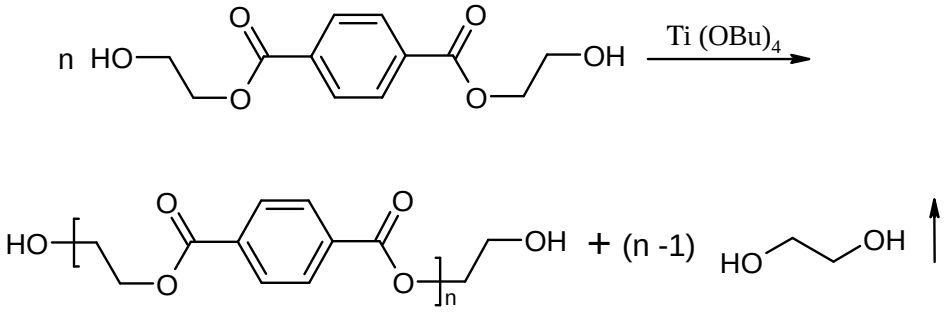

Scheme 3.1 Polycondensation of BHET.

Table 3.3 Wave number of detected IR band and corresponding chemical group

Wave number [cm^{-1}]	**Chemical group** [-]
2941	CH_2
3650	O-H
1052	C-O

4- Mass transfer limitations in polycondensation reaction are neglected.

Fitting of nonisothermal data to different reaction models results in widely varying Arrhenius parameters. This problem had been addressed by different authors [6-9]. The way of obtaining trustworthy kinetic parameter is to extract them in a way that is independent of reaction model. A viable alternative method is based on the model–free isoconversional method and allows obtaining unambiguous values of activation energy by considering of its dependency on reaction conversion. Friedman isoconversional method [6] applied in these studies (equation 3.10), is derived by taking the logarithm of reaction rate equation of nonisothermal experiment (equation 3.9) with constant heating rate, β=dT/dt:

$$\frac{dx}{dT} = \frac{k_0}{\beta}\exp(-\frac{E_a}{RT})\ f(x) \tag{3.9}$$

$$\ln(\frac{dx}{dT})_x = \ln[k_{0,x} f(x)] - \frac{E_{a,x}}{RT_x} \tag{3.10}$$

where x is conversion and *f(x)* represents the reaction progress as function of conversion. The linear plots between $\ln(dx/dT)_x$ and $1/T_x$ determine the value of E_a (activation energy) at different conversion. The software package, Thermokinetic from Netzsch company was

used for determination of activation energy of nonisothermal experiments. Figure 3.6, represents dependency of overall activation energy of nonisothermal reaction on conversion. It is observed that in the conversion range of 0 to 80%, activation energy remains constant with a value of 92±4 kJ mol^{-1}. Increasing of activation energy at higher conversion might be due to the presence of side reactions which affect overall activation energy. This value of activation energy (92 kJ mol^{-1}) was used for the determination of frequency factor by application of simulation software.

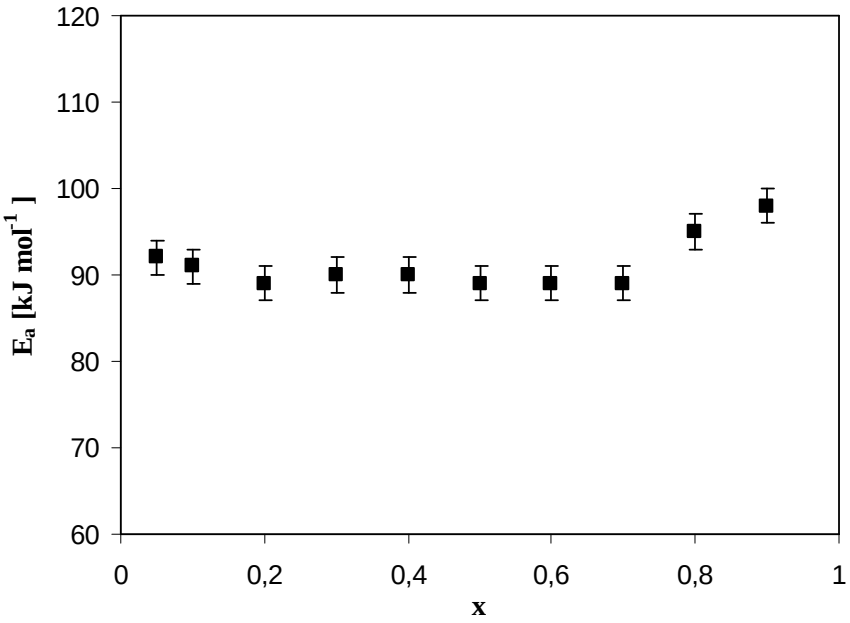

Figure 3.6 Dependency of activation energy on conversion of nonisothermal reaction evaluated by Friedman method [6].

The reaction order with respect to hydroxyl end groups concentration, was determined with integration method. Best fitting was achieved by plotting of experimental data with a second order reaction kinetic (Figure 3.7). Therefore the reaction rate, R [mol l^{-1} min^{-1}], can be written as following:

$$R = -\frac{1}{2}\frac{d[OH]}{dt} = k_0 \exp[\frac{-E_a}{RT}]\,[OH]^2 \qquad (3.11)$$

k_0 is overall frequency factor [l mol^{-1} min^{-1}] and E_a is overall activation energy.

The PREDICI [10] software package was used for detailed kinetic modeling. It was applied to fit experimental conversion-time curves. The fitting parameter was frequency factor for initial overall activation energy of 92 kJ mol^{-1}. Figure 3.8 shows experimental and simulated data with second order kinetic for nonisothermal run. The fitting quality indicates second order kinetic is able to predict polycondensation progress.

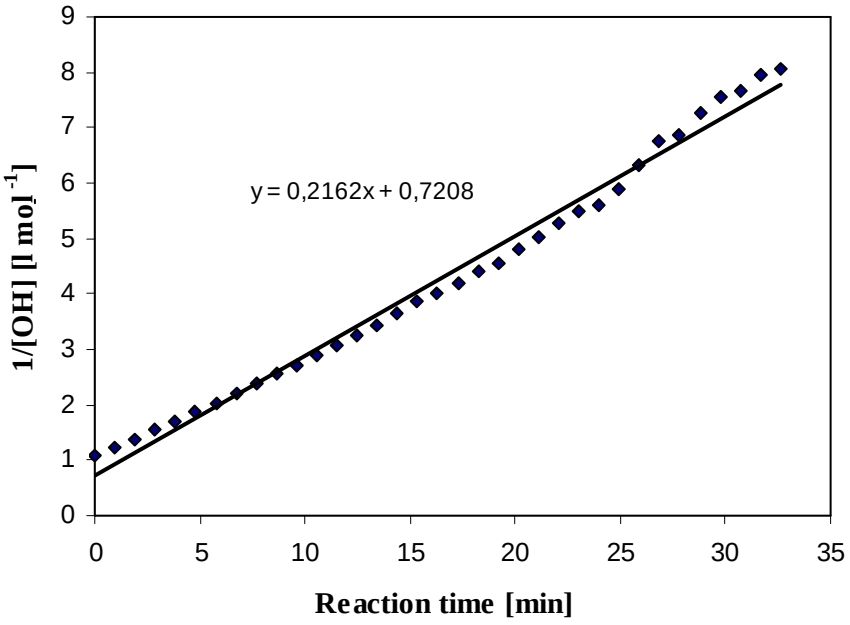

Figure 3.7 Fitting of the experimental data with second order kinetic with respect to hydroxyl end groups concentration.

The overall frequency factor is depending on catalyst concentration and it increases linearly with increasing initial catalyst concentration (Figure3.9).

Kinetic studies of isothermal experiments in TGA are not easy task. The reason is the preheating of reaction mixture to reach the isothermal regime which has severe effect on hydroxyl end groups concentration before reaching to isothermal temperature. Further more, this effect is more severe with increasing catalyst concentration. The investigation is only possible at very low catalyst concentration (10 mol ppm), which led to the results of 89±4 kJ mol^{-1} for overall activation energy and 4.5×10^{7} l $mol^{-1}min^{-1}$ of overall frequency factor.

In order to check the kinetic results of TGA, polycondensation was run in lab scale stirred tank reactor. Due to low temperature of the reaction and efficient vacuum to remove by-product, kinetics of polycondensation was assumed to be chemistry controlled till 260°C. Furthermore, the analysis of polymeric product showed that the side products are negligible at this temperature. However the concentration of side products like carboxyl end groups is increasing at higher temperature. Moreover, polycondensation at 250°C for longer time (more than 180 min) leads to polymer precipitation because the melting point of reaction product is higher than reaction temperature.

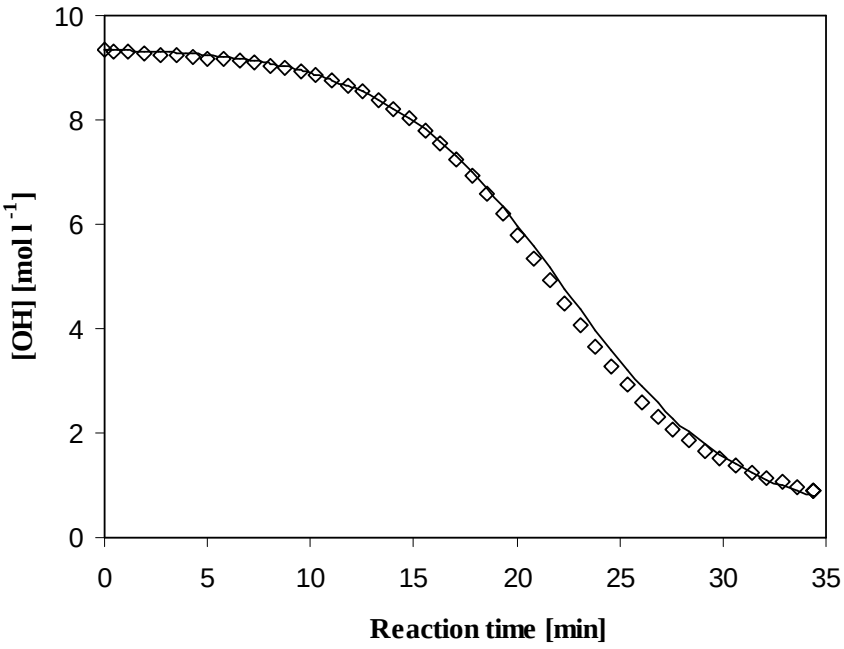

Figure 3.8 Fitting of experiments (dots) with model, [Cat 1]: 10 mol ppm, nonisothermal run.

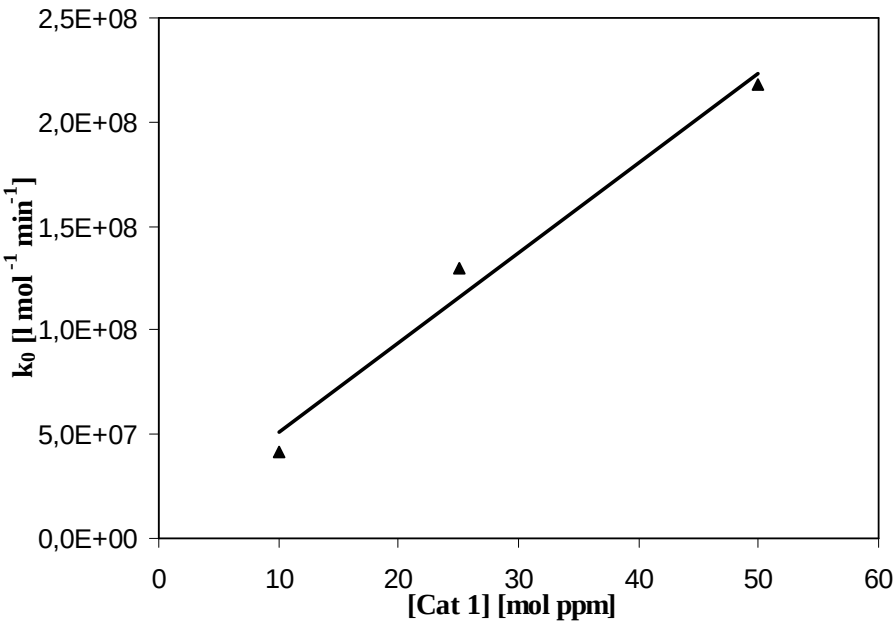

Figure 3.9 Effect of catalyst concentration on overall frequency factor

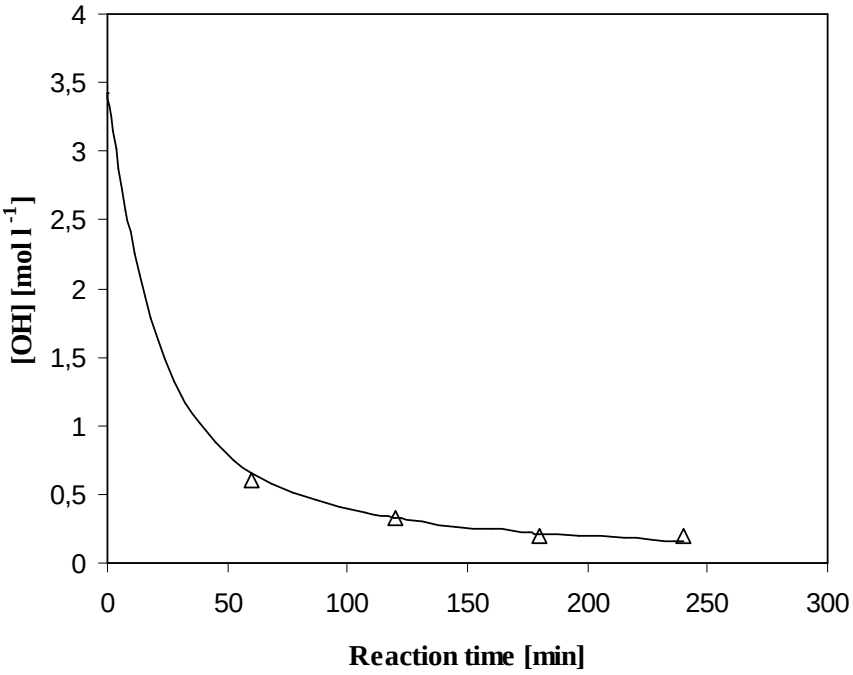

Figure 3.10 Fitting of experiments (dots) with model, [Cat 1]:10 mol ppm, in STR at 260°C under vacuum.

Therefore, overall rate constant of polycondensation reaction with applied assumption could be just obtained at 260°C which leads to a value of 1.3×10^{-3} l mol^{-1} min^{-1}. This leads to requirement of developing a more complex model of polycondensation reaction which can cover total reaction temperature range. This comprehensive model will be discussed in chapter 4.

3.4.4 Kinetic of polymer decomposition

Figure 3.11, represents the thermograms of thermal decomposition of PET synthesized by titanium and antimony catalysts. Onset of decomposition depends strongly on the heating rate.

The basic kinetic equation used to describe a decomposition reaction can be expressed by rewriting of equation (3.9) as

$$\frac{dx}{dt} = \beta \frac{dx}{dT} = k(T)\, f(x) \tag{3.12}$$

$$\beta \frac{dx}{dT} = k \exp(-\frac{E_a}{RT})(1-x)^n \tag{3.13}$$

x can be calculate by following relationship:

$$x = \frac{m_0 - m_t}{m_0 - m_f} \tag{3.14}$$

where m_0 is initial sample mass, m_t is sample mass at time t and m_f is mass of residual sample.

At maximum rate, $\frac{d^2x}{dT^2} = 0$, therefore, following equation can be used to calculate activation energy:

$$\frac{\beta}{RT_m^{\ 2}} = \frac{nk}{E_a}(1-x)^{n-1}\exp(-\frac{E_a}{RT_m}) \tag{3.15}$$

where T_m, is temperature at maximum reaction rate. By plotting ln (β/RT_m^2) versus $1/T_m$, the slope will be corresponding to E_a (Figure 3.12 and 3.13).

Activation energy of 176 kJ mol^{-1} and 200 kJ mol^{-1} was obtained for decomposition of PET synthesised by titanium and antimony catalysts respectively. That is an indication that titanium catalyst also activates degradation reaction of polymer chain. The reasons of stronger effect of catalysts on decomposition reaction in comparison to results in chapter 2, might be the higher titanium concentration (50 wt ppm compare to 20 wt ppm), higher molecular weight of polymer and higher temperature of synthesis of polymer (temperature of 280°C and 260°C).

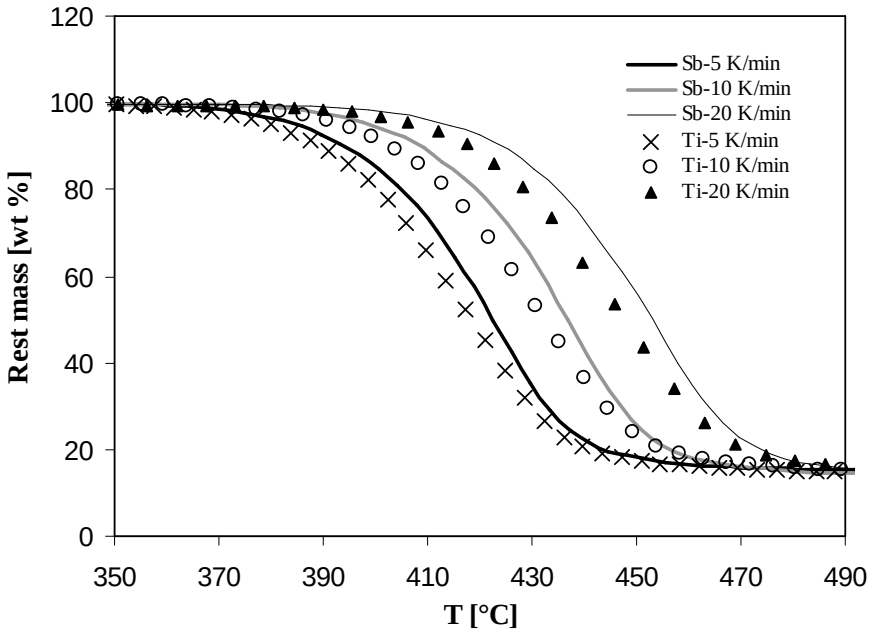

Figure 3.11 Thermograms of PET decomposition with different catalysts at different heating rates.

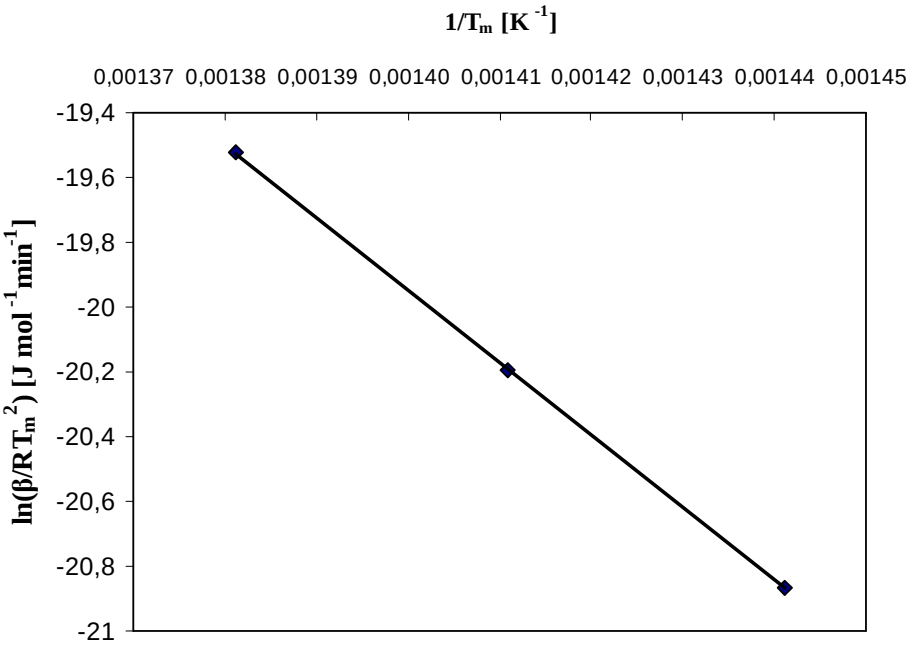

Figure 3.12 Plot of ln (β/RT_m^2) versus $1/T_m$ for Cat 1.

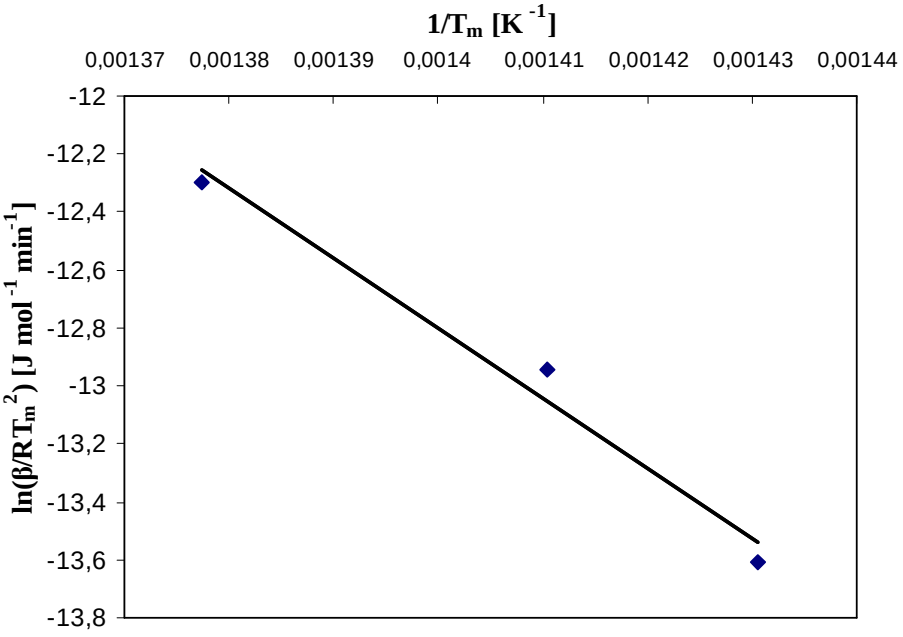

Figure 3.13 Plot of ln (β/RT_m^2) versus $1/T_m$ for antimony.

3.5 Conclusion

Thermogravimetric analysis is a suitable method for fast screening of catalyst of polycondensation reaction, since reaction is characterized by mass loss. However, the method of thermogravimetry for quantitative kinetic studies of polycondensation reactions

should be used only if another independent method is confirming the thermogravimetry results. Furthermore, this technique is a suitable technique for evaluation of polymer degradation.

3.6 References

[1] G. A. Gamlen, T.H. Shah, J.I. Bhatty, D. Dollimore, *Acta. Thermochim*., **106**, 105 (1986)

[2] W. Zimmerer, *PhD Thesis*, Swiss Federal Institute of Technology, Lausanne (1997)

[3] Th. Rieckmann, S. Völker, *Chem. Eng. Sci*., **56**, 945 (2001)

[4] F.-A. El-Toufaili, G. Feix, K.-H. Reichert, *Macromol. Mater. Eng*., **291**, 114 (2006)

[5] F.-A. El-Toufaili, G. Feix, K.-H. Reichert, *Thermochim. Acta*, **432**, 101 (2005)

[6] H. Friedman, *J. Polymer. Sci. C*, **6**, 183 (1963)

[7] S. Vyazovkin, N. Sbirrauoli, *Macromol. Chem. Phys*., **200**, 2294 (1999)

[8] R. B. Prime, *Polym. Eng. Sci*., **13**, 365 (1973)

[9] F.-X. Perrin, T. M. H. Nguyen, J.-L. Vernet, *Macromol. Chem. Phys*., **208**, 718 (2007)

[10] M. Wulkow, *Macromol. Theory. Simul*., **5,** 393 (1996)

Chapter 4: Modeling of Kinetic, Molecular Weight and Molecular Weight Distribution of Polyethylene Terephthalate Synthesis Catalyzed by Titanium Tetrabutoxide in Melt Phase

Abstract

Low molecular weight oligomers of polyethylene terephthalate were used to conduct the polycondensation reaction in lab scale stirred tank reactor at isothermal conditions (260 to 280°C) under vacuum (1 mbar) with titanium tetrabutoxide as catalyst (10 wt ppm). The reaction was run for different times and the product produced was analyzed with respect to molecular weight and molecular weight distribution and concentration of side products.

A mathematical model was developed including the polycondensation reaction, all major side reactions and mass transfer processes. With this model conversion of reaction, molecular weight and, concentration of side products can be modeled very well. In case of molecular weight distribution deviation between simulation and experiments are observed. Kinetic data of polycondensation process was extracted from simulation work and indicates that titanium tetrabutoxide is a more active but less selective catalyst than antimony triacetate. This is due to the fact that activation energies of all chemical reactions involved are much lower in case of titanium catalyst at conditions studied.

4.1 Introduction

Modeling in general has a high potential value to industry in terms of reactor design, scale up, process optimization, product structure control and reactor stability and safety. Consequently, great effort has gone into model development for PET process. However, due to many uncertainty surrounding to mechanism of catalyzed polycondensation; a wide range of models and kinetic results exist which often differ significantly. Moreover, the reaction kinetics of the polycondensation process is complicated by presence of side reactions and is still under investigation and is not unambiguously determined. The published data depend on the specific experimental procedures and applied catalysts and the resulting kinetic parameters vary with the assumed kinetic model and the applied data fitting procedure [1-13]. Table 4.1 represents published kinetic data of polycondensation reaction in synthesis of PET. The presented results were achieved by different determination methods. Effect of catalyst concentration is mostly included in the rate constant.

Table 4.1 Published kinetic data of polycondensation reaction of PET synthesis[1-13]

Year	Auther	Catalyst	K [-]	T [°C]	Ea [kJ mol^{-1}]	k [l^n mol^{-m} min^{-1}]
1960	Challa	No	$K=K(P_n)$	195-282	96	-
1968	Fontana	Pb, Zn, Ca, Sb	0.5	152-228	-	-
1969	Stevenson	Sb_2O_3	0.36	275	59 (Sb_2O_3), 167 (no cat)	0.6
1971	Hovenkamp	Sb_2O_3, Zn, Mn, Pb, Ca	0.8	197	-	-
1973	Tomita	Zn	-	270-300	99	-
1978	Yokoyama	Sb_2O_3	1	275,280,285	77 (Sb_2O_3), 167 (nocat)	$0.3\text{-}1.62\times10^{-1}$
1979	Chegolya	H^+, TPA	0.5	214,234,244	102	7.3
1980	Rafler	$SbAc_3$	-	270		1.55×10^{-1}
1980	Reimschuessel	H^+,Sb_2O_3	$\Delta S=-80.3$, $\Delta H=-38.1$	202,215,226	115(Sb_2O_3), 91.4 (H^+), 205 (no cat)	-
1986	Ravindranath	Sb_2O_3	0.5	290	77.3	6.8×10^5
1989	Yamada	Sb_2O_3	-	240-265	11.7	-
2000	Collins	No	-	270,280,290	168	-
2001	Rieckmann	No	-	287	92	8.9
2006	El-Toufaili	HT	-	dynamic	92	4.3×10^8

In general three types of methods were applied for kinetic investigation of polycondensation reaction: semi batch stirred tank reactor, thin film and thermal analysis method in which the micro scale of reactor is causing high specific surface area of reaction mass. The melt viscosity of reaction mixture increases rapidly with progressing polycondensation. As the polycondensation reaction is a reversible equilibrium reaction, the macro kinetics of the polycondensation process becomes more and more limited by the mass transfer of the volatising EG at higher conversion and temperature. A good reactor design should employ this knowledge concerning rate limitations. It should also provide a maximum specific surface area, ensuring minimum mass transfer distances, respectively an utmost thin polymer film.

The aim of this chapter is to evaluate kinetic parameters of titanium tetrabutoxide catalyzed PET synthesis and develop a mathematical model to predict conversion, molecular weight and concentration of side products.

4.2 Experimental part

4.2.1Chemicals

Oligomer with properties shown in table 4.2 was supplied by Equipolymers GmbH. A 2:1 weight ratio mixture of o-dichlorobenzol and phenol was from Organo Spezial Chemie GmbH. The chemicals used for analysis were bromophenol blue (>99%), chloroform (>98%), o-cresol (>99%) and potassium hydroxide solution in ethanol 0.1 N, which were supplied by Merck. All the reactants were used in the experiments without further purification and without especial treatments, except in the case of Cat 1, which was mixed with EG and kept under an inert atmosphere.

Table 4.2 Properties of oligomers used for polycondensation

$\mathbf{M_n}$ [mol/g]	$\mathbf{P_n}$	**[COOH]** [mmol kg^{-1}]
889	4-5	30

4.2.2 Polycondensation in lab scale stirred tank reactor

In previous studies, polycondensation was run in a glass reactor heated by salt bath to desired temperature, but due to better heat transfer from heating medium to reaction mixture, better temperature control and more safety during reaction run, glass reactor was replaced by metal reactor made of aluminium (Figure 4.1-b).

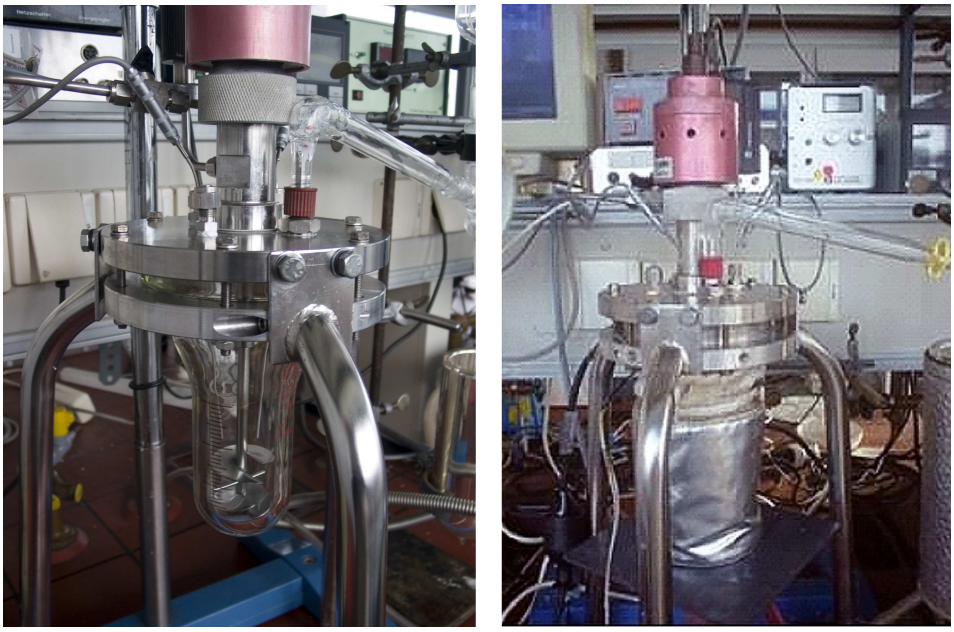

(a) (b)

Figure 4.1 (a) Glass reactor with helical stirrer, (b) Aluminium reactor equipped with electrical heater.

200 g of oligomers was filled into the 200 ml aluminium reactor and melted under nitrogen flow with stirring speed of 200 rpm. Catalyst was added to the melt and the reaction was stared by applying vacuum at different reaction temperature (260, 270, 280°C). The by- product of reaction, EG, was collected in a flask right after the condenser which was cooled by a mixture of water and triethylene glycol at temperature of -5°C. After a certain reaction time (2, 3, 4 h) polycondensation was stopped by purging with nitrogen. Due to instability of temperature and pressure, sampling at shorter reaction time was not reliable. The PET was removed from reactor in melt phase and cooled down to room temperature under nitrogen flow.

Reactor was equipped with two temperature sensor, one pressure sensor and one torque measurement sensor located on the motor of magnatice coupled stirrer. The presence of the second temperature sensor is due to safety reasons. Figure 4.2 shows the flow diagram of polycondensation setup.

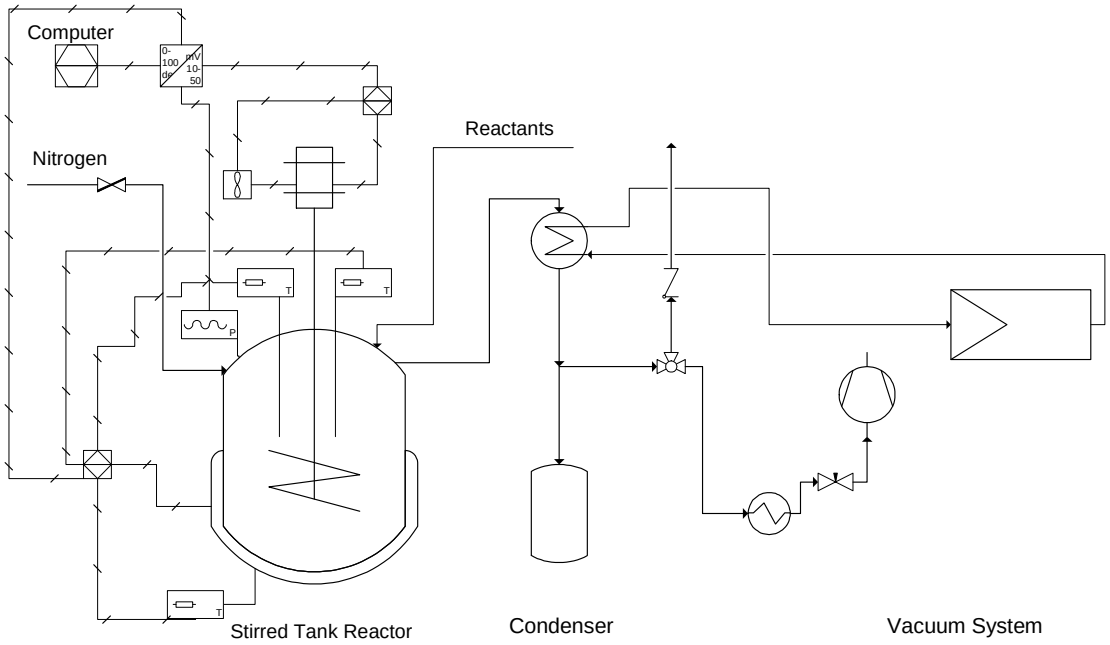

Figure 4.2 Flow diagram of polycondensation setup.

4.2.3 Polymer characterization

4.2.3.1 Determination of intrinsic viscosity of polymer

10 g of polymer was placed in a strainer and cooled by liquid nitrogen. The polymer was immediately ground to powder in a centrifugal mill (RETZSCH MZ 100) with 0.5 mm mesh bottom. The ground polymer was dried at constant temperature of 100°C in a halogen moisture analyzer of METTLER HG53. The dried sample was then dissolved in solvent mixture of phenol and 1,2-dichlorobenzene with a phenol concentration of 50 wt%. Homogeneous sample was filled in sample bottles and place in auto sampler of IV measurement instrument (SCHOTT AVSPro). The inner temperature of capillary was maintained at 25°C. The time that sample solution needs to pass the capillary is detected and the viscosity of the solution was calculated with the analytical equation supplied by Equipolymers GmbH. The measuring system is very precise and reproducible (error of ± 0.8).

By using of polymer samples with known molecular weight and measuring of intrinsic viscosity (IV), the following equation was defined to describe relation between number average molecular weight (M_n) and IV.

$$\ln(M_n) = IV^{1.4706} + 2.3458 \qquad (4.1)$$

4.2.3.2 Determination of carboxyl end groups concentration of polymer

1 g of polymer was added as powder in a titration flask along with 35 ml solvent (o-cresol/chloroform). The sample was dissolved for 15 min at 170°C in a heating block system and then cooled down to room temperature. The carboxyl end groups of polymer were titrated against 0.05 N potassium hydroxide using tetrabromophenol blue in ethanol as an indicator. The concentration of carboxyl end groups was calculated by application of following equation.

$$[COOH] = \frac{103(Q - B)}{m} \tag{4.2}$$

where Q [mmol] = consumed KOH [ml] × 0.05 [mol l^{-1}] × t

B [mmol] = solvent without sample= consumed KOH [ml] × 0.05 [mol l^{-1}] × t

m = mass of substance in g

t = titer for 0.05 N KOH by using bromobenzoic acid

The error of analysis was calculated to be ± 1%.

4.2.3.3 Determination of diethylene glycol content of polymer

About 1 g of the ground PET together with 30 ml methanol and zinc acetate as catalyst and tetraethylene glycol dimethyl ether as internal standard were introduced into a pressure container. The container was heated for 2 h at 220°C in an oven. The PET material was decomposed to diethylene glycol and methyl isophthalate.

The reaction solutions are analyzed by gas chromatography (PERKIN ELMER GC – Autosystem XL) after cooling to ambient temperature. The DEG and IPA amounts are calculated from the areas of the DEG and IPA ester peaks in relation to the internal standard peak. The GC was calibrated with defined amounts of DEG and IPA ester before.

4.2.3.4 Determination of acetaldehyde content of polymer

0.1 to 0.3 g of the ground PET sample is introduced into a 22 ml head space vial and closed with a PTFE-coated seal. Vials are tempered in a head space oven (headspace auto sampler - HS-40XL (PERKIN ELMER)) at 150°C for 90 minutes and then analyzed by GC (GC - AutoSystem XL (PERKIN ELMER)). The calibration is done by total evaporation of different acetaldehyde water mixtures.

4.2.4 Reproducibility of torque measurement and polymer viscosity

Figure 4.3 shows the diagram of torque of stirrer during polycondensation reaction at 260°C and 200 rpm for three runs. The obtained curves for all three measurements are in good agreement.

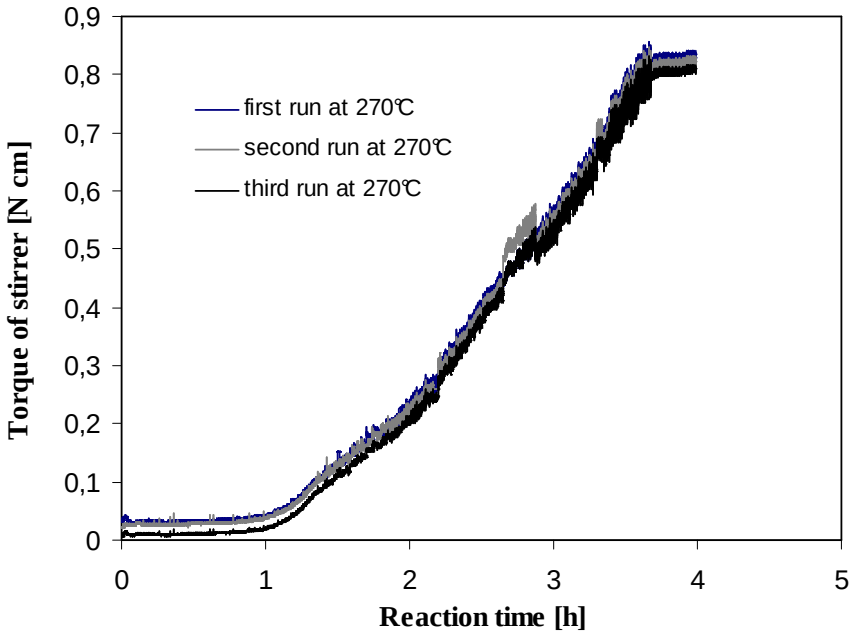

Figure 4.3 Reproducibility of torque of stirrer at three different runs

The reproducibility was also tested for intrinsic viscosity of PET, at different temperature and time. Table 4-2 shows the results. Each reported value is the average value of 3 different polycondensation runs for the certain temperature.

Table 4.3 Reproducibility of intrinsic viscosity of PET at different temperature and time. [Cat 1]: 10 wt ppm

Reaction temperature [°C]	**Reaction time** [h]	**IV** [dl g^{-1}]
260	3	0.465±0.004
260	4	0.518±0.005
270	3	0.522±0.005
270	4	0.602±0.006

4.3 Reaction model

The kinetic modeling of polycondensation was done based on following assumption:

Equal reactivity of functional end groups irregardless of polymer chain length (According to Flory theory).

A comprehensive model for PET formation was developed taking into account kinetic data, equilibrium data, and mass transfer processes for the volatilisation of major by-products, EG and water. Primary modeling in chapter 3 shows that a simple model including only irreversible polycondensation reaction (reaction 1) could fit experimental data at lower reaction temperature 260°C in which mass transfer and side reaction are not significant and polycondensation is just chemistry control. At higher temperature, and higher reaction viscosity, mass transport phenomena play an important role and polycondensation is controlled by evaporation of EG. Moreover, side reactions are more evident at high temperature. The following reactions are considered for modelling of PET synthesis:

Table 4.4 Reactions used for modeling

Nr.	Reaction scheme
1.	Polycondensation reaction 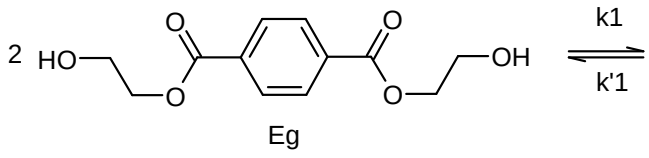 Eg 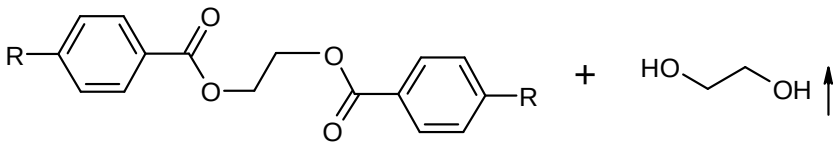 Z EG
2.	Polymer degradation 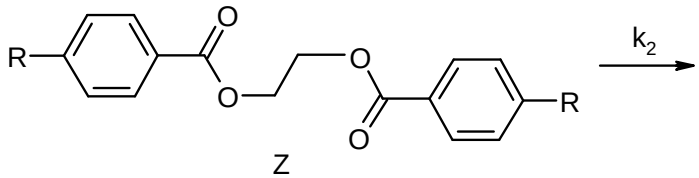 Z 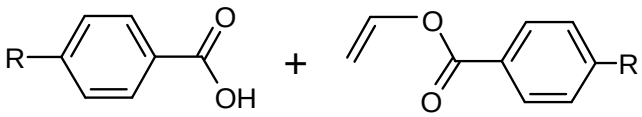 E_c E_v

3. Formation of AA

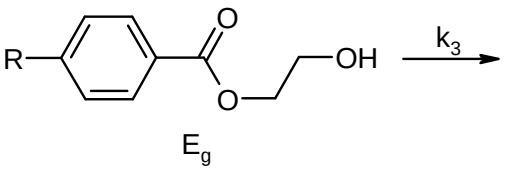

E_g

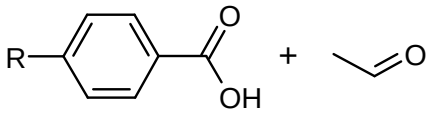

E_c AA

4. Formation of AA

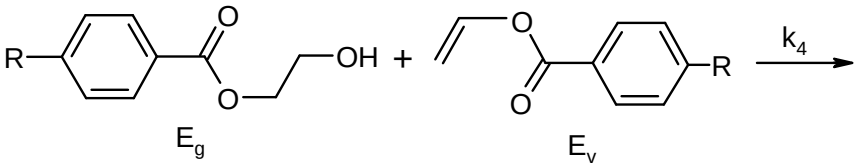

E_g E_v

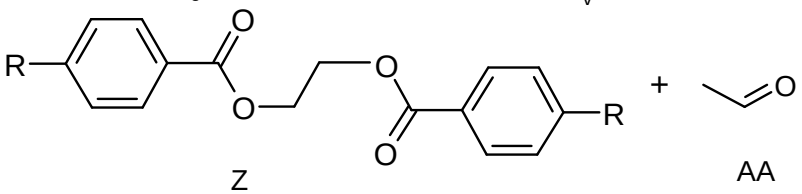

Z AA

5. Esterification reaction

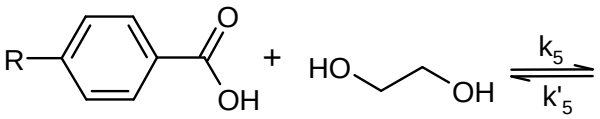

E_c EG

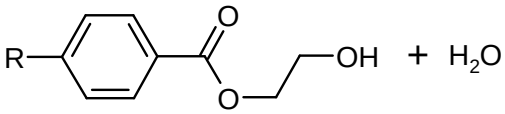

E_g W

6. Esterification reaction

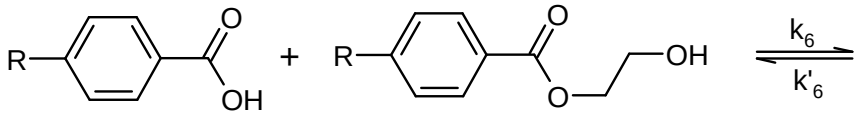

E_c E_g

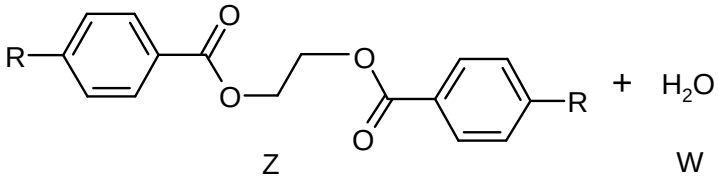

Z W

7. Formation of DEG

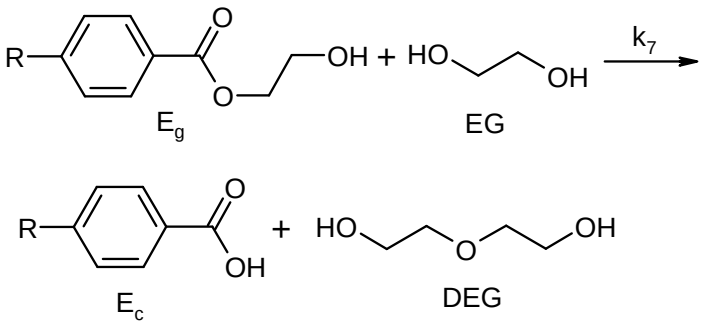

8. Formation of DEG

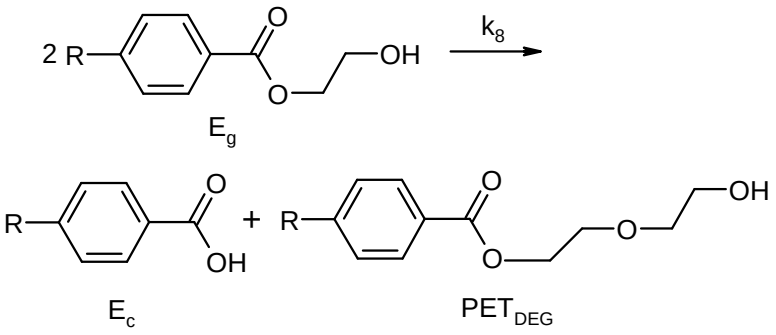

9. Formation of DEG

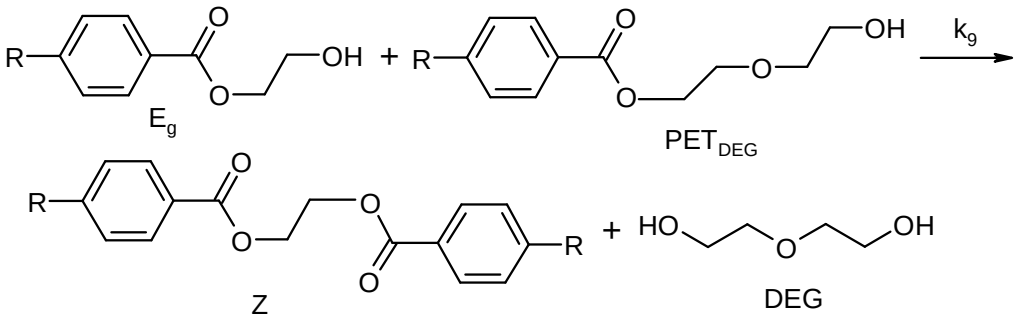

The rate expression of reactions 1-9 have following forms:

$$R_1 = k_1\left([Eg]^2 - \frac{[Z][EG]}{K_1} \right) = k_{1,0}[cat]\left([Eg]^2 - \frac{[Z][EG]}{K_1} \right) \quad (4.3)$$

$$R_2 = k_2\,[Z] \quad (4.4)$$

$$R_3 = k_3[Eg] \quad (4.5)$$

$$R_4 = k_4[Eg][Ev] \quad (4.6)$$

$$R_5 = k_5\left([Ec][EG] - \frac{[Eg][W]}{K_5} \right) \quad (4.7)$$

$$R_6 = k_6\left([Ec][Eg] - \frac{[Z][W]}{K_6}\right) \quad (4.8)$$

$$R_7 = k_7[Eg][EG] \quad (4.9)$$

$$R_8 = k_8[Eg]^2 \quad (4.10)$$

$$R_9 = k_9\left([PET_{DEG}][Eg] - \frac{[Z][DEG]}{K_9}\right) \quad (4.11)$$

where, k_1, and $k_{4\text{-}9}$ are second order rate constants, and k_2, k_3 are first order rate constants. K_1 is equilibrium constant of polycondensation reaction, K_5 and K_6 are equilibrium constants of esterification reactions. In equation 4.3, catalyst concentration is excluded from rate constant ($k_{1,0}$). In all other rate equations, concentration of catalyst is incorporated into the rate constant. It is assumed that catalyst concentration remains constant in the course of polycondensation.

In order to simplify the process of fitting parameters to experimental data and simplify the mathematical model, three main assumptions were done, following the general trend published for antimony catalyzed PET synthesis.

1- Irregardless of the end groups, the polycondensation reactions have the same rate constant. The assumption eliminates the need of considering three separated rate constants for the glycolate, DEG and vinyl end groups ($k_1 = k_4 = k_9$), and simplify the process of parameter fitting.
2- Two esterification reactions have the same rate constant, irregardless of the reactants involved ($k_5=k_6$).
3- All the side reactions of the chain ends have same probability of reacting and therefore, have same rate constant ($k_3 = k_7 = k_8$).

Mass transfer limitations

It was discussed that the melt viscosity increases with progressing polycondensation. As the transesterification reaction is a reversible equilibrium reaction, polycondensation process becomes more and more limited by the mass transfer of EG evaporation.

Modeling of PET synthesis catalyzed by titanium catalysts without application of mass transfer effect could not give the reliable fitting to the experimental results. Especially at elevated temperature where the viscosity of the reaction mixture increases strongly and transfer of by-product from reaction mixture is more problematic. Therefore it is needed to

consider a variable mass transfer coefficient of EG with respect to the degree of polymerization and temperature. The equation was introduced first by Reickmann et al.[3]:

$$k_m = k_{m,0} \exp(-0.043 P_n)(1 + 0.1(T - 267°C)) \quad (4.12)$$

Where k_m is the mass transfer coefficient, P_n is the degree of polycondensation, T is the temperature of the reaction mixture and $km,_0$ is the initial value of the mass transfer coefficient, which in the case of the different conditions in the system can be obtained by fitting to the experimental data.

Therefore the rate of mass transfer of EG express as follows:

$$R_m = k_l a([EG]_L - [EG]_0) = k_m([EG]_L - [EG]_0) \quad (4.13)$$

$[EG]_l$ is concentration of EG in melt phase and $[EG]_0$ is interfacial concentration. Furthermore, similar equation can describe the rate of mass transfer of water

$$R_w = k_w([W]_L - [W]_0) \quad (4.14)$$

$[W]_l$ is concentration of water in melt phase and $[W]_0$ is interfacial concentration. For calculation of mass transfer coefficient of water, the following initial assumption was considered and the final value was obtained by fitting.

$$k_w = (m_{EG} / m_w)^{1/2} k_m \quad (4.15)$$

The interfacial concentration of EG and water can be obtained by considering vapour-liquid phase equilibrium concept. In the present work only the total content of DEG (free DEG and DEG incorporated in the polymer chain) could be measured. Furthermore, since the vapour pressure of AA is very high at polycondensation temperature, it is assumed that AA is removed instantly at it formed. The low molecular weight oligomers have very low vapour pressure and are assumed to be non volatile. Therefore, initially the phase equilibrium in the interface is considered just only for EG and water. The interfacial concentration $[i]_0$ or the corresponding mole fraction, x_i, (i: EG, Water) of each volatile in the interface can be calculated from the vapour pressure P_i^0 and the activity coefficient γ_i taken from the Flory–Huggins model. In this work, the values reported by Laubriet et al. [7] are used:

$$[i]_0 = \left(\frac{[PET]}{1 - (x_{EG} + x_w)} \right) x_i \quad (4.16)$$

The vapour phase is assumed to follow the ideal gas low.

$$x_i \gamma_i P_i^0 = P_t y_i \quad (4.17)$$

Vapour pressure for EG and water is calculated by

$$\ln P_{EG}^{0} = 49.703 - \frac{8576.7}{T} - 4.042\ln(T) \tag{4.18}$$

$$\ln P_{W}^{0} = 18.568 - \frac{4047.66}{T - 33.3} \tag{4.19}$$

At polycondensation reaction temperature, vapour pressure of water was calculated to be much higher and the partial pressure of water at reaction pressure is smaller than EG. Therefore, the phase equilibrium is considered for EG which means vapour phase contain only EG and interfacial concentration of water is zero.

For calculation of activity coefficient:

$$\gamma_{EG} = \frac{1}{m_i}\exp\left[1 - \frac{1}{m_i} + \chi_{PET}\right] \tag{4.20}$$

In which m_i is the ratio of molar volume of polymer to molar volume of EG, χ_{PET} is Flory-Huggins interaction parameter and is taken approximately as 1.3 for EG.

The volume of the melt phase occupied by EG per volume of reaction mixture is given by:

$$\upsilon = \frac{M_{EG}[EG]_L}{\rho_{EG}} \tag{4.21}$$

and the molar volume of polymer is calculated by

$$\overline{\upsilon} = \frac{1 - \upsilon}{[PET]} \tag{4.22}$$

The material balance at vapour-liquid phase equilibrium are expressed by

$$y_{EG} = 1 \tag{4.23}$$

$$x_{EG} + x_{PET} = 1 \tag{4.24}$$

Hence, equation 4.16 is rewritten as

$$[EG]_0 = \left(\frac{[PET]}{1 - x_{EG}}\right)x_{EG} \tag{4.25}$$

The material balance equations of reaction components are:

$$\frac{d[Eg]}{dt} = -2R_1 - R_3 - R_4 + R_5 - R_6 - R_7 - 2R_8 - R_9 \tag{4.26}$$

$$\frac{d[EG]_L}{dt} = R_1 - R_m - R_5 - R_7 \tag{4.27}$$

$$\frac{d[AA]}{dt} = R_3 + R_4 \quad (4.28)$$

$$\frac{d[DEG]}{dt} = R_7 + R_9 \quad (4.29)$$

$$\frac{d[Ev]}{dt} = R_2 - R_4 \quad (4.30)$$

$$\frac{d[W]}{dt} = R_5 + R_6 - R_w \quad (4.31)$$

$$\frac{d[Ec]}{dt} = R_2 + R_3 + R_7 + R_8 - R_5 - R_6 \quad (4.32)$$

$$\frac{d[PET_{DEG}]}{dt} = R_8 - R_9 \quad (4.33)$$

$$\frac{d[Z]}{dt} = R_1 - R_2 + R_4 + R_6 + R_9 \quad (4.34)$$

The kinetic parameters which were used for a first fitting test are taken from literature [1, 3] and are listed in table 4.5. The activation energy of PET degradation was the value obtained by degradation study in TGA in chapter 3.

Table 4.5 Data used for parameter estimation

Reaction	**Rate constant**	$\mathbf{k_{0,i}}$ [l^n mol^{-m} min]	$\mathbf{E_a}$ [$kJ\ mol^{-1}$]	**K** [-]
Poylcondensation	$k_1=k_6=k_9$	6.80×10^5	77.4	0.5
Degradation of PET	k_2	3.09×10^9	176.0	-
Acetaldehyde formation	$k_3=k_6$	4.16×10^7	95.0	-
Esterification of E_c	$k_4=k_5$	1.04×10^6	73.6	1.25
DEG formation	$k_7=k_8$	4.16×10^7	95.0	-

The software packages, PREDICI® from company CiT GmbH and Berkley Madonna were applied to develop the model. The simulation was performed with following steps:

- Sensitivity studies which was applied to find out how dramatic the effect of varying one constant might be for a certain property or variable and also for whole simulation. The following priorities were found: 1) rate constant of polycondensation, 2) rate constant of degradation, 3) rate constant of side reactions involved at chain end, 4) rate constant of esterification and 5) mass transfer coefficient.
- Parameter estimation which was based on fitting of reaction rate constants to the reliable set of experimental data

4.4 Experimental results

Effect of temperature on the reaction progress was studied by running polycondensation at different reaction temperatures for different times.

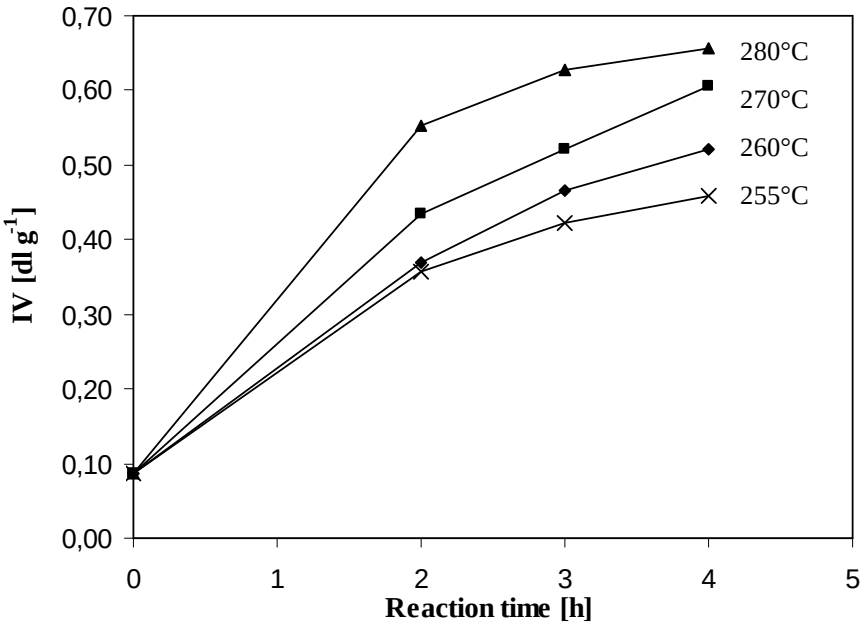

Figure 4.4 Intrinsic viscosity of PET at different temperatures ([Cat 1]: 10 wt ppm).

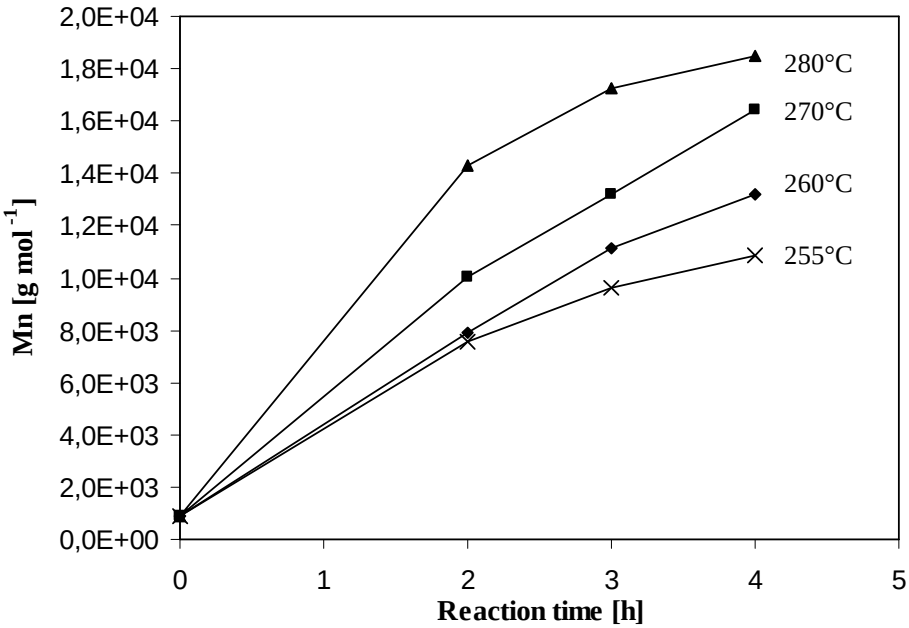

Figure 4.5 Number average molecular weight of PET at different temperatures ([Cat 1]:10 wt ppm).

Figure 4.4 and 4.5 show increase of IV and M_n of PET during synthesis with 10 wt ppm of Cat 1 at different temperatures. The progress of molecular weight with reaction time at high temperature shows a deviation from linear behaviour expected of a simple irreversible second order reaction. The reasons might be presence of backward reaction, increase of rate of side reactions and mass transfer limitations caused by high viscosity of reaction mixture with progress of reaction.

Effect of variation of catalyst concentration on Mn of polymer is shown in figure 4.6. During polycondensation reaction in presence of 30 wt ppm of Cat 1, the increase of viscosity after 3.5 h was very strong and stirrer was not able to rotate. It seems variation of molecular weight deviates from linearity in presence of 30 wt ppm of catalyst. Therefore, this concentration is the border to enter to completely mass transfer control regime at 260°C.

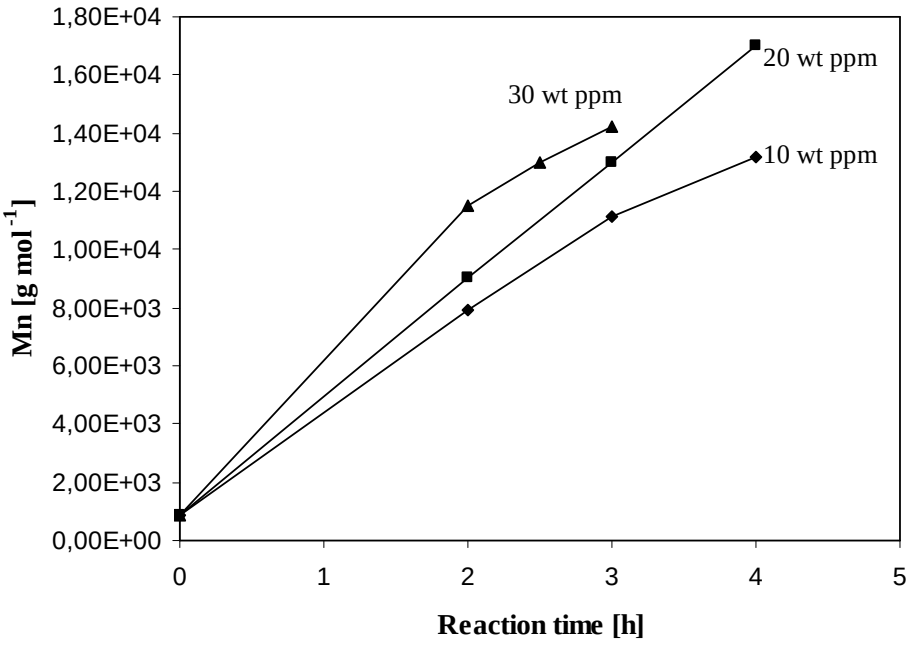

Figure 4.6 Number average molecular weight of PET at different Cat 1 concentrations (260°C).

Figure 4.7 and 4.8 shows the progress of formation of DEG during PET synthesis at different temperature and catalyst concentration. However, one should consider that the measured values are total amount of DEG. In general formation of DEG is severe at higher temperature which might be due to the high overall activation energy. Moreover, catalyst concentration did not have strong effect on formation of DEG. Furthermore, the DEG

content of all synthesised PET was much less than limited values for industrial production of PET.

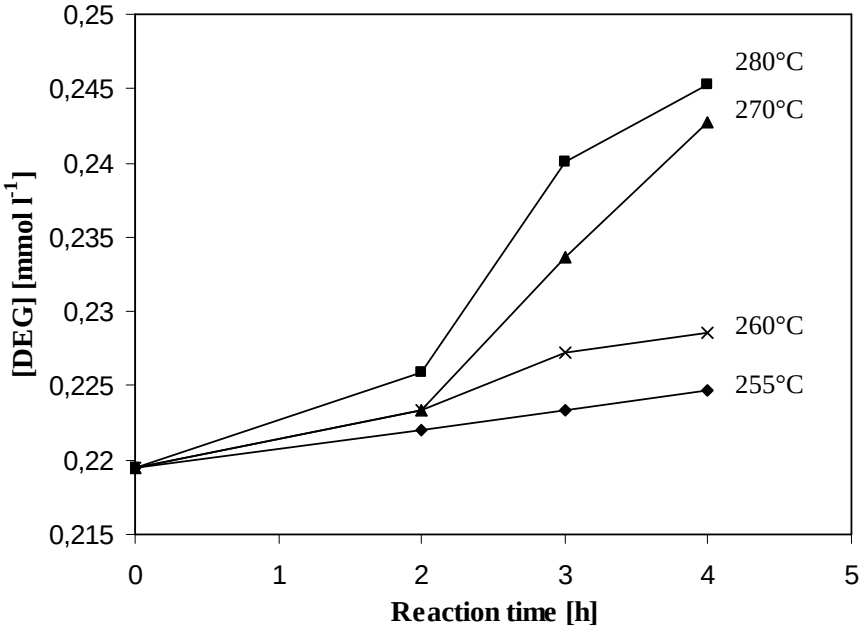

Figure 4.7 DEG formation at different temperatures ([Cat 1]: 10 wt ppm).

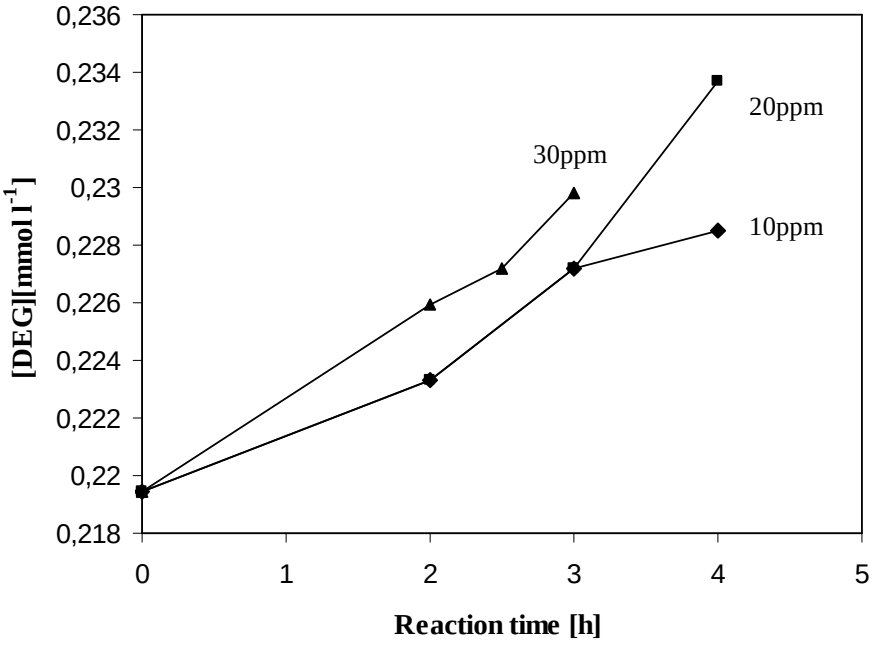

Figure 4.8 DEG formation at different Cat 1 concentrations (260°C).

4.5 Modeling results and discussion

Figure 4.9 presents fitting of reaction conversion with the reaction model presented in table 4.4 and the kinetic data in table 4.6.

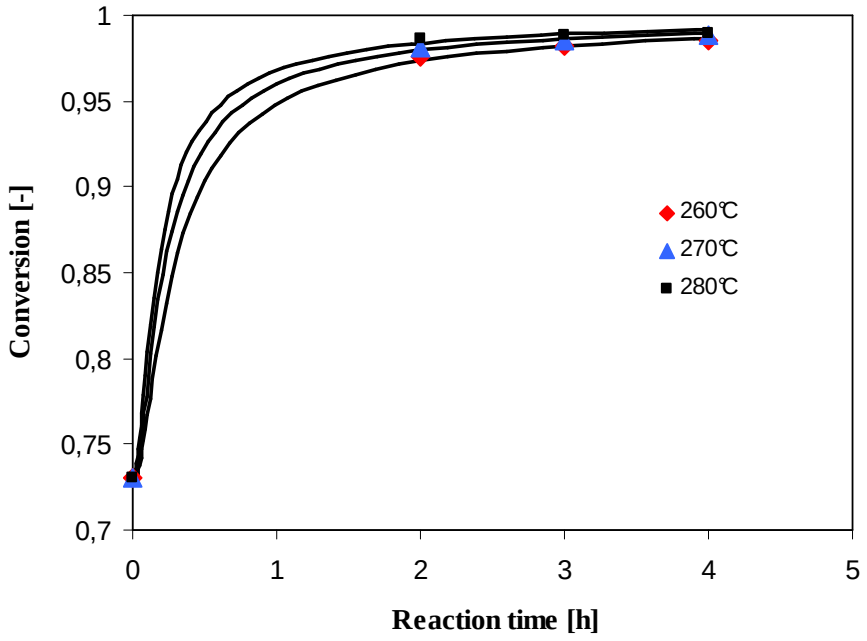

Figure 4.9 Fitting of conversion at different temperatures ([Cat 1]:10 wt ppm). Dots are experimental data and bold lines are model.

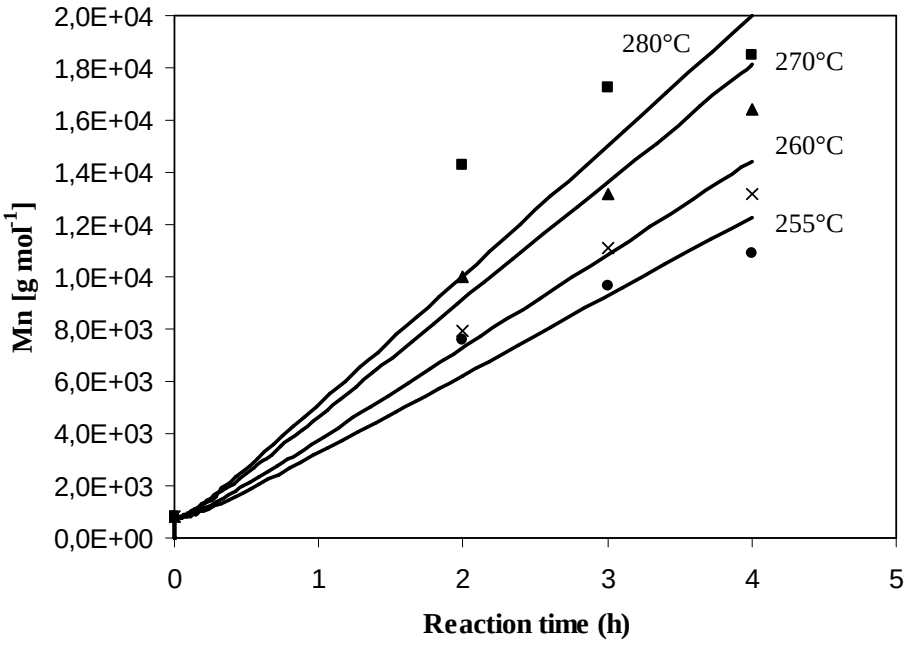

Figure 4.10 Modeling of number average molecular weight of PET at different temperatures in case of an irreversible polycondensation and absence of side reactions ([Cat 1]:10 wt ppm). Dots are experimental data and bold lines are model data.

One should consider that good fitting quality of reaction conversion could even be achieved by considering only an irreversible polycondensation reaction which is not the case for modeling of number average molecular weight (Figure 4.10). The most important

part of modeling is fitting of average molecular weight of PET which is influenced by side reaction and reaction temperature. The quality of fitting molecular weight of PET with the set of data in table 4.6 can be seen in figure 4.11.

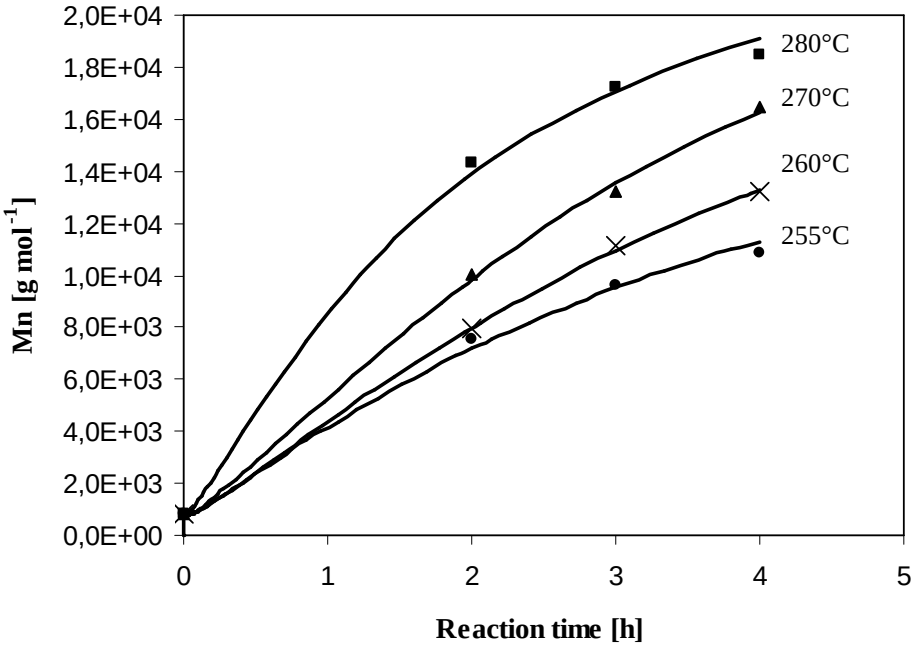

Figure 4.11 Fitting of number average molecular weight of PET at different temperature with the model introduced in session 4.3. The points are experimental data and the lines are simulations ([Cat 1]: 10 wt ppm).

The progress of M_n with reaction time at different temperatures is quite different from progress of conversion because it is more affected by increase of rate of side reactions and backward reaction. The following equations express the relation between number average molecular weight and degree of polycondensation and the reaction conversion. The α value is the ratio of concentration of carboxylic end group to the total end groups concentration. This value depends strongly to the rate of side reactions like esterification and polymer chain degradation and increases at high temperature.

$$P_n = \frac{1}{1-x} \tag{4.35}$$

$$M_n = 192P_n + 62 - 2(44\alpha) \tag{4.36}$$

$$\alpha = \frac{[COOH]}{[OH]+[COOH]} \tag{4.37}$$

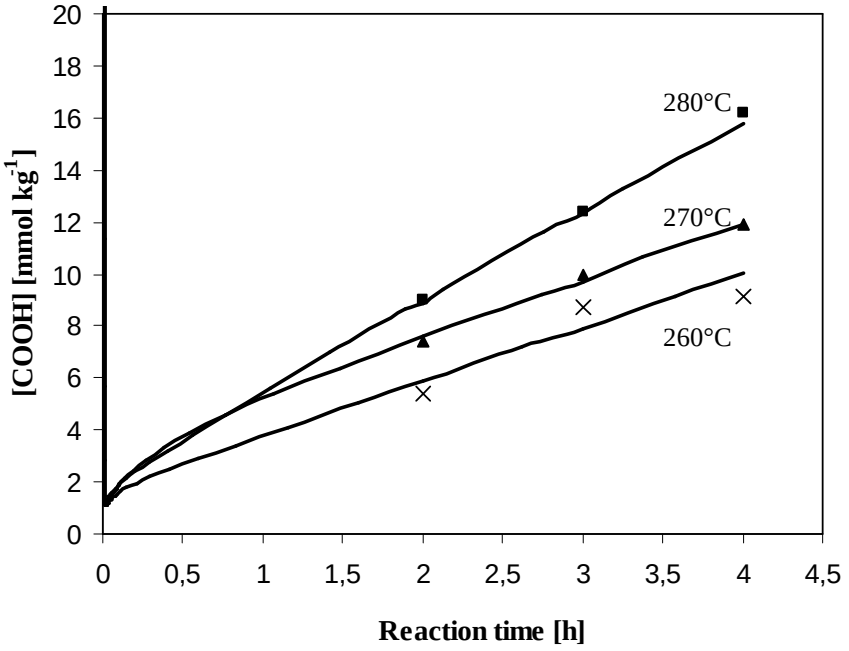

Figure 4.12 Fitting of carboxyl end groups concentration at different temperatures ([Cat 1]: 10 wt ppm). The points are experimental data and the lines are simulations.

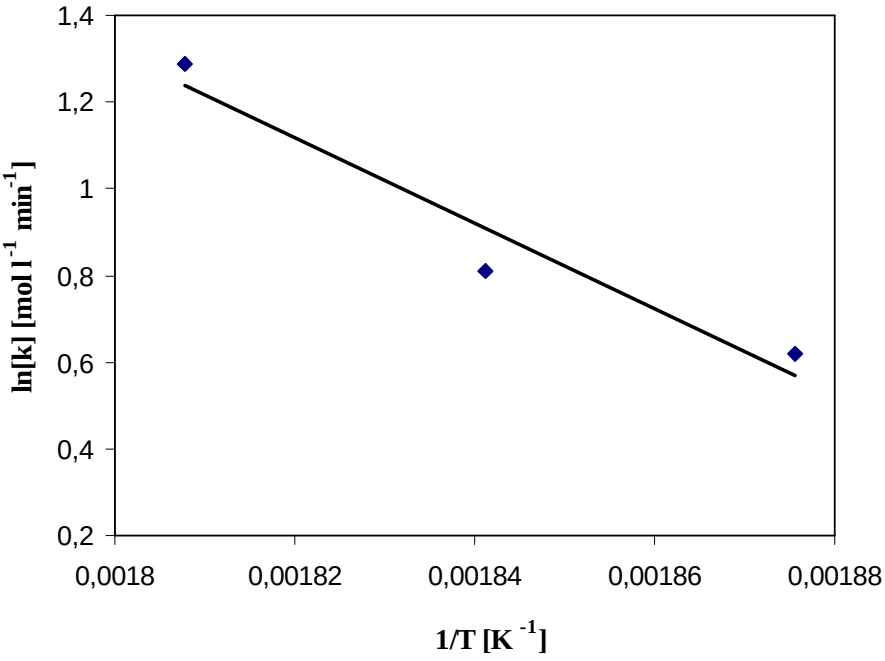

Figure 4.13 Arrhenius plot of overall rate constant of formation of carboxyl end groups during polycondensation of BHET oligomers.

The model can also predict variation of carboxyl end groups concentration in the polymeric product (Figure 4.12). The sharp decay of concentration of carboxyl end groups in the beginning of reaction is due to the initial strong increase in the esterification rate

caused by strong reduction of pressure which induces more efficient removal of by-product water [14]. By consumption of carboxyl end groups, the esterification rate reduces and the side reactions produce carboxyl end groups during reaction. Due to pressure instability of the system in the initial stage of the reaction, initial experimental data could not be obtained to smooth this sharp decay by fitting to experimental points. The experimental results show that overall rate of production of carboxyl end groups is a zero order reaction between 2 and 4 h of reaction time. By applying Arrhenius equation (Figure 4.13), the overall activation energy of formation of carboxyl end groups was calculated to have a value of 82 kJ mol^{-1}. One should consider that this value is an overall value and includes all side reactions which involve in formation or consumption of carboxyl end groups.

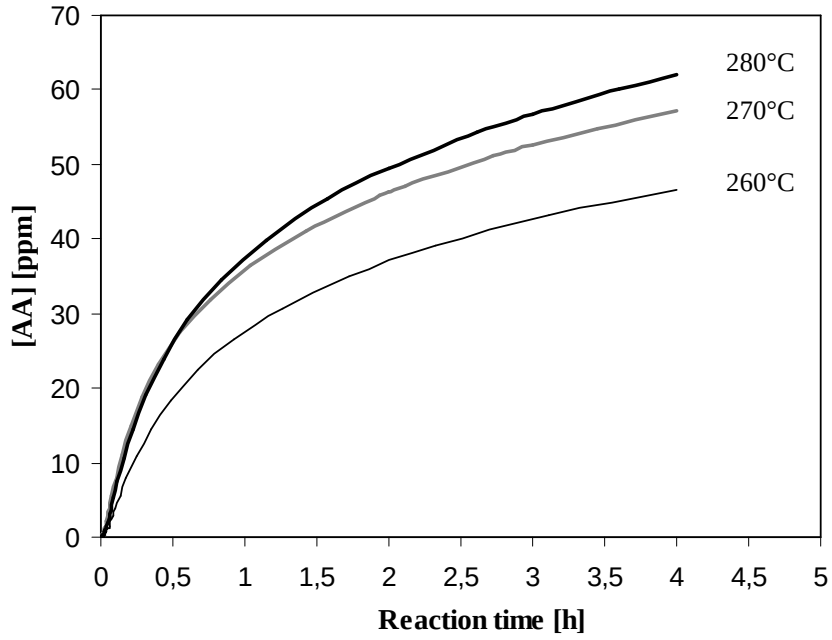

Figure 4.14 Simulation of AA concentration during polycondensation reaction ([Cat 1]:10 wt ppm).

Model could also predict the variation of concentration of AA and free DEG in the course of polycondensation reaction. However, unreliability of analytical results of determination of AA content caused by operational error during sampling and storage of PET samples led to variation of AA content even for the same sample. Therefore, it was not possible to do fitting process.

In case of DEG content, as mentioned the characterization method detected total amount of DEG, therefore the experimental results could not be fitted.

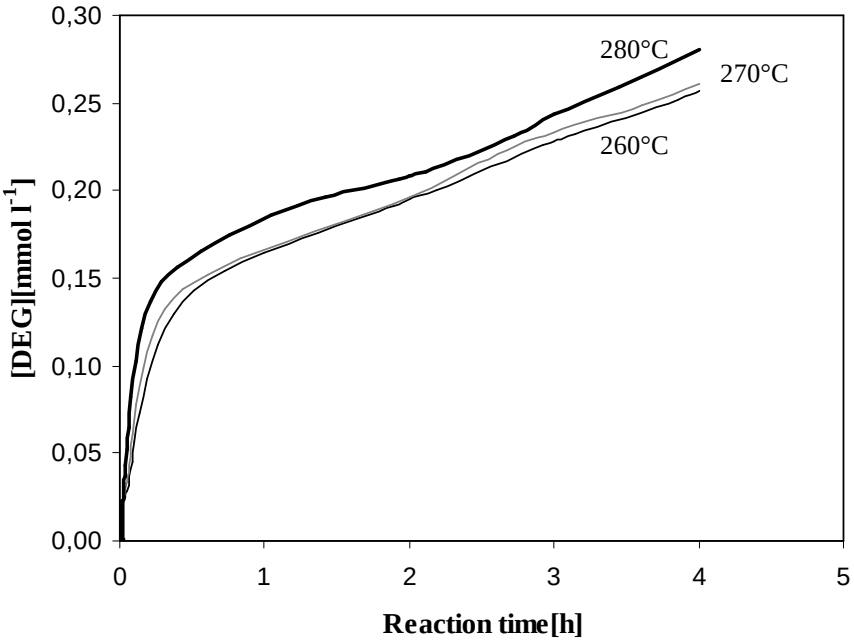

Figure 4.15 Simulation of increasing of free DEG concentration during polycondensation reaction ([Cat 1]: 10 wt ppm).

Table 4.6, presents kinetic data of optimal modeling of PET synthesis including side reactions and mass transfer process. The activation energy of 63 kJ mol^{-1} of polycondensation reaction with titanium catalyst is lower than the one of antimony catalyst (77 kJ mol^{-1}).

Table 4.6 Kinetic data obtained by simulation of PET synthesis in melt phase with Cat 1

Paratemer	Polycondensation*	PET degradation	AA formation	DEG formation	Esterification
Ea [kJ mol^{-1}]	63	165	71	71	48
$k_{0,i}$ [l^n mol^{-m} min]	4.8×10^7	7.85×10^9	2.91×10^4	2.91×10^4	5.73×10^3

* Effect of catalyst concentration on frequency factor is excluded.

Table 4.7 Initial overall mass transfer coefficient ($k_{m,0}$) for different temperatures

Reaction Temperature [°C]	$k_{m,0}$ [min^{-1}]
255	1.62
260	2.05
270	2.76
280	2.92

Table 4.7, shows the initial value of overall mass transfer coefficient ($k_{m,0}$) achieved by data fitting which increases with increasing temperature.

4.6 Modeling of molecular weight distribution

Modeling of molecular weight distribution (MWD) was executed using the same simulation program. The MWD of the polymer samples produced at 260°C and 280°C with 10 wt ppm of Cat 1 was simulated first by using the reaction scheme listed in table 4.4. The result of simulation was a very narrow MWD (PDI less than 2) for reaction at 260 and 280°C (Figure 4.16).

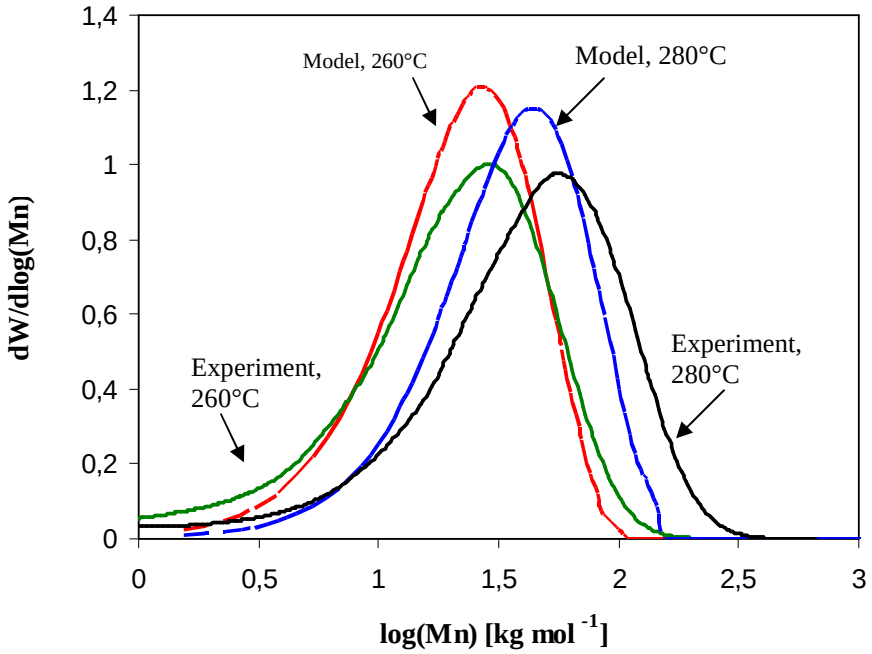

Figure 4.16 Molecular weight distribution of PET synthesised at 260 and 280°C [Cat 1]:10 wt ppm.

Table 4.8 Polydispersity index of PET after 4 h of reaction at different temperatures

Reaction Temperature [°C]	**Source**	**PDI** [-]
260	GPC	2.45
	Model	1.92
280	GPC	3.78
	Model	1.90

The PDI values obtained by GPC measurements (GPC 1100 of Agilent) and modeling are reported in table 4.7. The large differences between these values indicate the necessity to improve the model by introduction of side reactions leading to formation of short and long chain polymers which are missing in simulated MWD curve.

PET chains undergo interchange reactions. Interchange involves reaction between the terminal functional groups of the one polymer molecule with repeating units of another polymer chain. Free interchange corresponds to all repeating units in all polymer chain having equal probability of interchange. This is analogous to the concept of functional group reactivity independent of molecular size [11]. Therefore, interchange reactions does not affect the degree of polymerization but they can affect the MWD. The following interchange reaction was introduced in the reaction scheme of model and no effect on simulated MWD was found.

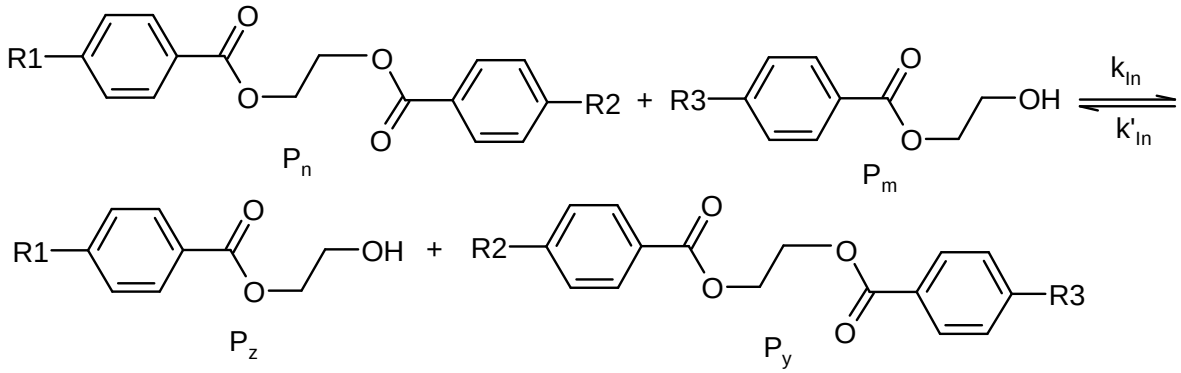

Scheme 4.1 Interchange reaction between hydroxyl end group and polymer chain repeating unit.

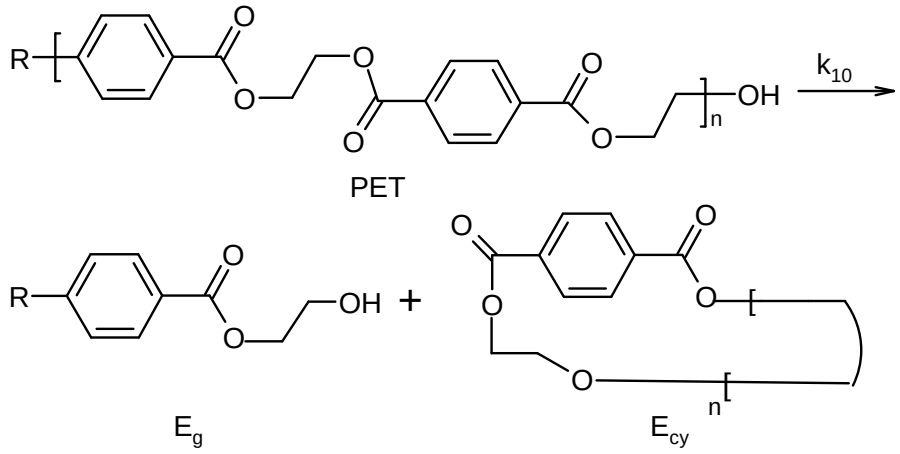

Scheme 4.2 Formation of cyclic oligomers by back biting mechanism.

Another side reaction which might affect MWD is formation of cyclic oligomers which is a slow reaction. Among the oligomers, the cyclic trimer has been postulated to be uniquely stable [15, 16]. This could be due to either a mechanism favouring the formation of trimer (kinetic control) or to trimer having a lower energy than other oligomers (thermodynamic control), thus decreasing of rate of further reaction [17]. A back biting mechanism

(cyclodepolymerization) has been proposed as a probable mechanism for oligomer formation [16] (Scheme 4.2).

By introducing of cyclization reaction in the model, the fitting of model to the GPC results improved specially at 260°C.

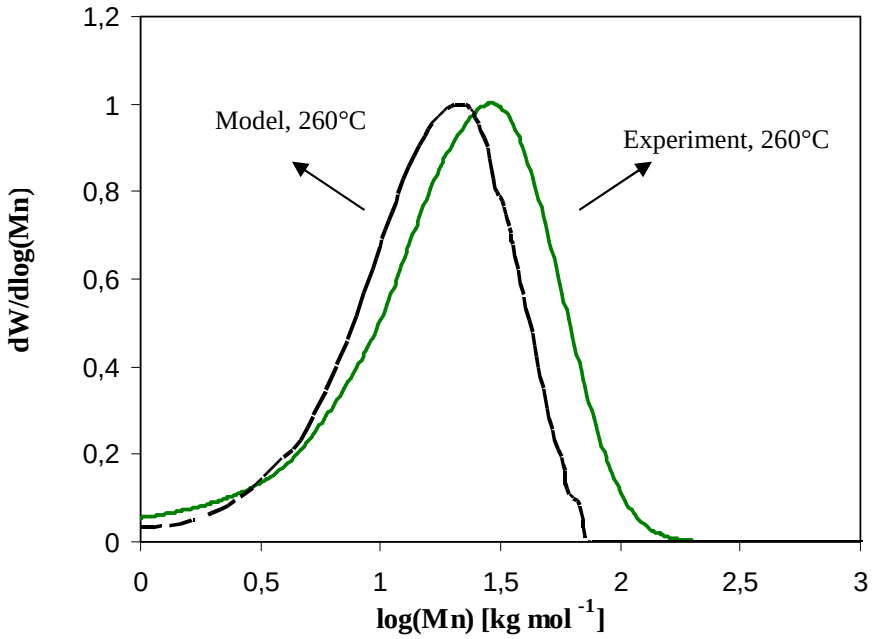

Figure 4.17 Fitting of molecular weight distribution of PET by modified model with cyclization reaction.

Table 4.8 Polydispersity index of PET after 4 h of reaction at 260°C

Reaction Temperature [°C]	**Source**	**PDI** [-]
260	GPC	2.45
	Modified model	2.21

4.7 Conclusion

A rather complex reaction scheme must be used to simulate PET synthesis especially when many parameters should be modeled.

In order to develop a very precise model for MWD, further side reactions should be introduce into the reaction scheme to cover whole range of molecular weight at elevated temperatures.

4.8 References

[1] K. Ravindranath, R. A. Mashelkar, *J. Appl. Polym. Sci.*, **26**, 3179 (1981)

[2] K. Ravindranath, R. A.Mashelkar, *J. Appl. Polym. Sci*., **2**7, 2625 (1982)

[3] J. Scheirs, T. E. Long, *Modern Polyesters: Chemistry and Technology of Polyesters and Copolyesters,* John Wiley & Sons (2003)

[4] F. -A. El-Toufaili, G. Feix, K.-H. Reichert, *Macromol. Mat. Eng.*, **291**, 114 (2006)

[5] W. Zimmerer, *PhD Thesis,* Swiss Federal Institute of Technology, Lausanne (1997)

[6] C.-K. Kang, *J. Applied Polym. Sci*. **63**, 163 (1997)

[7] C. Laubriet, B.LeCorre, K. Y.Choi, *Ind. Eng. Chem. Res.*, **30**, 2 (1991)

[8] C. M. Fontana, *J. Polym. Sci.*, Part A-1, **6**, 2343 (1968)

[9] K. Ravindranath, R. A. Mashelkar, *Polym. Eng. Sci.*, **22**, 610 (1982)

[10] K. Ravindranath, R. A. Mashelkar, *Polym. Eng. Sci.*, **22**, 619 (1982)

[11] K. Ravindranath, R. A. Mashelkar, *Polym. Eng. Sci*., **22**, 628 (1982)

[12] T. Yamada, Y. Imamura, *Polym. Plast. Technol. Eng.*, **28**, 811 (1989)

[13] L. Finelli , *J. Appl. Polym. Sci.*, **92**, 1887 (2004)

[14] G. W. Parshall, S. D. Ittel, Homogeneous *Catalysis*, 2nd Edition, John Wiley & Sons, INC (1992)

[15] I. Goodman, B. F. Nesbitt, *Polymer.*, **1**, 384 (1960)

[16] A. L. Cimecioglu, S. H. Zeronian, K. W. Alger, M. J. Collins, G. C. East, *Appl. J. Polym. Sci.*, **32**, 4719 (1986)

[17] L. H. Peebles, M. W. Huffmann, C. T. Ablett, *J. Polym. Sci., Part A-1*, **7**, 479 (1969)

Abbreviation

AA	Acetaldehyde
Abs	Absorbance
ADA	Adipic acid
AI	Activity index
BHET	Bis (hydroxyethylene) terephthalate
BPA	Bisphenol A
BPC	Bisphenol C
Bu	Butanol
Cat	Catalyst
CSD	Carbonated soft drink
DEG	Diethylene glycol
DMT	Dimethyl terephthalate
DPC	Diphenyl carbonate
DSC	Differential scanning calorimetry
E_c	Carboxyl terminal
E_{cy}	Cyclic terminal
EG	Ethylene glycol
E_g	Glycolate terminal
EGMB	Ethylene glycol monobenzoate
ET	Ethylene segment
E_v	Vinyl terminal
GC	Gas chromatography
GPC	Gel permission chromatography
HE	Hydroxy ethylene segment
HMD	Hexamethylene diamine
HPPA	High performance polyamide
HT	Hydrotalcite
IPA	Isophthalate
IR	Infrared spectroscopy
IV	Intrinsic viscosity
MTR	Melt to resin

MWD	Molecular weight distribution
PA	Polyamide
PA 6	Polyamide 6
PA 66	Polyamide 66
PDI	Polydispersity index
PBT	Polybuthylene terephthalate
PC	Polycarbonate
PE	Polyethylene
PE	Polyester
PET	Polyethylene terephthalate
PP	Polypropylene
PS	Polystyrene
PTA	Purified terephthalic acid
PUR	Polyurethane
PVC	Polyvinyl chloride
Sb	Antimony
SSP	Solid state polycondensation
STR	Stirred tank reactor
Syn.Elas	Synthetic elastomer
T	Terephthalic segment
TA	Thermal analysis
TBBPA	Tetrabromobisphenol A
TE	Terephthalate segment
TMBPA	Tetramethylbisphenol A
TGA	Thermogravimetric analysis
TVO	Trinkwasserverordnung
VK	Vereinfacht Kontinuierlich tube
W	Water
Z	Diester

Symbols

a_A	Activity of amine terminal	[-]
a_c	Activity of carboxyl terminal	[-]
a_L	Activity of polymeric amide	[-]
α	Ratio of concentration of carboxylic end groups to concentration of total end groups	[-]
AI	Activity index based on DSC measurment	[°C^{-1}]
AI	Activity index based on torque measurement	[mN cm min^{-1}]
B	Amount of solvent without sample for titration	[mmol]
β	Heating rate	[K min^{-1}]
C	Integration constant	[-]
$C_{P, MR}$	Heat capacity of the reference measuring system	[J K^{-1}]
$C_{P, MS}$	Heat capacity of the sample measuring system	[J K^{-1}]
$C_{P, R}$	Heat capacity of the reference	[J K^{-1}]
$C_{P,S}$	Heat capacity of the sample	[J K^{-1}]
[COOH]	Concentration of carboxyl end groups	[mol l^{-1}]
D	Difference in concentration of acid and amine end groups	[mol l^{-1}]
ΔH_R	Enthalpy of reaction	[J mol^{-1}]
E	Molar expansivity of polymeric segment	[l mol^{-1}K^{-1}]
[E]	Concentration of total end group of PET	[mol l^{-1}]
E_a	Activation energy	[J mol^{-1}]
$E_{a,x}$	Activation energy at x conversion	[J mol^{-1}]
$[EG]_0$	Interfacial concentration of ethylene glycol	[mol l^{-1}]
$[EG]_L$	Concentration of ethylene glycol in melt phase	[mol l^{-1}]
f(x)	Reaction progress as function of conversion	[-]
IV	Intrinsic viscosity	[dl g^{-1}]
K	Calibration constant of DSC	[J s^{-1} K^{-1}]
K_{app}	Apparent equilibrium constant	[-]
k	Rate constant of forward reaction	[l^{n}mol^{-m} min^{-1}]
k´	Rate constant of backward reaction	[l^{n}mol^{-m} min^{-1}]
k_c	Rate constant of forward catalyzed transesterification	[l^2 mol^{-2}min^{-1}]

$k´_c$	Rate constant of reverse catalyzed transesterification	$[l^2\ mol^{-2}min^{-1}]$
k_i	Rate constant	$[l^n mol^{-m}\ min^{-1}]$
k_h	Rate constant of hydrolysis	$[l^n mol^{-m}\ min^{-1}]$
$k_{1,0}$	Rate constant of polycondensation excluding of catalyst concentration	$[l^2 mol^{-2}\ min^{-1}]$
k_0	Frequency factor of Arrhenius equation of rate constant	$[l^n mol^{-m}\ min^{-1}]$
$k_{0,i}$	Frequency factor of Arrhenius equation of rate constant	$[l^n mol^{-m}\ min^{-1}]$
K_i	Equilibrium constant	[-]
$k_{m,0}$	Initial overall mass transfer coefficient	$[min^{-1}]$
k_m	Overall mass transfer coefficient of ethylene glycol	$[min^{-1}]$
k_u	Rate constant of uncatalyzed transesterification	$[l\ mol^{-1}min^{-1}]$
$k´_u$	Rate constant of reverse uncatalyzed transesterification	$[l\ mol^{-1}min^{-1}]$
k_w	Overall mass transfer coefficient of water	$[min^{-1}]$
m	Order of reaction rate constant	[-]
m	Mass of substance	[g]
m_0	Initial sample mass	[g]
m_f	Mass of residual sample	[g]
m_t	Sample mass at time t	[g]
m_i	Ratio of molar volume of polymer to volatile	[-]
M	Molar mass	
M_{BHET}	Molar mass of bis (hydroxyethylene) terephthalate	$[g\ mol^{-1}]$
M_{EG}	Molar mass of ethylene glycol	$[g\ mol^{-1}]$
M_n	Number average molecular weight	$[g\ mol^{-1}]$
M_T	Torque of stirrer	[N cm]
n	Order of reaction rate constant and number of polymer repeating units	[-]
$n_{t,EG}$	Amount of produced ethylene glycol at time t	[mol]
$n_{t,ET}$	Amount of ethylene segment at time t	[mol]
$n_{t,HE}$	Amount of hydroxyl ethylene segment at time t	[mol]
$n_{t,TE}$	Amount of terephthalate segment at time t	[mol]
[OH]	Concentration of hydroxyl end groups	$[mol\ l^{-1}]$
[P]	Concentration of end product of polyamidation	$[mol\ l^{-1}]$

$[P_{eq}]$	Concentration of end product of polyamidation at equilibrium	[mol l^{-1}]
P_p^0	Vapour pressure of phenol	[Pa]
P_{DPC}^0	Vapour pressure of diphenyl carbonate	[Pa]
P_{EG}^0	Vapour pressure of ethylene glycol	[Pa]
P_w^0	Vapour pressure of water	[Pa]
P_n	Degree of polymerization	[-]
Q	Amount of consumed KOH for titration	[mmol]
$\dot{Q}_{Chem}$	Reaction heat flow	[J s^{-1}]
$\dot{Q}_R$	Heat flow to the reference	[J s^{-1}]
$\dot{Q}_S$	Heat flow to the sample	[J s^{-1}]
R	Reaction rate	[mol $l^{-1}min^{-1}$]
R	Gas constant	[J mol^{-1} K^{-1}]
R_i	Reaction rate constant (i=1-10)	[mol $l^{-1}min^{-1}$]
R_m	Rate of mass transfer of ethylene glycol	[mol $l^{-1}min^{-1}$]
R_{MS}	Heat flow resistance	[K s J^{-1}]
R_w	Rate of mass transfer of water	[mol $l^{-1}min^{-1}$]
ρ	Density	[g ml^{-1}]
t	Time	[min]
τ	Time constant	[s]
T	Temperature	[°C]
T_{max}	Temperature at maximum polycondensation rate	[°C]
T_m	Temperature at maximum polymer decomposition rate	[°C]
T_0	Polycondensation onset temperature	[°C]
T_{MS}	Temperature of measuring system	[°C]
T_s	Sample temperature	[°C]
γ_A	Activity coefficient of amine	[-]
γ_c	Activity coefficient of carboxyl acid	[-]
γ_{EG}	Activity coefficient of ethylene glycol	[-]
γ_i	Activity coefficient of volatile	[-]
γ_l	Activity coefficient of polymeric amide	[-]
γ_w	Activity coefficient of water	[-]

V	Reaction volume	[l]
V_m	Molar volume of polymeric segment	[l mol^{-1}]
V_m^{298}	Molar volume of polymeric segment at 298 K	[l mol^{-1}]
V_m^T	Molar volume of polymeric segment at T temperature	[l mol^{-1}]
V_t	Volume of the melt at time t	[l]
V_{Vdw}	Molar Van der Waals volume of polymeric segment	[l mol^{-1}]
υ	Volume of melt occupied by volatile species per volume of mixture	[-]
$\overline{\upsilon}$	Molar volume of polymer in melt phase	[l mol^{-1}]
$[W]_0$	Concentration of water in gas phase	[mol l^{-1}]
$[W]_l$	Concentration of water in melt phase	[mol l^{-1}]
x_A	Mole fraction of amine terminal in liquid phase at phase equilibrium	[-]
x_c	Mole fraction of carboxyl terminal in liquid phase at phase equilibrium	[-]
x	Conversion	[-]
x_i	Mole fraction of volatile in liquid phase at phase equilibrium	[-]
x_l	Mole fraction of amine terminal in liquid phase at phase equilibrium	[-]
x_{EG}	Mole fraction of ethylene glycol in liquid phase at phase equilibrium	[-]
x_w	Mole fraction of water in liquid phase at phase equilibrium	[-]
χ_{PET}	Flory-Huggins coefficient	[-]
y_i	Mole fraction of volatile in vapour phase	[-]
y_{EG}	Mole fraction of ethylene glycol in vapour phase	[-]
y_w	Mole fraction of water in vapour phase	[-]

Appendix I

Table 1 IR spectra of mixture of Cat 1 and EG (Cat 1*)

Wave number(cm^{-1})	Vibration Type	Observation
3600-3000	O-H stretch	The absorption of ethylene glycol is around 3300cm^{-1}. However the mixed system shows the peak around 3318cm^{-1}, value which is in the same range as the butanol (BuOH) peak.
3000-2700	C-H stretch	At higher reaction time, the peaks looks more like the catalyst absorption peaks with the difference that around 2841cm^{-1} the shoulder, dissapears or is almost neglectable for the products obtained.
1600-1200	C-H bending	The absorption peaks in this region look more like the ones of butanol.
1200-1000	C-O stretch	
1000-600	C-H bending	

Table 2 ^{1}H and ^{13}C NMR data of mixture of Cat 1 and EG

Position in molecule *	EG		EG:$Ti(OBu)_4$ (2:1)	
	^{1}H	^{13}C	^{1}H	^{13}C
$CHCl_3/CDCl_3$	7.26	77.16	7.26	77.03
1	3.72	63.79	-	-
2	3.72	63.79	-	-
α			3.63	62.70
β			1.55	34.85
γ			1.37	18.89
δ			0.92	13.84

*Numbers/symbols represent the following:

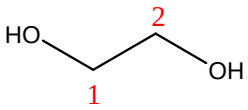

Ethylene glycol

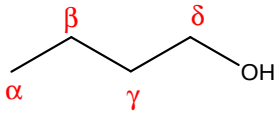

1-Butanol

Appemdix II

Table 1 TGA data of nonisothermal run for calculation of activation energy based on model free method for [Cat 1]:10 mol ppm

5 K min^{-1}		**10 K min^{-1}**		**20 K min^{-1}**	
T [°C]	**Mass loss** [%]	**T** [°C]	**Mass lass** [%]	**T** [°C]	**Mass loss** [%]
110.43	100	110.40	100	110.40	100
114.2035	99.98019	113.5705	99.99124	113.84872	99.99501
117.977	99.97235	117.341	99.97317	117.58744	99.98694
121.7505	99.96623	121.1115	99.94554	121.32616	99.96946
125.524	99.96623	124.882	99.93347	125.06488	99.94832
129.2975	99.96826	128.6525	99.91552	128.8036	99.92889
133.071	99.96259	132.423	99.90101	132.54232	99.90676
136.8445	99.94486	136.1935	99.89013	136.28104	99.88515
140.618	99.9124	139.964	99.871	140.01976	99.86346
144.3915	99.87604	143.7345	99.84504	143.75848	99.83909
148.165	99.81226	147.505	99.81432	147.4972	99.81941
151.9385	99.72787	151.2755	99.78263	151.23592	99.7998
155.712	99.61522	155.046	99.73861	154.97464	99.77378
159.4855	99.46275	158.8165	99.68624	158.71336	99.74494
163.259	99.24068	162.587	99.63436	162.45208	99.70913
167.0325	98.99254	166.3575	99.54687	166.1908	99.67117
170.806	98.67285	170.128	99.41242	169.92952	99.61421
174.5795	98.30445	173.8985	99.25539	173.66824	99.55143
178.353	97.83801	177.669	99.07714	177.40696	99.47614
182.1265	97.28768	181.4395	98.85535	181.14568	99.39221
185.9	96.66406	185.21	98.58913	184.8844	99.2868
189.6735	95.91849	188.98051	98.27414	188.62312	99.16078
193.447	95.1003	192.75101	97.89808	192.36184	99.02275
197.22051	94.17388	196.52151	97.46119	196.10056	98.83742
200.99401	93.17481	200.29201	96.94165	199.83928	98.63029
204.76751	92.0986	204.06251	96.36539	203.57799	98.38802
208.54101	90.94942	207.83301	95.69213	207.31671	98.10369
212.31451	89.7627	211.60351	94.96134	211.05543	97.77996
214	89.15	215.37401	94.15778	214.79415	97.39876
216.08801	88.54771	219.14451	93.15527	218.53287	96.9632
219.86151	87.34372	222.91501	92.2904	222.27159	96.40712
223.63501	86.17081	226.68551	91.25648	226.01031	95.78713
227.40851	85.05072	230.45601	90.18559	229.74903	95.08849
231.18201	84.01266	234.22651	89.05003	233.48775	94.3814
234.95551	83.06447	237.99701	87.99672	237.22647	93.62994
238.72901	82.21086	241.76751	86.90162	240.96519	92.84081
242.50251	81.43924	245.53801	85.76727	244.70391	91.99272
246.27601	80.78927	249.30851	84.83721	248.44263	91.09208
250.04951	80.24793	253.07901	83.89647	252.18135	90.16601
253.82301	79.76796	256.84951	83.00939	255.92007	89.2022
257.59651	79.3404	260.62001	82.21317	259.65879	88.30435
261.37001	78.99084	264.39051	81.52365	263.39751	87.39067

5 K min^{-1}		10 K min^{-1}		20 K min^{-1}	
T [°C]	**Mass loss** [%]	**T** [°C]	**Mass lass** [%]	**T** [°C]	**Mass loss** [%]
265.14351	78.68923	268.16101	80.92659	267.13623	86.48977
268.91701	78.4304	271.93151	80.39738	270.87495	85.49447
272.69051	78.20953	275.70201	79.92472	274.61367	84.47694

Table 2 TGA data of nonisothermal run for calculation of activation energy based on model free method for [Cat 1]: 50 mol ppm

5 K min^{-1}		10 K min^{-1}		20 K min^{-1}	
T [°C]	**Mass loss** [%]	**T** [°C]	**Mass lass** [%]	**T** [°C]	**Mass loss** [%]
130.05	100	129.73	100	130.05	100
132.889	99.7631246	133.10086	99.7618936	133.38824	99.98223
135.728	99.5161113	136.47172	99.4860068	136.72648	99.96214
138.567	99.2230661	139.84258	99.2363385	140.06472	99.93871
141.406	98.9278035	143.21344	98.9683144	143.40296	99.91483
144.245	98.5570626	146.5843	98.6584119	146.7412	99.88658
147.084	98.1082765	149.95516	98.2911606	150.07944	99.85212
149.923	97.6151065	153.32602	97.9215875	153.41768	99.80373
152.762	97.0723661	156.69688	97.4472734	156.75592	99.74749
155.601	96.3730013	160.06774	96.9870289	160.09416	99.67637
158.44	95.5503711	163.4386	96.3551767	163.4324	99.58956
161.279	94.6574924	166.80946	95.6417831	166.77064	99.4875
164.118	93.5592108	170.18032	94.8248844	170.10888	99.37663
166.957	92.3224743	173.55118	93.8482803	173.44712	99.23369
169.796	90.9343223	176.92204	92.7805156	176.78536	99.063
172.635	89.2646262	180.2929	91.4485989	180.1236	98.84311
175.474	87.4302392	183.66376	89.8841409	183.46184	98.60734
178.313	85.3683794	187.03462	88.1508008	186.80008	98.31466
181.152	83.0847257	190.40548	86.0217639	190.13832	97.96574
183.991	80.6132844	193.77634	83.8138212	193.47656	97.41665
186.83	77.8290466	197.1472	81.2695361	196.8148	97.07948
189.669	74.9506573	200.51806	78.0782032	200.15304	96.48549
192.508	71.8106867	203.88892	75.4123188	203.49128	95.90261
195.347	68.5409989	207.25978	72.015305	206.82952	95.25019
198.186	65.1895497	210.63064	68.8105484	210.16776	94.53856
201.025	61.7409945	214.00151	65.2487072	213.506	93.80124
203.864	58.3339308	215	63.4349633	216.84424	93.02863
206.703	54.979977	217.37237	61.3225638	220.18248	92.21294
209.542	51.634039	220.74323	58.224003	223.52072	91.36515
212.381	48.4634837	224.11409	54.5396592	226.85896	90.51608
215.22	45.3132261	227.48495	51.2007728	230.1972	89.67205
218.059	42.4581058	230.85581	47.924002	231.1	89.37
220.898	39.8400343	234.22667	44.6482153	233.53544	88.81399
223.737	37.2590768	237.59753	41.6787843	236.87368	87.98459
226.576	34.8733064	240.96839	38.9407833	240.21192	87.1671

5 K min^{-1}		10 K min^{-1}		20 K min^{-1}	
T [°C]	**Mass loss** [%]	**T** [°C]	**Mass lass** [%]	**T** [°C]	**Mass loss** [%]
229.415	32.6619264	244.33925	36.3384488	243.55016	86.35736
232.254	30.6119442	247.71011	33.775343	246.8884	85.5429
235.093	28.5825845	251.08097	31.2690637	250.22664	84.78882
240.771	25.1415573	257.82269	27.0260556	256.90312	83.57388
243.61	23.464364	261.19355	24.9723707	260.24136	83.033
246.449	21.8282266	264.56441	23.285011	263.5796	82.40065
246.449	21.8282266	264.56441	23.285011	263.5796	82.40065
249.288	20.1903165	267.93527	21.8027364	266.91784	81.95701
252.127	18.8889828	271.30613	20.3680417	270.25608	81.5381
254.966	17.6922352	274.67699	19.2484953	273.59432	81.22696
257.805	16.4970314	278.04785	18.1619087	276.93256	80.88435
260.644	15.3063425	281.41871	17.1395767	280.27081	80.55982
277.678	11.0892686				
280.517	10.6636524				

Table 3 TGA data of nonisothermal run for calculation of activation energy based on model free method for [Cat 1]: 100 mol ppm

5 K min^{-1}		10 K min^{-1}		20 K min^{-1}	
T [°C]	**Mass loss** [%]	**T** [°C]	**Mass loss** [%]	**T** [°C]	**Mass loss** [%]
118.91	100	130.05	100	136.23	100
121.9718	99.99371	133.0488	99.9807	139.0988	99.9819366
125.0336	99.98465	136.0476	99.96169	141.9676	99.9637725
128.0954	99.96498	139.0464	99.9344	144.8364	99.943169
131.1572	99.95469	142.0452	99.9053	147.7052	99.9172734
134.219	99.91813	145.044	99.86653	150.574	99.8859045
137.2808	99.88254	148.0428	99.81506	153.4428	99.8454938
140.3426	99.82178	151.0416	99.75233	156.3116	99.795124
143.4044	99.75017	154.0404	99.68878	159.1804	99.7341198
146.4662	99.65307	157.0392	99.55023	162.0492	99.6781053
149.528	99.53297	160.038	99.42475	164.918	99.601215
152.5898	99.36443	163.0368	99.26517	167.7868	99.5117651
155.6516	99.16439	166.0356	99.08111	170.6556	99.4015706
158.7134	98.89016	169.0344	98.84948	173.5244	99.270712
161.7752	98.59254	172.0332	98.5709	176.3932	99.1210946
164.837	98.22437	175.032	98.24107	179.262	98.9548854
167.8988	97.77659	178.0308	97.85845	182.1308	98.7545757
170.9606	97.25096	181.0296	97.41857	184.9996	98.5180182
174.0224	96.64805	184.0284	96.9097	187.8684	98.2562608
177.0842	95.9708	187.0272	96.32925	190.7372	97.9398496
180.146	95.2122	190.026	95.6931	193.606	97.5887027
183.2078	94.38958	193.0248	94.99644	196.4748	97.134881
186.2696	93.48793	196.0236	94.11383	199.3436	96.6377152
189.3314	92.54938	199.0224	93.35729	202.2124	96.1295522

5 K min^{-1}		**10 K min^{-1}**		**20 K min^{-1}**	
T [°C]	**Mass loss** [%]	**T** [°C]	**Mass lass** [%]	**T** [°C]	**Mass loss** [%]
226.073	83.03895	232.0092	84.28173	236.638	88.0704611
229.1348	82.54755	235.008	83.66534	239.5068	87.3647603
232.1966	82.08587	238.0068	83.09766	242.3756	86.6663574
235.2584	81.65295	241.0056	82.62293	245.2444	86.0171046
238.3202	81.2097	244.0044	82.18174	248.1132	85.3851592
241.382	80.82065	247.0032	81.75309	250.982	84.78172
244.4438	80.46942	250.002	81.35986	253.8508	84.2306867
247.5056	80.15696	253.0008	80.9863	256.7196	83.8019037
250.5674	79.85173	255.9996	80.6136	259.5884	83.3899946
253.6292	79.56634	258.9984	80.26788	262.4572	82.9305582
256.691	79.32764	261.9972	79.95391	265.326	82.4432406
259.7528	79.11411	264.996	79.69449	268.1948	82.1034035
262.8146	78.95002	267.9948	79.42451	271.0636	81.6928854
265.8764	78.81195	270.9936	79.18957	273.9324	81.3804558
268.9382	78.68226	273.9924	78.98564	276.8012	81.018221
272	78.58595	276.9912	78.81251		
275.0618	78.49239				
278.1236	78.40162				

Appendix III

Table 1 Experimental data of lab scale stirred tank reactor

[Cat 1] [wt ppm]	**Temperature** [°C]	**Time** [h]	**IV** [dl g^{-1}]	**M_n** [g mol^{-1}]	**Conversion**	**[COOH]** [mmol kg^{-1}]	**[AA]** [ppm]	**[DEG]** [%]
10	260	2	0.37	7.93E+03	0.976	5.4	5.2	1.73
10	260	3	0.47	1.11E+04	0.983	8.7	6.4	1.76
10	260	4	0.52	1.32E+04	0.985	9.1	4.6	1.77
10	255	2	0.36	7.56E+03	0.974	4.9	4.1	1.72
10	255	3	0.42	9.65E+03	0.980	7.0	4.0	1.73
10	255	4	0.46	1.09E+04	0.982	7.6	6.9	1.74
20	260	2	0.40	9.05E+03	0.979	10.2	5.6	1.76
20	260	3	0.52	1.30E+04	0.985	11.6	8.4	1.76
20	260	4	0.66	1.86E+04	0.990	13.7	12.7	1.81
30	260	2	0.42	9.48E+03	0.980	12.1	9.7	1.75
30	260	2.5	0.49	1.20E+04	0.984	13.7	9.2	1.75
30	260	3	0.55	1.42E+04	0.986	14.2	11.0	1.78
0	260	4	0.19	3.04E+03	0.935	2.9	10.8	1.76
10	270	2	0.43	1.00E+04	0.981	7.4	8.1	1.73
10	270	3	0.52	1.32E+04	0.985	10.0	15.4	1.81
10	270	4	0.61	1.64E+04	0.988	11.9	8.7	1.88
10	280	2	0.55	1.43E+04	0.987	9.0	8.0	1.75
10	280	3	0.63	1.72E+04	0.989	12.4	16.1	1.86
10	280	4	0.66	1.85E+04	0.990	16.2	12.7	1.90
250 - Sb	260	4	0.42	9.53E+03	0.980	4.6	3.4	1.78
250 - Sb	260	3	0.37	8.00E+03	0.976	4.1	3.9	1.80
250 - Sb	260	2	0.33	6.62E+03	0.971	2.3	2.7	1.75

Table 2 Analytical data of intrinsic viscosity for PET synthesised at 270°C, [Cat 1]: 10 wt ppm

No.	**Times measured for the solvent** [s]	**Times measured for the sample** [s]	**Viscosity Number [ml g^{-1}]**
1	266.31	361.28	61.701
2	266.34	361.48	
3	266.19	361.06	
4	265.99	361.05	
5	266.00	361.41	
6	265.96	361.14	
7	266.18	361.83	
8	265.99	361.8	
9	265.87	361.72	
10	265.93	361.84	
Average	266.07	361.46	
St. Deviation	0.16	0.32	
Porcentual error	0.18%	0.27%	

Table 3 Analytical data of determination of carboxyl end groups concentration for PET synthesised at 270°C, [Cat 1]:10 wt ppm

KOH solution concentration [M]	**Weight of the sample used** [mg]	**Volume of KOH solution for titration** [ml]	**Acid number** [mg KOH g^{-1}]	**[COOH]** [mmol kg^{-1}]
0.1	237.09	0.47	6.47	11.87

Table 4 Rate constants of polycondensation of BHET oligomers catalyzed by Cat 1 at different temperature

Temperature [°C]	**Polycondensation** [l mol^{-1} min^{-1}]	**Degradation** [min^{-1}]	**Esterification** [l mol^{-1} min^{-1}]	**Side reactions** [l mol^{-1} min^{-1}]	**Initial overall mass transfer coefficient** [min^{-1}]
255	4.65E-02	3.70E-07	1.03E-01	2.69E-03	1.62
260	5.08E-02	6.52E-07	1.10E-01	3.15E-03	2.05
270	6.52E-02	1.00E-06	1.34E-01	4.75E-03	2.76
280	8.90E-02	2.25E-06	1.68E-01	5.41E-03	2.92